論文 / 著書情報
Article / Book Information

題目(和文)	
Title(English)	Hazardous Antibiotic Bacterial Residue Utilization by Hydrothermal Treatment Combined with Combustion
著者(和文)	MaDachao
Author(English)	Dachao Ma
出典(和文)	学位:博士（工学）, 学位授与機関:東京工業大学, 報告番号:甲第9940号, 授与年月日:2015年6月30日, 学位の種別:課程博士, 審査員:吉川　邦夫,竹下　健二,高橋　史武,時松　宏治,梶谷　史朗
Citation(English)	Degree:, Conferring organization: Tokyo Institute of Technology, Report number:甲第9940号, Conferred date:2015/6/30, Degree Type:Course doctor, Examiner:,,,,
学位種別(和文)	博士論文
Type(English)	Doctoral Thesis

TOKYO INSTITUTE OF TECHNOLGY

Hazardous Antibiotic Bacterial Residue Utilization by Hydrothermal Treatment Combined with Combustion

Ma Dachao (馬大朝)

Department of Environmental Science and Technology
Tokyo Institute of Technology

Doctoral Dissertation

June 2015

Title: Hazardous Antibiotic Bacterial Residue Utilization by Hydrothermal Treatment Combined with Combustion

Abstract:

Bacterial residue from the antibiotic production (ABR) is one kind of the typical bio-waste with high moisture content, high nitrogen content and dangerous antibiotic substances. The present study proposed new method to deal with ABR by hydrothermal treatment (HTT) combined with combustion. The batch-scale and pilot-scale HTT of ABR were respectively conducted to prepare solid biofuels from ABR. The process optimization, the mass balance and the energy balance was discussed based on the experimental data. It was found that HTT can dramatically upgrade the fuel properties of ABR. Moreover, the antibiotic substance in ABR can be remarkably decomposed (almost 100%) by HTT. After that, the NO emission characteristic of raw ABR and treated ABR was investigated in the fixed bed combustion and the air-staged combustion (ASC). The results show that HTT combined with ASC can significantly reduce the NO emitted from ABR combustion by 58%. As a result, a low cost and low emission system combining HTT with combustion was established and tested to be feasible for the management of hazardous ABR.

Table of Content

Abstract: 1

Table of Content 1

Chapter 1 introduction 1

1.1. Antibiotic industry and its bacterial residue 1

1.2. The problems of antibiotic bacterial residue 4

1.3. Optional methods for antibiotic bacterial residue management 5

- Incineration 5
- Landfill after steam autoclaving (sterilization) 5
- Microbial composting to make fertilizer 6
- Animal feed 7
- Waste to biogas fuel by anaerobic digestion 7
- Gasification 8

1.4. Waste to solid fuel by hydrothermal treatment 8

1.5. Utilization of solid biofuel by combustion 11

1.6. Study proposal and objective 13

1.7. Study outline 14

References 16

Chapter 2 Lab Scale Hydrothermal Treatment of Antibiotic Bacterial Residue 18

2.1. Introduction 18

2.2. Experimental procedures and analytical methods 19

2.2.1. Antibiotic bacterial residue source 19

2.2.2. Experimental procedures and hydrothermal treatment apparatus 19

2.2.3. Analytical methods on dewaterability of ABR 21

2.2.4. Analysis of the solid product 22

2.2.5. Analysis of the liquid products 24

2.3. Results and discussions 26

2.3.1. Effect of hydrothermal treatment on dewaterability of antibiotic bacterial residue 26
2.3.2. Effect of hydrothermal treatment on the properties of products 29
2.3.3. Fundamental understanding on hydrothermal treatment of antibiotic bacterial residue 37
2.3.4. Mass and energy recovery in the solid fuels 43
2.4. Conclusions 45
References 48
Chapter 3 Pilot Scale Hydrothermal Treatment of Antibiotic Bacterial Residue 50
3.1. Introduction 50
3.2. Apparatus and experimental methodologies 51
3.2.1. Pilot scale hydrothermal treatment plant and the experimental procedures 51
3.2.2. Analytical methods 55
3.3. Results and discussions 58
3.3.1. Properties of the products from hydrothermal treatment of antibiotic bacterial residue 58
3.3.2. Mass balance and energy balance in the hydrothermal treatment process 62
3.3.3. Modification study on hydrothermal treatment process 66
3.3.4. The modified hydrothermal treatment performance in full scale plant 71
3.4. Conclusions 73
References 75
Chapter 4 Combustion Behaviors of Hydrothermally Treated Antibiotic Bacterial Residue 77
4.1. Introduction 77
4.2. Material and Methodology 78

4.2.1. Fuel characterization 78
4.2.2. Combustion and pyrolysis tests 82
4.2.3. Slagging and fouling tendency calculation 85
4.3. Results and discussions 87
4.3.1. NO emission characteristics of burning ABR-based biofuels 87
4.3.2. Ash behavior and slagging/fouling tendency 101
4.4. Conclusions 107
References 109
Chapter 5 Conclusions and future works 111
5.1 Conclusions 111
5.2 Recommendations for future work 114
Reference 115
Acknowledgement 117

Chapter 1 introduction

1.1. Antibiotic industry and its bacterial residue

The discovery and beginning usage of antibiotic medicine two centuries ago was a great milestone in the history of human beings resisting deadly bacterium against diseases. Since then on, we have benefited from antibiotic medicine for hundreds of years and this will last forward on. Nowadays, the antibiotic is not only used for the pharmaceutical treatment of human beings, but also used for the promoting growth and therapy of meat animals. It is reported by Chinese Fishery Equipment and Engineering Network that in 2014, the consumption of antibiotic in Chinese meat industry is proximately estimated as much as 0.2 million ton, which was higher than 50 wt.% the amount for human usage [1]. As the development of pharmaceutical industry and the meat industry, the demand and production of the antibiotic has kept annually increasing and reached considerable amount. Taking Denmark as an example [2], as shown in Figure 1.1, the pig production in Denmark shown by the yellow curves keep increasing annually. As a result, the antibiotic usage increased even though there is a dropping in antibiotic consumption from 1996 - 1999 due to the limitation on the usage for grow promotion. Also, it is reported that the antibiotic production reached 0.3 million ton/a in 2012 in China and 0.4 million ton/a all around the world [3].

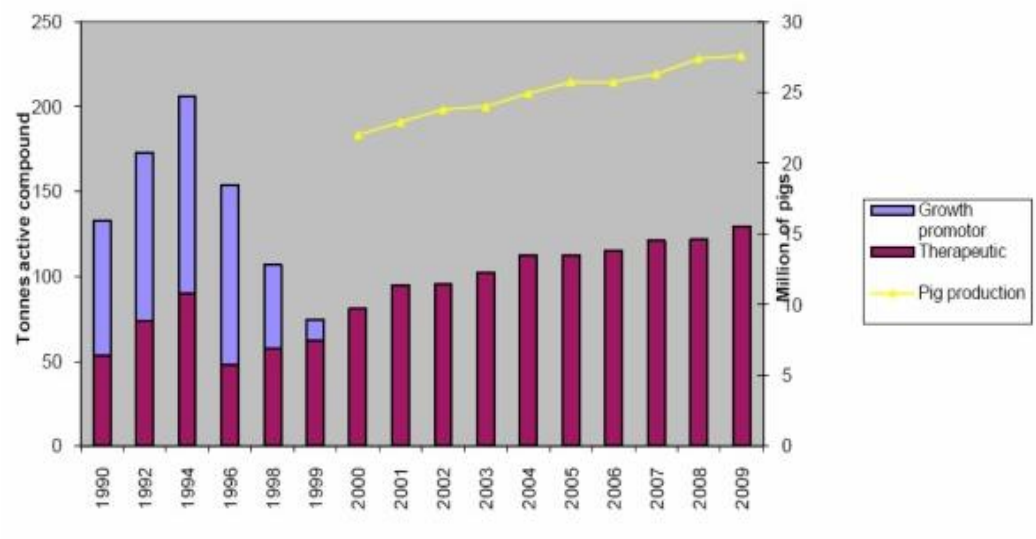

Figure 1.1. Antibiotic usage in all type of animals in Denmark and rate in pig production

As shown in Figure 1.2, the antibiotics are produced industrially by a process of fermentation, where the source microorganism is grown in large containers containing a liquid growth medium. Once the process is completed, the antibiotic will be extracted and purified to a crystalline product [4]. At the same time, the process releases almost ten times amount of wet bacterial dreg as residue[3]. Thus, in 2012, the amount of antibiotic bacterial residue (ABR) from the antibiotic production was almost 4 million ton.

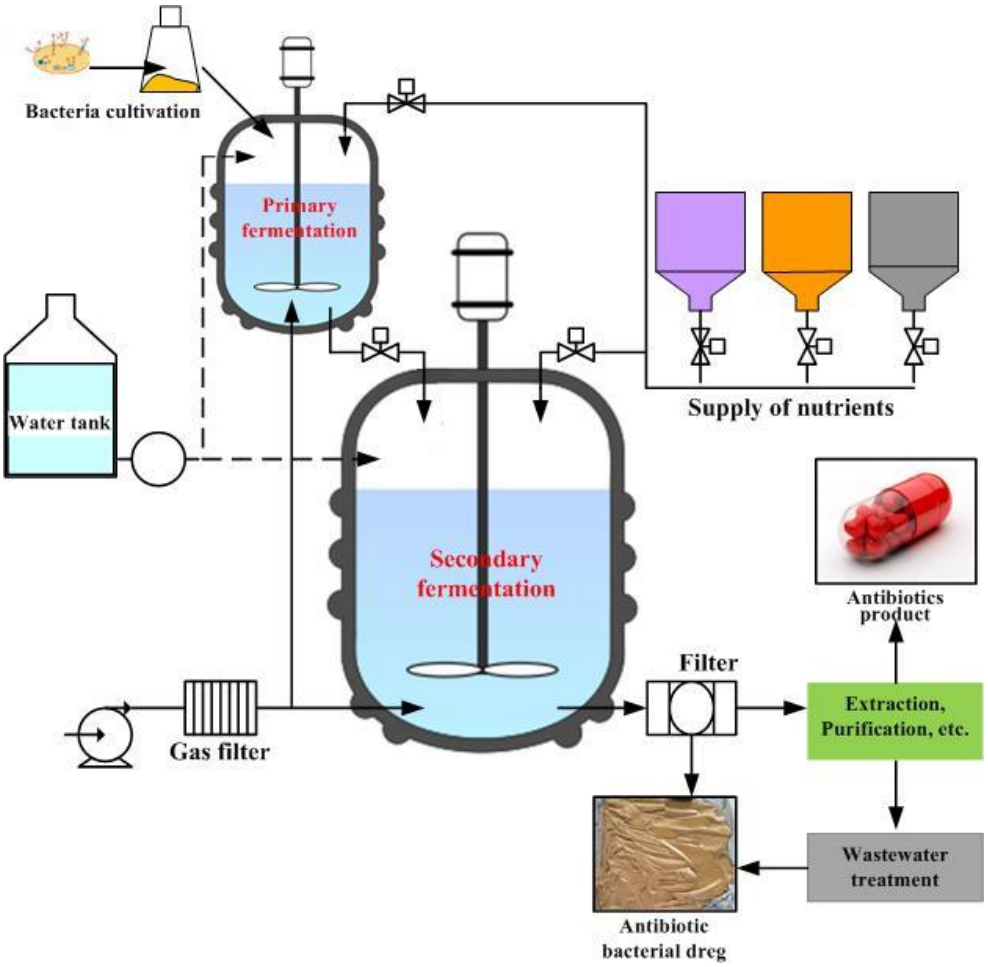

Figure 1.2. The antibiotic production process

ABR are mainly consisted of antibiotic mycelia, culture medium and metabolite residues[5]. These constituents lead to high protein (30-40%) and high heating value of ABR. Besides, some chemicals are added into the solution for the abstraction of the antibiotic. There is also small amount of antibiotic remaining in ABR.

Table 1.1 Basic analysis of ABR

	proximate analysis (%)				HHV[b] (MJ/kg)	ultimate analysis(%)				
	M	VM[b]	A[b]	FC[b]		C	H	N	S	O[c]
Cephalosporin ABR	82.6[a]	91.6	8.4	--	19.4	43.5	6.7	7.7	0.8	33.7
Terramycin ABR[5]	5.1[d]	69.4	12.1	18.4	16.8	41.4	5.0	8.9	0.9	34.0
Penicillin ABR[5]	12.7[d]	81.6	7.3	11.2	17.5	44.1	6.3	9. 5	1.4	32.8

a. As received; b. Dry basis; c. By difference; d. steam dried

Basic analysis of one kind ABR from the antibiotic production process in a medical factory located in Hebei Province, China is presented in Table 1.1. It can be seen that the moisture content of ABR as received basis is as high as 82.6 wt. %. The volatile mater in the dry basis material is 91.6 wt. %, meaning the organic compound occupy the main proportion of the dry basis material. The fixed carbon is undetectable in the raw ABR. Because of the high content of protein, the atomic concentration of nitrogen in ABR is as high as 7.7 wt. %. The higher heating value (HHV) is around 19.4 MJ/kg. Besides, two kinds of ABR from previous study [5]were listed in Table 1.1, showing similar feature of high content of volatile matter, HHV and nitrogen. The difference in FC might be caused from the difference in the analysis methods in different study.

1.2. The problems of antibiotic bacterial residue

Antibiotic resistance threats the effective treatment of an ever-increasing range of infections caused by bacteria, parasites, viruses and fungi. It results in reduction in the efficacy of antibacterial, antiparasitic, antiviral and antifungal drugs, making the treatment of patients difficult, costly, or even impossible. For this sake, the surveillance of antibiotic drug usage and the antibiotic substance has caused a worldwide concerning [6]. A lot of papers have been focused on the risk of residue antibiotics in the environment, but it is difficult to estimate the impact of the trace antibiotic to the environment [5, 7]. Under this background, the remnants antibiotics (6 wt.%) in ABR makes it hazardous and has been listed as a dangerous waste in the legal regulations and needed to be dealt with in regulated ways [8].

There are several typical features for ABR, such as high moisture content as high as 80 wt.%, bad odor and high concentration of nutrient. In the viewpoint of transportation cost and environmental security, the normal disposing ways such as landfill or open dumping is not fit for this biomass waste which will lead to high cost,

secondary pollution to water or air. Because of the high protein content (30~40wt.% as dry basis) [5], ABR used to be recycled as animal feed or organic fertilizer. However, the antibiotics will flow into the food chain of human beings [7]. Besides, the odor will diffuse to the air. Therefore, it was forbidden to use ABR in these ways. As ABR is in the list of dangerous industrial wastes in the legal regulation [8], the pharmaceutical companies were forced to treat this biomass wastes in proper way [9]. The management of ABR is not profitable. It thus has become a critical problem for the pharmaceutical companies. The production of the antibiotic medicine keeps increasing year by year leading to the increasing in production of ABR. Development of feasible technology and method for its management is in urgent need.

1.3. Optional methods for antibiotic bacterial residue management

- **Incineration**

Incineration is a common thermal waste treatment method which fits for almost all the biomass waste and municipal waste. It can reduce the amount and volume of waste to ash, converting organic part to energy at the same time [10]. However, the ABR is high in moisture content as high as 80 wt. %, which will consume a lot of latent heat while subjected into a thermal process. For this reason, the overall calorific value of ABR is too low to sustain constant combustion process unless additional heat is supplied by combusting additional fossil fuel. What is more, the exhausted gas of incineration should be well cleaned to control the emission of pollutants, such as fly ash, NOx and SOx. These will lead to very high operation cost around 300 USD/ton. There is no doubt that the high treatment cost by incineration will eliminate the economic feasibility and block the application of it.

- **Landfill after steam autoclaving (sterilization)**

Landfill disposal is one of the most common waste management methods which

can avoid the spreading of hazardous substance into the environment by controlling the land fill site well [11]. It is suitable for the dangerous waste which is difficult to be reused. As hazardous industrial waste, while dealt by land fill disposal, the transportation, storage, filling and management of land fill site should be controlled strictly according to the management regulations[12]. These processes are high cost.

Regarding high moisture content, the weight density of ABR is low which will spend a lot of land fill site space. Besides, high nutrient content and antibiotic substance content might be released out of the land fill site then lead to secondary pollution. In addition, because ABR is slurry like material and has bad odor, the transportation and storage of ABR will be a big problem that is difficult to be fixed. Considering the cases abovementioned, direct land fill disposal will not be a feasible method to manage ABR.

- **Microbial composting to make fertilizer**

The ABR is consisted of organic substance, organic acid, nitrogen, potassium and microelement. Especially the protein content in ABR is as high as 30~40 wt. % in dried basis. It is possible to utilize ABR as organic fertilizer. In this method, ABR will be subjected into a microbial digestion process to inactivate the antibiotics in the residue. Then the residue can be dried to produce fertilizer.

However, the residual antibiotic in ABR is difficult to be totally inactivated by microbial digestion. If using this residue as fertilizer, the residual antibiotic will sustain in the environment and lead to potential venture for ecosystem. Furthermore, ABR is difficult to be dried even after being treated by microbial digestion. The drying process will be a big part of the treatment energy cost for this method. Therefore, it is necessary to evaluate and control the venture of utilizing ABR as fertilizer and low cost drying process is needed to be found.

- **Animal feed**

In ABR, 30~40 wt. % of dry basis is protein. The most common method to treat ABR is to pre-treat the residue to remove the antibiotic, then, use it as animal feed. The micro scale of antibiotic in ABR will be helpful for the growth of animal. However, the problem of this method is that the antibiotic will flow from the animal into the food chain of animal and human beings and then be discharged into the environment, which will boost the evolution of super bacterium that can resist to the antibiotic medicine and cause potential venture for ecosystem. This will be an unpredictable venture to environment and human beings. For this reason, using ABR as animal feed was forbidden in many countries. Other method to manage this waste is needed to be explored.

- **Waste to biogas fuel by anaerobic digestion**

Around 90 wt. % of the dry basis ABR is organic compound which can be recycled as biomass energy. Through the anaerobic digestion, the organic compound in ABR can be converted to methane gas, which is a kind of biogas fuel. The final residue from the digestion will have a stable property that is easier to be managed than the raw ABR and can be used as organic fertilizer.

However, it has been proven that antibiotics has toxic effect on the microbial bacteria which will largely reduce the biogas production yield and difficult to keep the digestion continuously stable[13, 14], which makes this technology impractical for the treatment of ABR. The microbial cell wall which is mainly consisted of cellulose will obstruct the releasing of organic compound from the cell out to the solution. This will be the obstacle for fully utilizing the organic compound as gas fuel. Moreover, the antibiotic remaining in the final digested residue will cause the unpredictable venture to the ecosystem while using the residue as fertilizer. Thus, further treatment for this

method is needed, resulted in complex treatment process and high cost.

- **Gasification**

In addition to the technologies shown above, pyrolysis to produce syngas, oil product and char is also viable technology to manage biomass waste. The feed stock material of the pyrolyzer or gasifier should be as dry as 20 wt. % of moisture content. As the moisture content of the raw ABR is as high as 80 wt. %, direct treatment by gasification is not reasonable but pretreatment to dry it is needed before feeding into the reactor. But the drying process will be high cost. In the viewpoint of economy, this method is not viable.

1.4. Waste to solid fuel by hydrothermal treatment

Considering the high proportion of organic compound in the dry basis ABR, solid fuel production from ABR through a waste-to-energy process would be a promising method as it can not only suppress the environmental stress, but also supply recycling energy. However, the high moisture and nitrogen content restricts its further utilization as a clean and storable fuel. Besides, the remaining of small amount of antibiotic in the residue should be considered as a matter. Therefore, proper pretreatment for upgrading ABR is urgently needed.

Basically, hydrothermal treatment (HTT) of a biomass waste involves dehydration and decarboxylation of the waste to raise its carbon content and heating value. HTT has been widely used to simulate the natural coalification processes for a century, and from last decade the application has been further extended to the pretreatment of biomass feedstock for making high-quality biofuel or biomaterial [15, 16]. HTT can be divided into three main regions, liquefaction, catalytic gasification, and high-temperature gasification, depending on the processing temperature and pressure as shown in Figure 1.3 [16]. The pressure-temperature phase diagram for

pure water is superimposed to highlight the regions with respect to water's liquid-vapor co-existence behavior. The hydrothermal conversion via liquefaction pathways occurs generally between about 200 and 370 ℃, with pressures between about 4 and 20 MPa, sufficient to keep the water in a liquid state. At near-critical temperatures up to about 500 ºC, effective reforming and gasification generally requires catalytic enhancement to achieve reasonable rates and selectivity. At higher temperatures above 500 ºC, homogeneous gasification and thermolysis often occur.

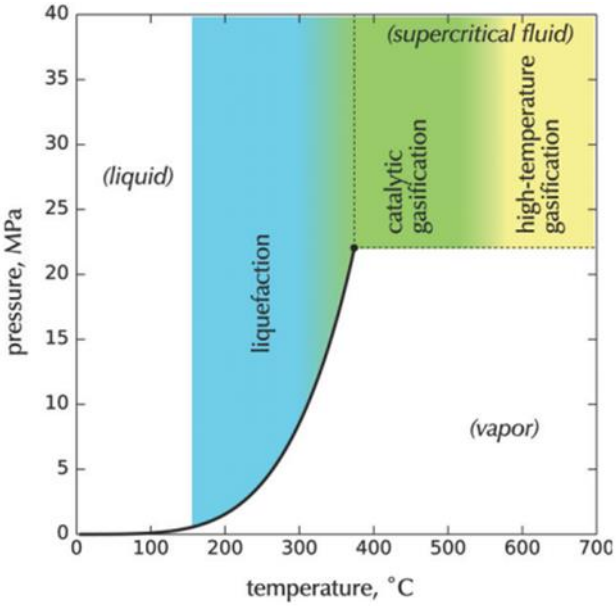

Figure 1.3. Hydrothermal treatment regions referenced to the pressure–temperature phase diagram of water[16].

In many previous studies, HTT under mild temperatures has been demonstrated as an effective technology to produce good quality solid fuel from high moisture content material such as sewage sludge, municipal solid waste (MSW), agricultural reside, etc. Namioka conducted studies to develop a two-stage system consisting of HTT and mechanical dewatering to supplant thermal drying for solid fuel production from sewage sludge [17, 18]. It was demonstrated that HTT can improve the dewaterability of various sewage sludge by Meng [19]. Prawisudha [20] demonstrated that the study of hydrothermal conversion of MSW to solid fuel clarifying that it was fit for MSW to fuel process and could remove chlorine from MSW through washing

process. Besides, Sakaguchi [21] applied HTT to upgrade brown coal to get high quality coal fuel, boosting up the calorific value and reducing the volatile mater of coal. Lu[22]investigated on the co-combustion behaviors of the hydrothermally treated MSW blending with various coals in different kinds of combustor primarily verifying the feasibility of utilization of the hydrothermally treated MSW as solid fuel. In some previous studies [23-25], model components were subjected to HTT under varies of conditions in order to get deeper understanding on the reaction mechanism of the biomass in high compressed and temperature water. Funke and Ziegler [26] stated in the review study that HTT can be defined as the combination of dehydration and decarboxylation. However, during HTT in the temperature range from 100 ℃ to 350 ℃, the reactions like hydrolysis, dehydration, decarboxylation, polymerization, aromatization, and etc. occur and the components interact with each other to achieve the final product from raw feedstock. The studies above illustrated that HTT is a feasible technology to approach high quality solid fuel from variety of high moisture material, offering an alternative route to reuse the biomass waste as storable and carbon neutral energy resource. Based on them, it can be expected that HTT is feasible for converting industrial ABR to solid fuel.

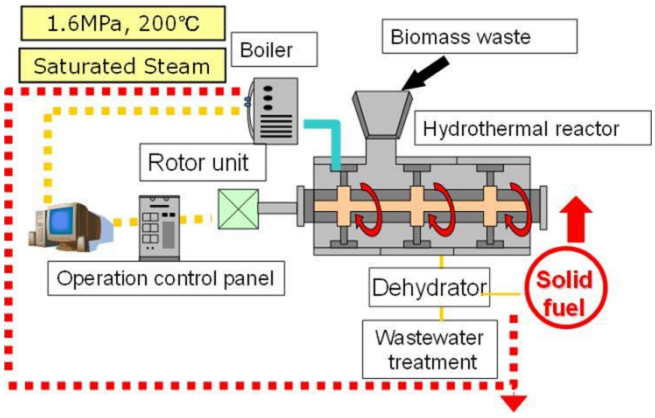

Figure 1.4 Sketch of hydrothermal treatment apparatus

However, the property of ABR which contains a certain amount of amino acid, oligose and metal ion are quite different from the reported biomass wastes that might

lead to a big difference in the reaction mechanism during HTT. Therefore, it is necessary to investigate the feasibility of fuel production from ABR by HTT. Biomass waste is often not homogenous due to which during HTT, some components in biomass wastes will affect the reaction pathway, the reaction rate and etc. For instance, the alkaline metal ion Ca^{2+} was proved to have a positive effect on improving the dewaterability of sludge [27]. Therefore, the usage of model components (e.g., lignin, hemicellulose) cannot give the exact information of chemical composition change of a real biomass waste while subjected in HTT. Furthermore, a number of researches were reported on high nitrogen content biomass [23, 24] showing that the combustion of them will cause emission of NOx which is well known as one of the most undesirable gaseous pollutants. Moreover, the effect of HTT on the biomass was mainly explored in term of physical properties and primary chemical properties by ultimate and proximate analysis. Thus, the differences between the model components and real biomass should be considered for the purpose of engineering practice. In one word, the effect of HTT on the properties of high nitrogen content biomass is still unknown ultimately. In order to get a deeper understanding of the effect of HTT on the chemical composition and the combustion practice of utilized ABR as solid fuel, further study is needed to be conducted.

1.5. Utilization of solid biofuel by combustion

Compared to chemical conversion technologies such as gasification for syngas, pyrolysis for bio-crude, liquefaction, digestion, etc, combustion is one of the most direct way to convert biomass into thermal energy or steam heat [28, 29]. Generally, combustion is a complex phenomenon which involves simultaneous coupled heat and mass transfers with chemical reactions and fluid flows. The essential process steps include drying, devolatilization, gasification, char combustion, and gas phase reactions[28]. Figure 1.5 schematically shows a typical combustion process of biomass particle.

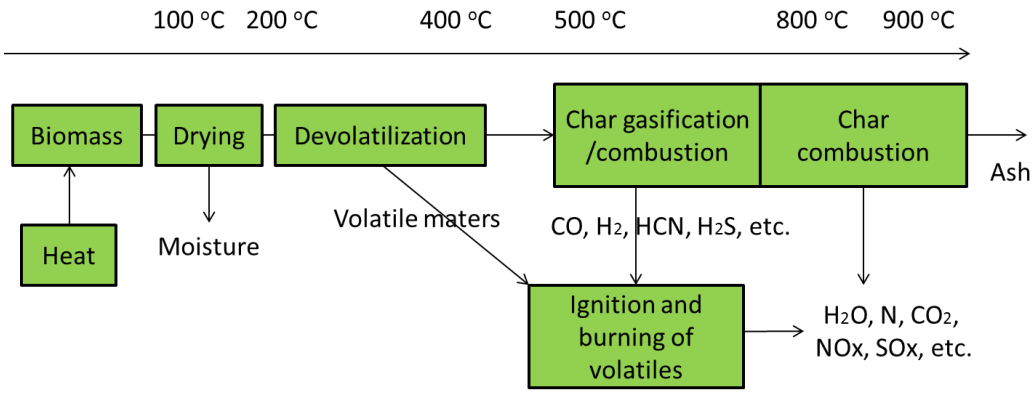

Figure 1.5 Schematic description of the combustion process of biomass particle

It has been found that, biomass materials show different combustion characteristics according to their elemental composition. Biomass combustion is a series of chemical reactions by which mainly carbon is oxidized to carbon dioxide, and hydrogen is oxidized to water. However, there are many elements that go into the combustion. Reaction for the combustion of a biomass fuel in air might take the following form, where the first reactant compound is a biomass fuel.

$$Cx_1Hx_2Ox_3Nx_4Sx_5Clx_6Six_7Kx_8Cax_9Mgx_{10}Nax_{11}Px_{12}Fex_{13}Alx_{14}Tix_{15} + nH_2O + n_2(1 + e)(O_2 + 3.76N_2) = n_3CO_2 + n_4H_2O + n_5O_2 + n_6N_2 + n_7CO + n_8CH_4 + n_9NO + n_{10}NO_2 + n_{11}SO_2 + n_{12}HCl + n_{13}KCl + n_{14}K_2SO_4 + n_{15}C + \cdots + \text{Energy}$$

It has been previously concluded that, compared to the fossil fuel combustion, biomass solid fuel combustion has advantages such as renewable fuel, low content of ash, high reactivity with high volatile matters, reduction of biomass wastes, carbon balance, etc. [29] even though, due to the different characteristics of biomass, there are some problems need to be settled down during the utilization of solid biofuel by combustion [29]. The biomass usually contains higher fraction of alkali metals (Na, K, etc.), silica and phosphorus in ash, which will lead to the problem of fouling, deposits, corrosion and agglomeration. Fouling or deposits are known as the ash covered on the surface of heat transfer equipment which will reduce the efficiency of radiant heat.

Corrosion will lead to the reduction of strength in equipment material that can be caused either directly by gas phase species, by deposits or by a combination of both. Agglomeration can occur as a result of accumulation of low-temperature-melting salts. Besides, it can also occur in the presence of silica from sand and calcium from fuel, potassium phosphate can react with silica forming low-temperature-melting silicates of potassium and calcium while phosphorous bounds with calcium. Agglomeration is harmful for boiler because it reduces the fluidization performance in boilers. In addition, some biomass fuels contain high protein or amino component which will lead to high nitrogen content, which will bring the concerning of NO_x emission, which is well known as the main source of acid rain and photochemical smog [30].

1.6. Study proposal and objective

For the previously stated problems about ABR, in this study, we propose to treat ABR by HTT combined with combustion. The task is to investigate the feasibility of solid fuel production from ABR by HTT; to optimize and scale up the HTT condition of ABR for the further application of this process; to discuss the effect of HTT on the combustion characteristics of ABR; finally to prove the feasibility of our proposal.

The systemic sketch for treatment of ABR is shown in Figure 1.6. ABR can be treated by HTT to produce high quality solid biofuel. At the same time, part of the ABR is converted into liquid phase. As the water from HTT contains solvable substance such as organic acid, salts, etc., wastewater treatment processes or some chemical methods are needed to recycle this part as green product. In the practical process, hot steam is needed to heat up the closed reactor to provide a high temperature and high pressure atmosphere. Thus, we propose to provide the hot steam needed by combusting the produced solid biofuel from the last step in a solid fuel firing boiler. The scope of this study is bounded by the blue dotted line circle shown in Figure 1.6.

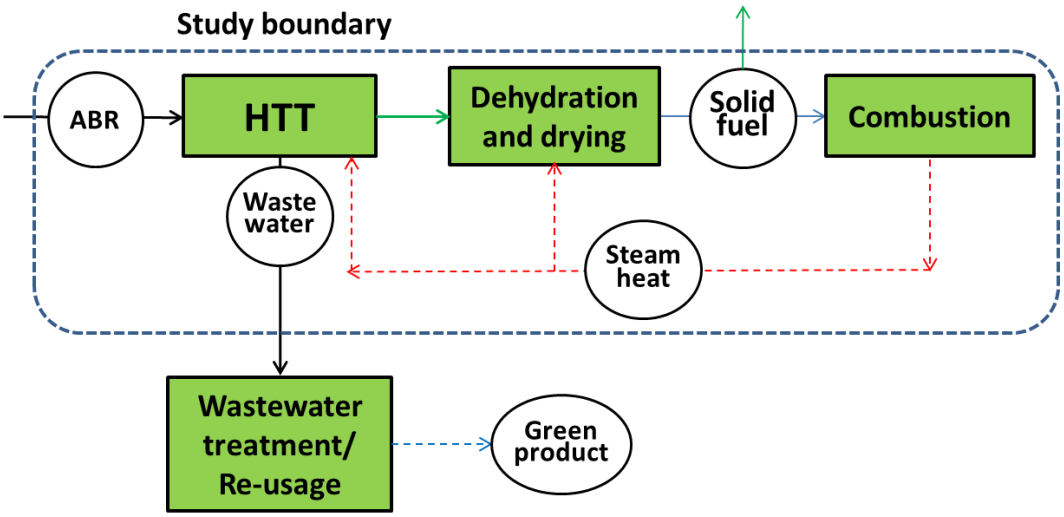

Figure 1.6. Process for treatment of ABR by HTT combined with combustion

1.7. Study outline

Based on the study proposal in section 1.6, this research is separately presented by 6 chapters. The content of each chapter is briefly shown as follows:

In chapter 1, the background and problems of antibiotic bacterial residue was described. The current alternative technologies for the management of ABR were introduced. In addition to that, the research progress of HTT for solid fuel production and the combustion of biomass solid fuel were briefly summarized. Then, we proposed combination of HTT and low NO combustion for the environmental friendly treatment of ABR.

Chapter 2 investigated the processing characteristics of HTT on ABR. The effects of the HTT operating parameters including the temperature and the holding time were discussed. The water removal performance of ABR varied with different experimental conditions was revealed. Besides, the mass balance during HTT was obtained. The decomposition of antibiotics substance in ABR via HTT was studied using a model solution. Based on the characterization of the products from HTT of

ABR, the mechanism involving is discussed.

In Chapter 3, in order to get more information about HTT of ABR for industrial application, HTT of ABR was conducted in a 2 m^3 large scale reactor. The properties of the solid product and liquid product were analyzed respectively. Besides, the mass balance and the energy balance during HTT and the dewatering process were discussed based on the large scale experimental results. In addition, a new process was developed to reduce the energy consumption of the total system.

In Chapter 4, the effects of HTT on the combustion performance of ABR was investigated. The dried raw ABR and the solid fuel obtained from 200 ˚C, 30min HTT were combusted in the thermogravimetric analyzer to reveal their combustion characteristics. In addition, the NO emission from the combustion of the samples was studied in a silica reactor under the conventional combustion mode and the air staging combustion mode. The co-combustion of coal and ABR was also conducted under the different blending ratios. The slagging or fouling indexes of the ash from ABR-based fuel was calculated and discussed.

Finally, in the final chapter, the main achievements of this research were summarized. Suggestion for the future plan was also stated.

References

[1] Network CFEaESaTI. http://www.fmiri.ac.cn/showGevTrend.aspx?id=4133. 2015.
[2] Administration DVaF. Facts sheet on the Danish restrictions of non-therapeutical use of antibiotics for growth promotion and its consequences 2010.

[3] 李再兴, 田宝阔, 左剑恶, 余忻, 沈洪艳, 王勇军, et al. 抗生素菌渣处理处置技术进展 [J]. 环境工程. 2012;30:72-5.

[4] Elander RP. Industrial production of beta-lactam antibiotics. Applied microbiology and biotechnology. 2003;61:385-92.

[5] 贡丽鹏, 郭斌, 任爱玲, 刘仁平, 宋汉宁. 抗生素菌渣理化特性. 河北科技大学学报. 2012:190-6.

[6] Organization WH. Antimicrobial Resistance Global Report on Surveillance2014.
[7] Hernando MD, Mezcua M, Fernandez-Alba AR, Barcelo D. Environmental risk assessment of pharmaceutical residues in wastewater effluents, surface waters and sediments. Talanta. 2006;69:334-42.
[8] China MoEPotPsRo. GB21907-2008 Discharge standards of water pollutants for pharmaceutical industry Bio-pharmaceutical category2008.
[9] COMMISSION TE. COMMISSION REGULATION (EU) No 37. Official Journal of the European Union. 2010.
[10] C.C. Lee GLH. Medical waste management incineration. Journal of Hazardous Materials. 1996.
[11] Giusti L. A review of waste management practices and their impact on human health. Waste management. 2009;29:2227-39.
[12] Vrijheid M. Health Effects of Residence Near Hazardous Waste Landfill Sites A Review of Epidemiologic Literature. Environmental health perspectives. 2000;108:101-12.
[13] Keith A. Loftin, Cynthia Henny, Craig D. Adams, Surampali R, Mormile aR. Inhibition of microbial metabolism in anaerobic lagoons by selected sulfonamides, tetracyclines, lincomycin, and tylosin tartrate. Environmental Toxicology and Chemistry. 2005;24:782-8.
[14] Sanz J, Rodriguez N, Amils âR. The action of antibiotics on the anaerobic digestion process. Applied microbiology and biotechnology. 1996;46:587-92.
[15] Savage PE. Organic Chemical Reactions in Supercritical Water. Chemical Reviews. 1999;99:603-22.
[16] Peterson AA, Vogel F, Lachance RP, Fröling M, Antal JMJ, Tester JW. Thermochemical biofuel production in hydrothermal media: A review of sub- and supercritical water technologies. Energy & Environmental Science. 2008;1:32.

[17] Namioka T, Miyazaki M, Morohashi Y, Umeki K, Yoshikawa K. Modeling and Analysis of Batch-Type Thermal Sludge Pretreatment for Optimal Design. Journal of Environment and Engineering. 2008;3:170-81.
[18] Namioka T, Morohashi Y, Yamane R, Yoshikawa K. Hydrothermal Treatment of Dewatered Sewage Sludge Cake for Solid Fuel Production. Journal of Environment and Engineering. 2009;4:68-77.
[19] Meng D, Jiang Z, Kunio Y, Mu H. The effect of operation parameters on the hydrothermal drying treatment. Renewable Energy. 2012;42:90-4.
[20] Prawisudha P, Namioka T, Yoshikawa K. Coal alternative fuel production from municipal solid wastes employing hydrothermal treatment. Applied Energy. 2012;90:298-304.
[21] Sakaguchi M, Laursen K, Nakagawa H, Miura K. Hydrothermal upgrading of Loy Yang Brown coal — Effect of upgrading conditions on the characteristics of the products. Fuel Processing Technology. 2008;89:391-6.
[22] Lu L, Namioka T, Yoshikawa K. Effects of hydrothermal treatment on characteristics and combustion behaviors of municipal solid wastes. Applied Energy. 2011;88:3659-64.
[23] Sunphorka S, Chavasiri W, Oshima Y, Ngamprasertsith S. Kinetic studies on rice bran protein hydrolysis in subcritical water. The Journal of Supercritical Fluids. 2012;65:54-60.
[24] Duan P, Dai L, Savage PE. Kinetics and mechanism of N-substituted amide hydrolysis in high-temperature water. The Journal of Supercritical Fluids. 2010;51:362-8.
[25] Aida TM, Sato Y, Watanabe M, Tajima K, Nonaka T, Hattori H, et al. Dehydration of d-glucose in high temperature water at pressures up to 80MPa. The Journal of Supercritical Fluids. 2007;40:381-8.
[26] Funke A, Ziegler F. Hydrothermal carbonization of biomass: a summary and discussion of chemical mechanisms for process engineering. Biofuels, bioproducts and biorefining. 2010;4:160-77.
[27] Neyens E, Baeyens J, Creemers C. Alkaline thermal sludge hydrolysis. Journal of Hazardous Materials. 2003;97:295-314.
[28] Khan AA, de Jong W, Jansens PJ, Spliethoff H. Biomass combustion in fluidized bed boilers: Potential problems and remedies. Fuel Processing Technology. 2009;90:21-50.
[29] Saidur R, Abdelaziz EA, Demirbas A, Hossain MS, Mekhilef S. A review on biomass as a fuel for boilers. Renewable and Sustainable Energy Reviews. 2011;15:2262-89.
[30] Glarborg P. Fuel nitrogen conversion in solid fuel fired systems. Progress in Energy and Combustion Science. 2003;29:89-113.

Chapter 2 Lab Scale Hydrothermal Treatment of Antibiotic Bacterial Residue

2.1. Introduction

In many previously reported research works[1], the hydrothermal treatment (HTT) has been demonstrated as a viable way for the treatment of high moisture content biomass wastes such as MSW [2, 3] and sewage sludge[4-7] for improving the dewaterability of these kinds of wastes then produce high quality solid fuel. In this viewpoint, we proposed that HTT is also feasible to upgrade the antibiotic bacterial residue (ABR) for solid fuel production. However, the feasibility of this proposal should be studied. Besides, ABR is high nitrogen content material, which might lead to high NOx emission while being subjected into combustion process. The nitrogen behavior during the upgrading process should be taken into account. The objectives of this chapter are to investigate HTT process characteristics of ABR, then, to discuss the viability of fuel production from ABR by HTT. Therefore, the study boundary in this chapter is shown in Figure 2.1.

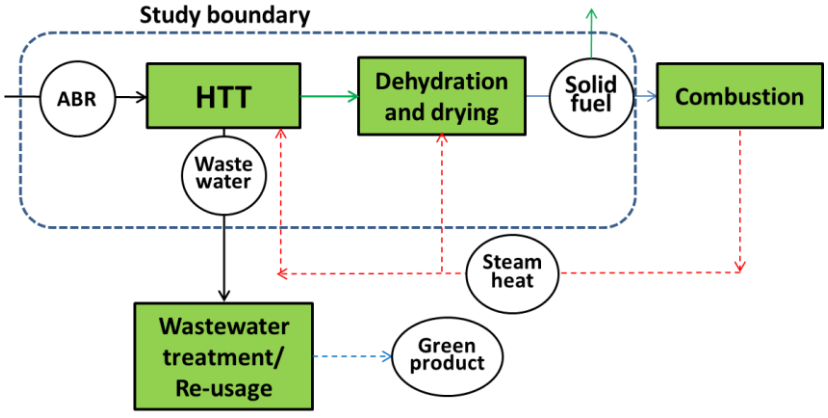

Figure 2.1 Study boundary of chapter 2

ABR will be firstly hydrothermally treated in a lab scale autoclave. The dewatering process of hydrothermally treated ABR was discussed. Then properties of ABR based solid fuels from various HTT conditions will be determined by several analysis methods such as the proximate analysis, the ultimate analysis, FTIR and XRF etc. The liquid products will also be tested by COD, spectrophotometer, etc.. A model solution will be treated in the autoclave to reveal the antibiotic behavior in HTT. The mass recycling and energy recycling from ABR by HTT will be discussed finally.

2.2. Experimental procedures and analytical methods

2.2.1. Antibiotic bacterial residue source

The antibiotic bacterial residue (ABR) used in this work was sampled from a cephalosporin production process in a medical factory located in Hebei Province, China. According to the process, it can be expected that ABR is mainly consisted of dead microbial cells and some nutrient constituents where nucleic acid, proteins, carbohydrates and lipid are existing. The basic analysis of sample is presented in Table 1.1.

2.2.2. Experimental procedures and hydrothermal treatment apparatus

In the lab scale study, the experimental procedure was conducted as shown in the flow chart of Figure 2.2. Firstly, ABR sample was hydrothermally treated in a batch type autoclave shown in Figure 2.3. After HTT, condensed liquid was obtained from the exhaust steam. Its ammonia concentration was measured. The residue from HTT (HTT-residue) was centrifuged to get wet centrifuged residue then dried to get solid fuels. The separated liquid and residue after the centrifuge were analyzed by various methods.

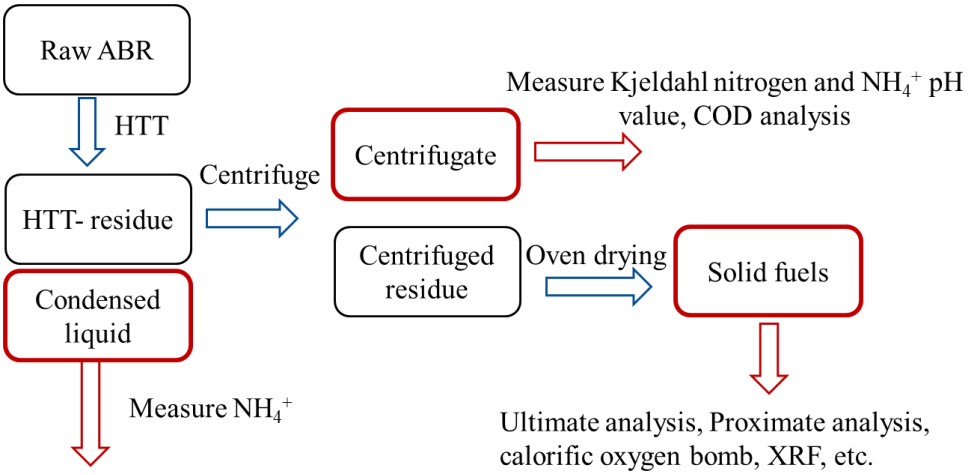

Figure 2.2 The experimental procedure of lab scale hydrothermal treatment of antibiotic bacterial residue

A bench-scale autoclave machine (Figure 2.3) was utilized in this study to conduct HTT, simulating the commercialized HTT process. As shown in Figure 2.3, the apparatus mainly consisted of a reactor with the capacity of 1.5 L circled by a heater. A condenser to cool down the exhaust gas containing steam is installed at the outlet of the reactor. Besides, a motor rotator is set to enhance the mixing of the sample with water and enhance heat transfer, which is very essential for the engineering practice. A cylinder filled with argon gas is connected to the reactor.

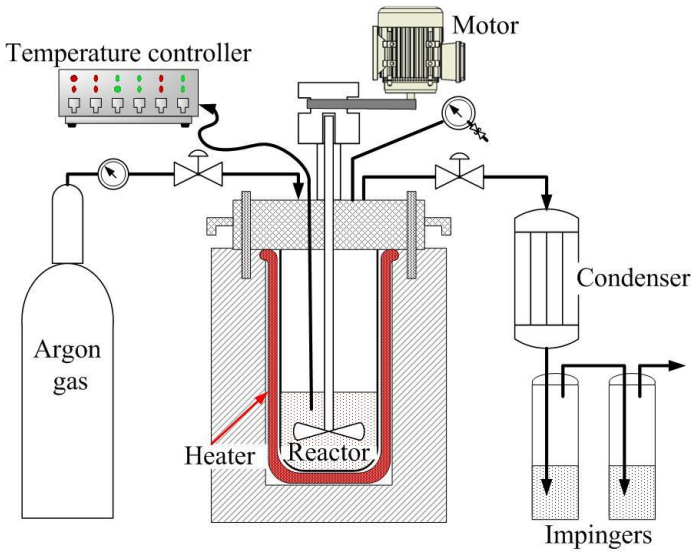

Figure 2.3. Schematic diagram of the autoclave system

ABR was firstly supplied to the reactor mixed with distilled water at the ratio of 5:2 (200 g sample and 80 g water) simulating HTT process that adds saturated steam as a heat agent to maintain the reaction[2, 8]. Before the experiment, argon was introduced to sweep out the air in the reactor to provide oxygen and nitrogen free environment, then the heater was started to heat up the reactor until reaching the target temperature, then held for 30 minutes to provide sufficient time for the reaction. The motor rotator was kept stirring at the fixed speed of 100 r/min during the reaction. The steam was discharged slightly out of the reactor to the condenser after finishing the reaction. Then the HTT-residue was collected after the temperature was cooled to 100 ℃. The condensed liquid in the condenser was also collected for the analysis. The detail HTT conditions are shown in Table 2.1.

Table 2.1. Summary of the operating conditions of experiments

HTT temperature (℃)	HTT holding time (min)	Others
160、180、200、220、240	30	Heating rate: 3 ℃/min, Rotate speed: 100 r/min, Atmosphere: argon, Material to water ratio: 5/2.
200	0、30、60	

2.2.3. Analytical methods on dewaterability of ABR

In order to know the effect of HTT conditions on the dewaterability of ABR, the sedimentation performance, the dehydration process and the drying process were discussed. Firstly, the HTT-residues were subjected into a set of bottles to tranquilly keep under room temperature condition for 24 hours to compare the sedimentation performance of different samples. The raw ABR was also subjected in this process for comparison.

Before being used as fuels, the material should be dried. HTT can improve the dewaterability of biomass waste which was proved by previous works[2, 8]. In the

real application process, the biomass waste should be mechanically dehydrated first then be dried so as it can sustain a stable combustion [9] In order to investigate the effect of HTT on the dewaterability of ABR, the HTT-residue and ABR were dehydrated in a centrifuge at the speed of 3000 r/min for 5 minutes. The weight loss of the samples was measured to know the dehydration performance of them. After that, the centrifuged residue was introduced to a drying oven to get dried solid biofuels. The drying condition was 105 ℃ for 48 hours. The weight loss of the samples during the drying process was measured every several hours so that we can evaluate the drying speeds of each sample. The calculation of the moisture content in the samples is presented in Equation 2.1 as follows.

$$M_x = \frac{m_x - m_f}{m_x} \qquad \text{Eq. 2.1}$$

Where M_x – the moisture in time x

m_x – the absolute weight of the samples in time x

m_f – the absolute weight of the samples after 48 hours of drying (Here the samples were assumed to be totally dried after 48 hours)

2.2.4. Analysis of the solid product

The dried solid biofuels dropped from the oven drying were milled to powder by a roller crusher. In order to confirm the uniformity of the solid biofuels for the downstream analysis, the powder like samples then were sieved through a 200 m filter

As a powerful tool for molecule observation, FTIR can detect the functional groups existing in the sample. As shown in Figure 2.4, it was applied to explore the organic chemical composition of solid biofuels for comparison, especially, to investigate the effects of HTT on nitrogen-containing functional groups in ABR. 1 mg of powder sample was mixed with 100 mg of KBr then pressed to thin film under the pressure of 10 MPa. After that, the thin film of each sample was analyzed by the

Fourier transform infrared spectrophotometer to get the bonding information in the absorption spectrogram. Since the spectrogram contains overlapping peaks, a de-convolution process was conducted by cure-fitting analysis in a data processing program to get individual peaks. The curve fitting function used in this work was Lorentz and Gauss functions.

Figure 2.4. FTIR analyzer

The study also characterized the solid biofuels using the X-ray Photoelectron Spectroscopy (XPS, ESCALAB250Xi). For the analysis, a sample was, in succession, dried in a vacuum dryer, degased at 10-7 Pa for 3 h and neutralized by Ar-ion sputtering. Monochromatic Al K Alpha (350W, hv =1486.8eV) X-ray was used to excite the fuel sample. All spectra were obtained at 20 eV of pass energy in the fixed transmission mode. The resolution and analysis area were 0.05 eV and 0.8 mm^{-2}, respectively. The analysis was automatically performed at 3 ~ 5 different positions on the surface to obtain the high-quality spectrum.

Metal contained in the fuel will become bottom ash or fly ash during combustion. The biofuels were analyzed by XRF to clarify the inorganic chemical constituents inside. The sieved powders were firstly pressed under a high pressure (20 kg) into tablet then were put into the multi channels analyzer. All the samples were detected in a vacuum chamber filled with helium. Data were recorded simultaneously.

2.2.5. Analysis of the liquid products

The separated liquid from the centrifugation and the condensed liquid obtained from the condenser were measured by several types of analysis. Firstly, the Chinese standard methods (GB/T 5009-2003, China) were used to measure the chemical oxygen demand (COD) of the separated liquid. The pH value of the liquids was directly measured by a pH meter (Mettler Toledo FE20). As shown in Figure 2.5, for the nitrogen behavior in the separated liquid, the liquid was diluted proper times to conduct ammonium ion (NH_4^+) determination by the spectrophotometer directly to get NH_4^+. Besides, Kjeldahl nitrogen (K-N) was also detected. The liquid was firstly digested under 240 ℃ to convert the nitrogen in organic compound into NH_4^+ and then distilled into acid absorbent (2 wt. % boric acid solution). The total NH_4^+ concentration was then measured by the spectrophotometer. Considering that the concentrations of nitrate and nitrite were undetectable, the total nitrogen concentration in all the separated liquid was defined as the total NH_4^+ concentration in the digested separated liquid. Here, we defined K-N in the separated liquid calculated by the total NH_4^+ concentration in the digested separated liquid subtracting the NH_4^+ concentration in the non-digested separated liquid.

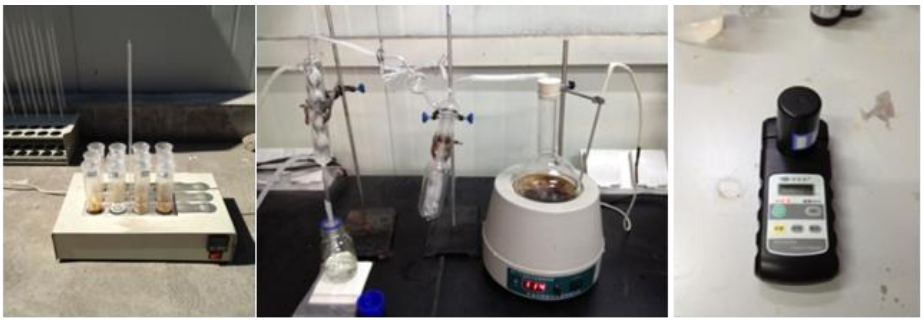

Figure 2.5 Procedure of nitrogen analysis for liquids

The HTT reaction was done in nitrogen free and oxygen free atmosphere, therefore, we can neglect the effect of NOx in the gas phase and consider the nitrogen

in the gas phase was represented by ammonia gas. The exhausting gas was swept slightly by argon gas out of the reactor to blow though an acid absorption bottle. The bottle was filled with absorbent (2 wt. % boric acid solution) for ammonia absorption. After absorption, the ammonium concentration in the solution was measured by the spectrophotometer. This part of the nitrogen was defined as gas-N.

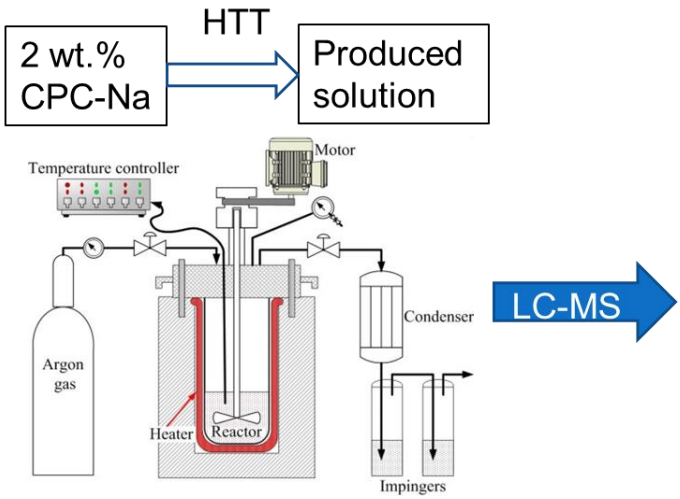

Figure 2.6. Procedure of antibiotic decomposing test by the hydrothermal treatment

There are so many organic species identified by Liquid chromatography–mass spectrometry (LC-MS) (Thermo Fisher Scientific, Q Exactive) in ABR and their liquid products after HTT, which made it hard to identify important intermediate and final products from HTT of cephalosporin C (CPC). Thus, it is almost impossible to determine its possible degradation pathway during HTT, and a solution with 2 wt.% cephalosporin C sodium (CPC–Na) was used to simulate the degradation process of remaining antibiotic matters during HTT of ABR. As shown in Figure 2.6, in order to test the behavior of the antibiotic in the HTT process, CPC-Na solution was treated by HTT under the condition of 180 ℃ for 30 minutes. The solution before and after HTT were then detected by the LC-MS to indentify the major chemical species in the liquid. The same separation conditions as the Agilent HPLC analysis were employed for the LC–MS analysis to ensure the similar retention times for the measured chemical

species contained in the objective products. The MS adopted the electrospray ionization (ESI) method to produce molecular ions.

2.3. Results and discussions

2.3.1. Effect of hydrothermal treatment on dewaterability of antibiotic bacterial residue

When ABR samples were dropped into the bottles shown in Figure 2.7, the fragment of solid ABR was floating in the bottles at the beginning. Because of gravity, particle settled down as the time went by. By pouring the upper part liquid, the liquid and the solid can be separated easily without consuming a lot of energy. The value of volume ratio of upper liquid part to lower solid part can reflect the sedimentation performance of the residue. For the same residence time, a larger value means better sedimentation performance.

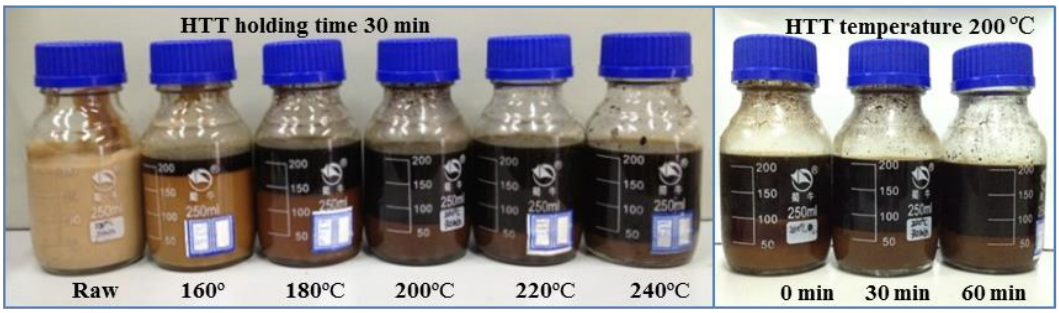

Figure 2.7. The sedimentation performance of samples obtained from different hydrothermal treatment conditions

In Figure 2.7, it can be seen that after the same residence time (24 hours), the sedimentation performance of ABR samples was different for different HTT conditions. For raw ABR, the fragment seems to be stable that no sedimentation phenomenon could be observed after 24 hours of the residence time. But for the HTT-residues of ABR, the sedimentation performance was shown in different level as a function of the HTT operating temperature and holding time. The higher

temperature or longer holding time was, the better performance was shown. This might attributed to HTT released the pectin substance which is high in hydrophilism from the surface of the solid into the liquid part.

To remove the water in the high moisture waste, one of the economic ways is the mechanical dewatering by centrifugation. Under high rotate speed, the substance in the centrifuge will bear high centrifugal force. The solid substance will be supported by the multihole wall of the centrifuge, while the liquid part will be supported by the binding force between water and solid substance. If the centrifugal force is boosted up beyond the maximum of this binding force, the liquid part will be separated from the solid part. In this case, the liquid and solid parts will be separated. Under the same rotating speed of the centrifuge and the same operating time, the lower moisture content it reach in the sample means the better dewaterability it is. After the centrifugation, the moisture content in ABR is still too high to be fed into the combustion process. Further drying process is needed to produce dry solid fuel. In this study, the centrifuged ABR samples were dried in a hot wind blowing oven.

Figure 2.8 showed the effect of the HTT operating temperature (a) and holding time (b) on the centrifugation and drying performance of ABR. The vertical coordinate gives the moisture content (M) of the samples after the centrifugation calculated by Eq. 2.1. Relatively, the horizontal was consisted of two parts, the centrifugation and the oven drying. It can be observed that at the timing of the completion of the centrifugation, the moisture content of all the hydrothermally treated ABRs was lower than the raw ABR. The highest moisture content could be seen at around 75 wt. % in the raw ABR and the lowest moisture content was shown to be around 25 wt. % in the sample which was hydrothermally treated under the temperature of 240 ℃. Under the holding time of 30 minutes, the higher HTT operating temperature it was, the lower moisture content was shown, meaning that HTT improved the centrifugation performance of ABR and higher temperature do

favor to the centrifugation performance. According to the Jiang's study[10], it should be caused by the broken water-holding structure of ABR after the hydrothermal process, which is conducive to further mechanical sludge dewatering.

For the oven drying, big difference could be seen between the raw ABR and the hydrothermally treated ABR. At the same drying time, the moisture content of the hydrothermally treated ABR was much less than the raw ABR. It took no more than 1 hour to be dried to 80% dry weight for them. But for raw ABR, it took 10 hours. It means that the oven drying speed of ABR was largely improved by HTT. As Namioka stated [7], the improvement in the drying process is probably caused by HTT to convert the bound water to free water. There is no big difference in the drying performance among the hydrothermally treated ABR at different HTT operating temperatures, indicating that the drying performance is not sensitive to the HTT temperature under the studied conditions. When the temperature reached 220 ℃, it seems that the drying speed of the sample was slightly slowed down compared to the sample treated under lower temperatures. And the sample treated at 240 ℃ showed prominent decreasing of drying speed compared with other hydrothermally treated samples. The explanation of this phenomenon might be the polymerization reactions of the fragments from the hydrothermal degradation [11]. The inserted picture in Figure 2.8 (a) showed the appearance of the hydrothermally treated sample at 240 ℃. Apparently, there was tar like substance formed by the polymerization reactions. This substance might show a high ability of hydrophilism that led to the elimination of the drying performance. For the improvement of the drying performance, the best HTT temperature should be 200 ℃.

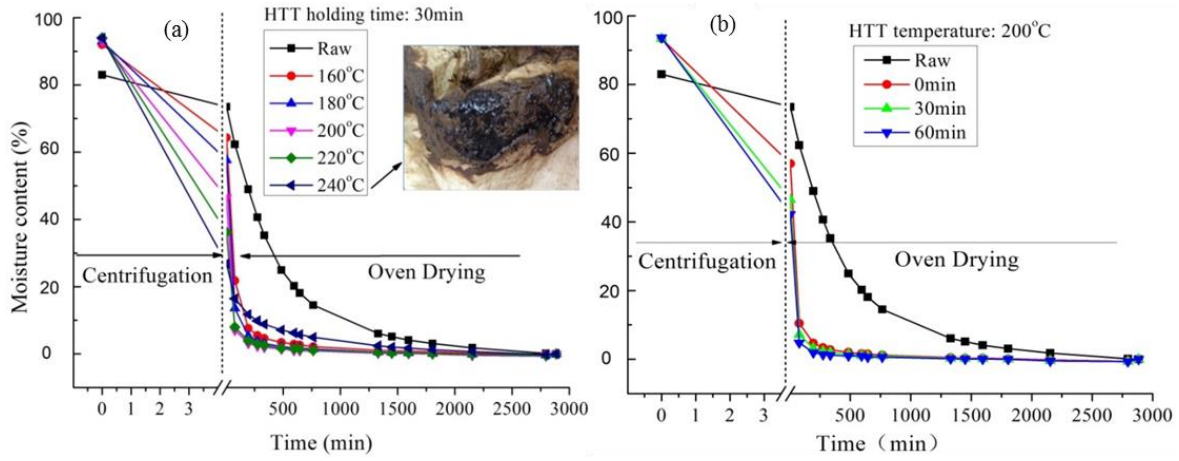

Figure 2.8. The effects of the hydrothermal treatment temperature (a) and the holding time (b) on the dewaterability of antibiotic bacterial residue

Figure 2.8 (b) shows the effect of the HTT holding time on the centrifugation and drying performance of ABR. Under the same HTT temperature of 200 ℃, the longer HTT holding time, the lower moisture content was shown, meaning that the longer holding time could boost the centrifugation performance of the bacterial residue. However, there was no big difference in the drying speed among different HTT temperatures for the treated samples. With a longer holding time, the drying speed of the sample was slightly faster. In a word, the dewaterability of ABR could be improved by HTT.

2.3.2. Effect of hydrothermal treatment on the properties of products

Properties of solid biofuels

Table 2.2 shows the properties of HTT produced solid biofuels at different temperatures and the raw dried ABR. The equilibrium moisture of the fuels shown in Table 2.2 represents the moisture content of a fuel first dried in oven and then kept at the atmospheric conditions for 48 hours. It was 5.8 wt.%, 3.6 wt.% and 2.3 wt.% for the dried ABR and HTT produced solid biofuels at 160 ℃ and 220 ℃, respectively. Thus, raising the HTT temperature can also decrease the moisture adsorption ability

of ABR. From the aspect of the solid fuel storage after drying, this is a highly desirable fuel property.

The higher heating value (HHV) of the biofuels was increased from 19.3 kJ/g for the dried raw ABR to 26.5 kJ/g for the biofuel from HTT at 220 ℃. As the HTT temperature increased, HHV of the resulting biofuels (after drying) gradually elevated, revealing that HTT improved the energy density of ABR based biofuels. The increase in the fuel heating value with raising the HTT temperature would be due to the gradual increase of the removal of oxygen and nitrogen from the solid matters of ABR during HTT. Table 2.2 shows also the lower heating values (LHVs), corresponding to HHVs, to indicate the net heating values of all the solid biofuels from HTT at different temperatures[12].

Table 2.2 Properties of solid biofuels from antibiotic bacterial residue at different HTT temperatures.†

Property parameters	Raw	160 ℃	180 ℃	200 ℃	220 ℃
Moisture (wt.%) (after centrifugation)	73.6	65.0	58.3	48.7	39.5
Moisture (wt.%)‡ (equilibrium)	5.8	3.6	2.8	2.4	2.3
Volatile mater (wt.%)	93.2	90.0	87.5	85.2	79.1
Ash (wt.%)	6.8	10.1	12.5	14.8	19.8
Fixed carbon (wt.%)	--	--	--	--	1.1
HHV (kJ/kg)	19.3	20.8	23.1	24.6	26.5
LHV (kJ/g)	16.7	18.6	21.0	22.6	24.4
C (wt.%)	43.5	47.1	51.2	53.3	55.1
H (wt.%)	6.7	6.5	6.4	6.6	6.7
N (wt.%)	7.7	6.3	6.2	5.8	5.6
O (wt.%)	42.1	40.1	36.2	34.3	32.6

a.† Element contents are based on dry-ash-free basis and the others on dry basis.
b.‡ It is the moisture after keeping the oven-dried biofuel in air for 48 h.

The biofuels from raw and HTT treated ABR mostly had high content of volatile matters (VM) but zero fixed carbon (FC) except for the 220 ℃ HTT produced solid

biofuels. HTT at the higher temperature tended to decrease the volatile matters content (from 93.2 wt.% to 79.1 wt%) and raise the ash content (from 6.8 wt.% to 19.8 wt.%) in the HTT produced solid biofuels. For the fuel from 220 ℃ HTT, an fixed carbon content of 1.1 wt.% appeared, indicating a light degree of carbonization to the carbonaceous matters [11]. Thus, degradation reactions such as hydrolysis, dehydration and decarboxylation definitely occurred during HTT to result in devolatilization. The higher the HTT temperature, the more severe the degradation reactions, resulted in lower volatile but higher ash contents in the fuels.

Table 2.2 shows that the oxygen (O) content in the HTT produced solid biofuels gradually decreased from 40.1 wt.% to 32.6 wt.%, whereas the carbon (C) content gradually increased from 47.1 wt.% to 55.1 wt.% with raising the HTT temperature from 160 ℃ to 220 ℃. These variations in the element composition corresponded actually to the gradual increase of HHV and LHV. Thus, we can view HTT as a process to upgrade ABR for solid biofuel. HTT also reduced the nitrogen (N) content in the solid biofuels from 7.7 wt.% in the raw ABR to 5.6 wt.% in the 220 ℃ HTT produced solid biofuel, and the higher HTT temperature led to the lower N content.

From the results of the X-ray fluorescence shown in Table 2.3, the relative concentration for most of the metals in the form of oxides and phosphor, sulfur, and chlorine element in ABR and the HTT produced solid biofuels can be determined. One severe problem for fuel combustion is that the hazardous metals contenting in ash. However the interesting finding was that the concentration of hazardous heavy metals in the samples was low as undetectable except for a trace of nickel and strontium which even was undetectable in ABR and in low temperature HTT produced solid biofuels. Hence, there is no need to concern about the heavy metal emission while utilizing this ABR based fuels which should be considered as a critical problem in coal combustion.

The relative concentration of the alkalis metal of sodium and potassium was reduced by HTT as a function of the temperature. In addition, the sulfur and chlorine concentrations also showed a great reduction trend where sulfur concentration was reduced from 7.36 wt.% to 2.63 wt.% and the chlorine relative concentration was reduced from 0.34 wt.% to 0.08 wt.%. The higher HTT temperature, the lower concentration of them can be observed. It can be stated that HTT had desulfurization and dechloridation effect on ABR. Therefore, the conceivable corrosion problem for the combustor led by alkalis, acid salts in ABR will be receded after HHT by removing these elements. Furthermore, organic sulfur and chlorine in the fuels is the precursor of severe pollutants such as SOx, dioxin. In this viewpoint, the desulfurization and dechloridation effect is very positive performance to upgrade ABR by HTT. The most prominent existing metal is calcium, which sources from calcium salt adding during the antibiotic cephalosporin production process. It had been proven by the previous researcher that Ca^{2+} has a positive effect on the dewater ability of biomass by the thermal hydrolysis reaction [13]. The concentration of magnesium and calcium who act a promoting effect to resist the corrosion of the furnace wall showed a trend of increasing after HTT. Besides, the concentrations of aluminum and silica were decreased due to their forms of solvable ion in ABR resulting in being dissolved into the water then removed. On the contrast, the heavier metal iron seems to be condensed in the residue.

Table 2.3. XRF analysis of ashes for biofuels from antibiotic bacterial residue at different hydrothermal treatment temperatures.

Metal(wt.%)	raw	160 ℃	180 ℃	200 ℃	220 ℃
Na_2O	1.6	0.8	0.6	0.4	0.3
MgO	1.2	0.8	1.0	1.8	2.2
Al_2O_3	0.3	0.1	0.1	0.1	0.1
SiO_2	0.8	0.4	0.3	0.2	0.2
K_2O	4.8	1.8	1.2	0.8	0.6
CaO	60.3	81.0	79.3	70.5	66.0
MnO_2	--	--	0.1	0.1	0.1
Fe_2O_3	0.6	0.7	0.7	1.0	1.2
ZnO	0.1	0.1	0.1	0.1	0.2
SrO	--	--	0.1	0.1	0.1
P_2O_5	12.0	6.3	8.2	17.9	22.4
SO_4	18.0	7.8	8.2	6.9	6.6
Cl	0.3	0.2	0.1	0.1	0.1

Properties of liquid products

Figure 2.9 shows the COD concentration in the liquid from centrifugation (centrifugate) from different HTT conditions. By increasing the HTT temperature from 180 ℃ to 200℃, the COD concentration increased for all the samples with different HTT holding times. For instance, it was around 200g/L to 225g/L at the zero holding time. By increasing the HTT holding time, the COD concentration were significantly elevated by around 50% from 200g/L to 300g/L for the 200℃ HTT. During HTT, the hydrolysis of the organic substance or so called depolymerization will decompose the particle of the solid matter into smaller size particles[14]. The higher temperature and longer holding time will obviously enhance the hydrolysis reaction. As a result, the higher temperature and longer holding time will help the solid ABR dissolve into liquid or become smaller particles and go into the centrifugate from the filter during the centrifugation. Such a high COD make the centrifugate high potential to be a good feedstock after diluted for biogas production by anaerobic digestion.

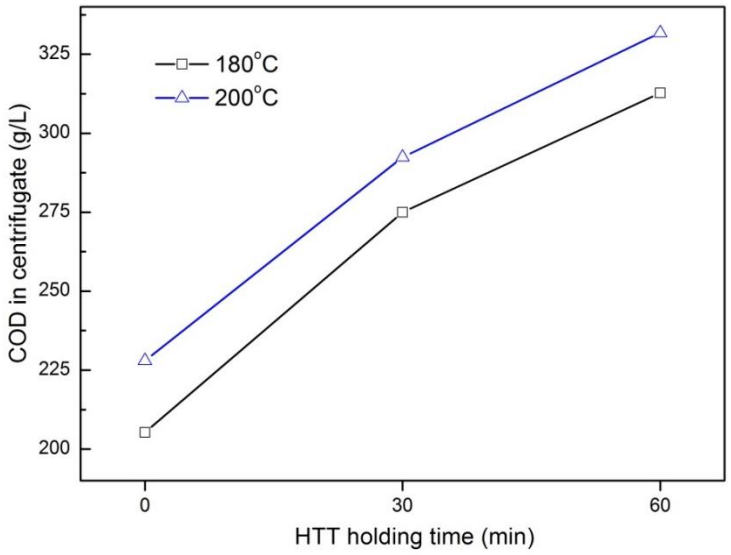

Figure 2.9. COD of the centrifugates from different HTT conditions

The pH value and the nitrogen concentration in the liquids are shown in Figure 2.10. After HTT, the pH value in the centrifugate increased and it kept increasing as the HTT temperature raised up from 160 ℃ to 240 ℃. The longer holding time also can boost the increase of the pH value. This can be explained by the hydrolysis of protein [15] in HTT that will produce ammonia which is basic gas that increased the pH value. This can be further verified by the NH_4^+ concentration especially it appeared a higher value as the temperature going up or the HTT holding time becomes longer. The ammonia in the condensed liquid should be attributed to the ammonia gas escaped from the reactor in the exhaust gas. Due to the escaped ammonia gas from the reactor, the NH_4^+ concentration in the centrifugate (red line) showed a drop trend after the HTT with the temperature higher than 200 ℃. The jumping in the NH_4^+ concentration in centrifugate or condensed liquid at 160 ℃ or 220 ℃ might be due to the uncertainty of the operating process. Therefore, the total amount of the N in the liquids but not only its concentration should be considered.

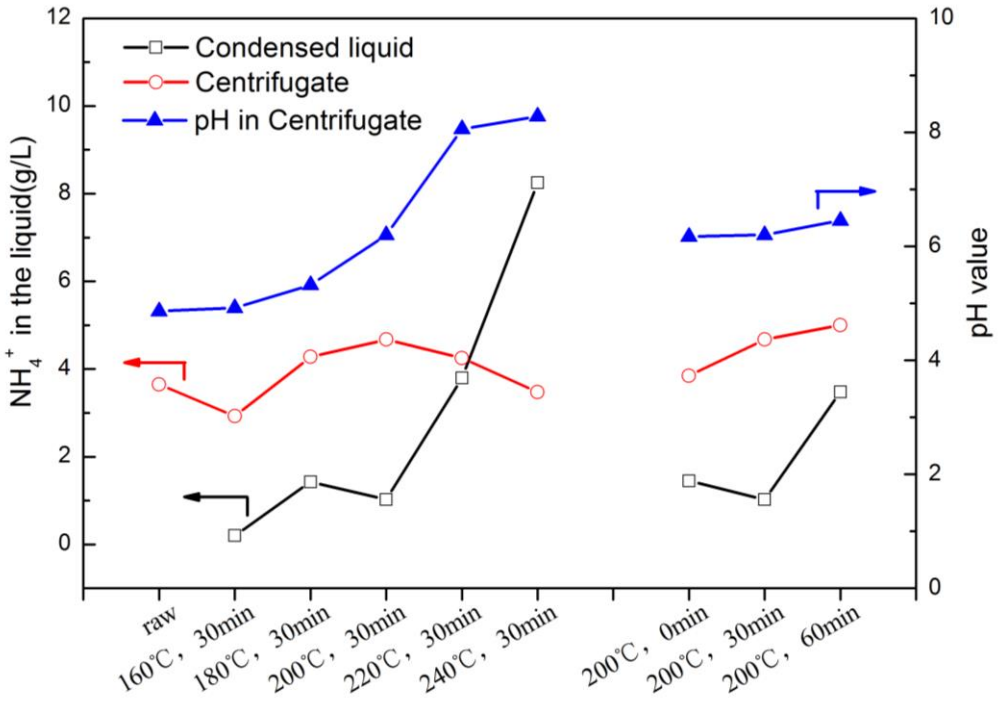

Figure 2.10. Effect of hydrothermal treatment conditions on the ammonia concentration and pH value of the liquid products

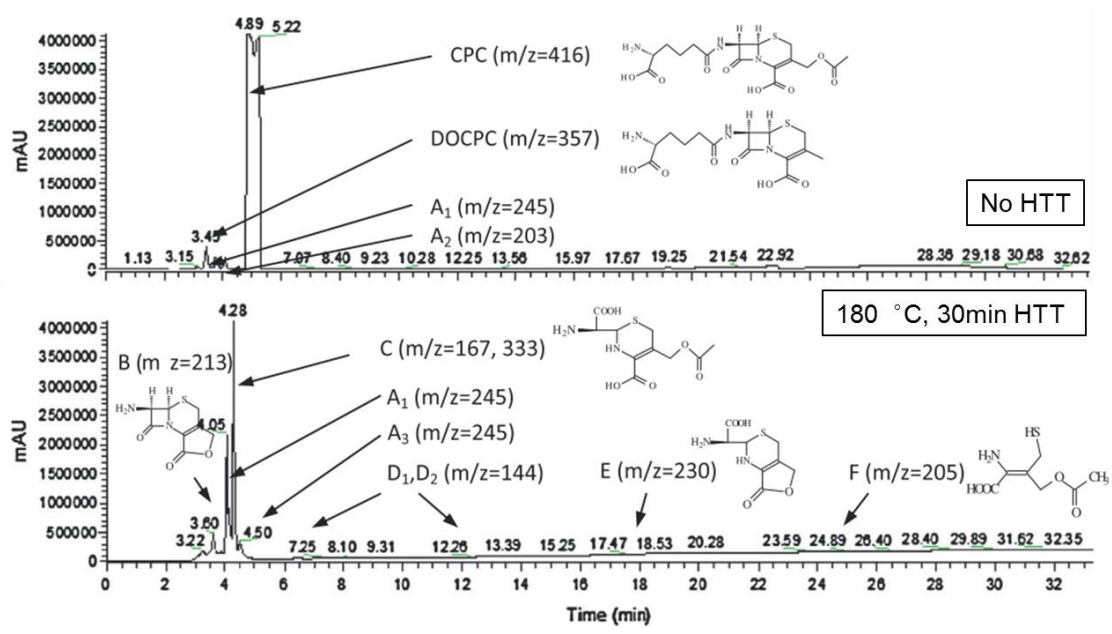

Figure 2.11. Results of LC–MS analysis for CPC–Na solution of 2.0 wt.% and its resulting solution after HTT at 180 ℃ for 30 min.

Figure 2.11 presents the LC–MS spectra for the CPC–Na solution before and

after HTT. For CPC (molecular weight, 415), its LC retention time is about 5 min and its molecular ion's m/z equals to 416 after combined with one H^+ during ESI in MS detection. DOCPC (m/z = 357), a dominant intermediate product in CPC production by fermentation, was also identified at the LC retention time of about 3.45 min and its molar percentage was about 3.8% according to the percentage of its peak area to the total peak area of CPC and DOCPC. Also by the peak area percentage, a total content of about 0.06% of CPC and DOCPC was determined in the tested ABR, which indicated the potential serious environmental pollution [16, 17]. However, no obvious CPC and DOCPC peaks were detected in the solution after HTT, showing complete decomposition of the antibiotic substance in the process of HTT.

As shown in Table 2.3, after HTT of the 2 wt.% CPC-Na solution under the same conditions as those adopted for HTT of ABR, more than 99.8% antibiotics (including CPC and DOCPC) were decomposed. Besides indispensable products of small molecular organic acids from HTT of the CPC–Na solution at 180 ℃ for 30 min, the recognized species by LC–MS mainly included the followings: (1) D-a-amino adipic acid, the common side chains of CPC and DOCPC, which is harmless and exists in corn cob and is usually used as one of the fermentation substrates for CPC production, (2) the products from deacetylation (followed by lactonization) and b-lactam ring opening of 7-ACA, backbone structure of CPC, and (3) their derivatives, as shown in Fig. 8b. Since the inhibition effect of b-lactam antibiotics on bacteria comes from their unique b-lactam ring and stereoscopic carboxyl structure attached to C2 in the thiazine ring, all the recognized species lost their antibacterial properties (see Figure 2. 10).

Table 2.3. Decomposition percent of CPC by hydrothermal treatment under different conditions

HTT conditions	Decomposition ratio of CPC（%）*
100 °C, 30min	99
133 °C, 30min	99.5
160 °C, 30min	99.8
180 °C, 0min	99.8
180 °C, 30min	99.9
180 °C, 60min	99.9
200 °C, 30min	99.9
220 °C, 30min	99.9

*. The percentage of the total area of CPC and DOCPC peaks in LC spectrum of the HTP solution to that of the original CPC–Na solution.

Only trace amount of potentially harmful compounds left in HTT liquid, showing that HTT provides thorough safe disposal for ABR. Surprisingly, the 30 min HTT at temperatures of 100 and 130 ℃ allowed the decomposition of antibiotics by 99.0% and 99.5%, respectively (see Table 2.3). This means that the milder HTT conditions are also effective for the innocent treatment of ABR.

2.3.3. Fundamental understanding on hydrothermal treatment of antibiotic bacterial residue

The above results primarily demonstrated that it is feasible to upgrade the mycelial residue by HTT for solid fuel production. In order to investigate the chemical modification in the samples by HTT, further discussion was conducted in the following statement.

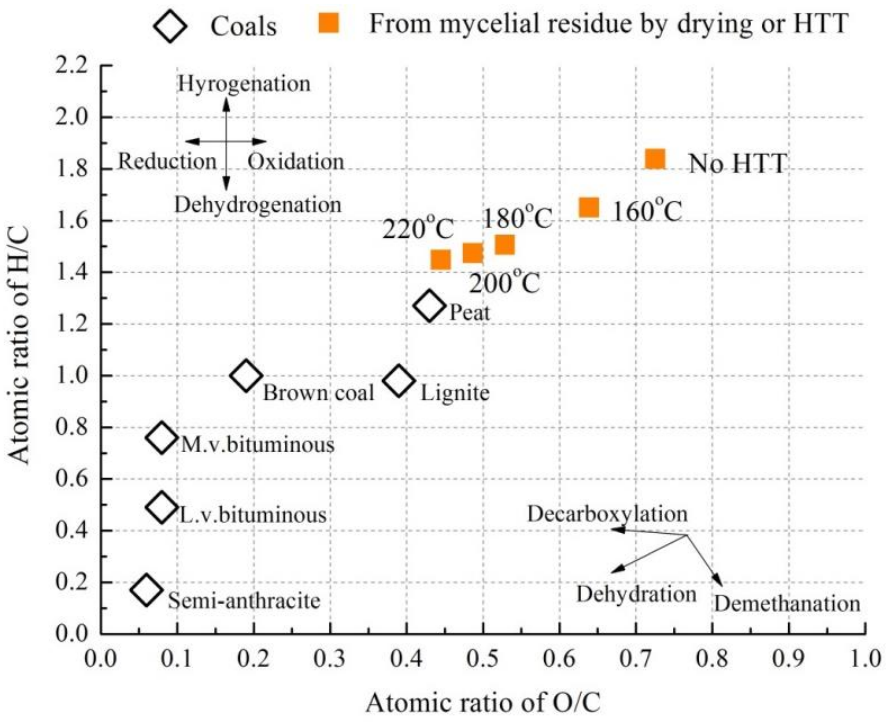

Figure 2.12. Coalification of mycelial residue during HTT[18]

Figure 2.12.shows the coalification trend of raw dried ABR and HTT ABR. The horizontal coordinate is the atomic ratio of oxygen to carbon and the vertical coordinate is the atomic ratio of hydrogen to carbon. For comparison, several coals [18] were also shown in the figure. As the temperature of HTT increased, the atomic H/C and O/C ratios of HTT ABR decreased. The atomic H/C and O/C ratios of solid biofuel produced at 220 ℃ were similar to the selected peat coal. Soaking in the high pressure and high temperature water, the pectin substances of ABR, which are abundant in oxygen and hydrogen, were removed from the surface of the noumenon fragment, resulting in massive loss of oxygen and hydrogen. Besides, the reduction and dehydration reactions during HTT could be considered as another force to reduce oxygen and hydrogen, where mainly hydrolysis and dehydration reactions occurred. With the temperature going up, a minor reaction of decarboxylation of the noumenon boosted the loss of oxygen, according to the previous studies [19]. This phenomenon implies that HTT has an interesting coalification effect on ABR in the viewpoint of atomic ratio of carbon, hydrogen and oxygen in which the evolution of biomass to

peat takes hundreds of years whereas HTT can achieve this process in hours. Ones can see that by setting the temperature higher than 180 ℃, the change of the atomic ratio of the solid products was much less than that at the lower HTT temperature (160~180 ℃), which means that the dehydration level increased faster at a lower temperature. As a result, the LHV increase was significant by increasing the HTT temperature from 160 to 180 ℃ (18.6~21MJ/kg) but was less significant when the HTT temperature was raised from 180 to 200 ℃ (21~24.4MJ/kg). Therefore, it is better to choose HTT temperature higher than 180 ℃ but not higher than 200 ℃ in the viewpoint of solid fuel upgrading.

As shown in Figure 2.13, the proportion of the solid-N in ABR based fuels was substantially decreased as the HTT temperature increasing from 66.8% for raw ABR to 19.0% for 220 ℃ hydrothermally treated ABR. However, the decreasing trend tended to be slower when the HTT temperature reached 200 ℃. This part of the nitrogen will be act as fuel nitrogen if the solid part is dropped to a thermochemical process as solid fuel. Correspondingly, the proportion of nitrogen in the liquid was increased as a function of the HTT temperature. Even the proportion of NH_4^+ in the liquid phase was increased, the ratio of K-N to NH_4^+ in the liquid phase was increased by increasing the HTT temperature. Besides, the proportion of the gas-N was increased slightly as the HTT temperature going up from 0% for 160 ℃ treated sample to 2.8% for 220 ℃ treated sample. The nitrogen distribution of the samples from various holding time was also shown in Figure 2.13. The longer holding time seems to be in favor of the conversion of solid-N to liquid-N and gas-N. Solid-N was mainly consisted of organic amide that was dissolved into liquid part becoming K-N during HTT due to the degradation of the big molecules into small ones [11]. At the same time, the K-N was converted to inorganic NH_4^+ and NH_3 gas [20]. The NH_3 gas was the gas-N. The HTT temperature and the holding time both boost the conversion path abovementioned.

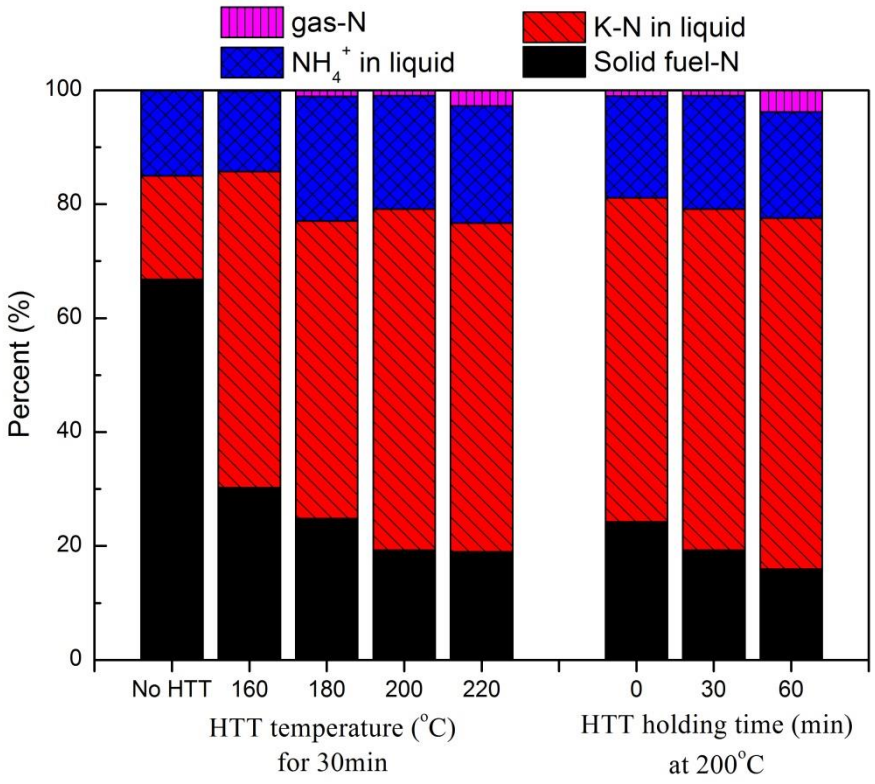

Figure 2.13. The effect of hydrothermal conditions on the nitrogen percentage distribution

The analysis by XPS has been used to determine the functional groups of carbon and nitrogen in coal and biomass chars in many literature studies [20, 21]. Figure 2.14 (a) and (b) show respectively the XPS spectra of carbon [C 1s in (a)] and nitrogen [N 1s in (b)] for the dried raw ABR and 220 ℃ and 30min HTT-ABR. The detailed information of the C 1s and N 1s curves was obtained by curve fitting function. Every deconvoluted peak (blue curve) typifies a specific bond of the element. The two inset tables in Figure 2.14 summarize the detailed characteristics of the deconvoluted peaks for the displayed C 1s and N 1s spectra, respectively. There, each area percentage was estimated as the area of the cited peak divided by the sum of the areas for all deconvoluted peaks.

In Figure 2.14 (a), the deconvoluted peaks centering at the binding energies (BEs) of 284.8 eV, 285.5 eV, 286.3 eV and 288.0 eV are respectively attributed to the C-C or C-H bonds, carbon in connection with amide or amine (C-N), carbon linking to

hydroxyl or ether groups (C-OH/C-OR) and carbon in carbonyl or quinonyl groups (C=O) [20]. By HTT, the percentage of the areas for all peaks representing C-OH/C-OR related to carbon and oxygen was greatly lowered from 21.7% to 8.4% due to the occurrence of dehydroxylation and decarbonxylation reactions. On the other hand, the area percentage of C-C and C-H increased from 64.9% to 80.3%. This result is also consistent with the results of ultimate analysis shown in Table 2.2.

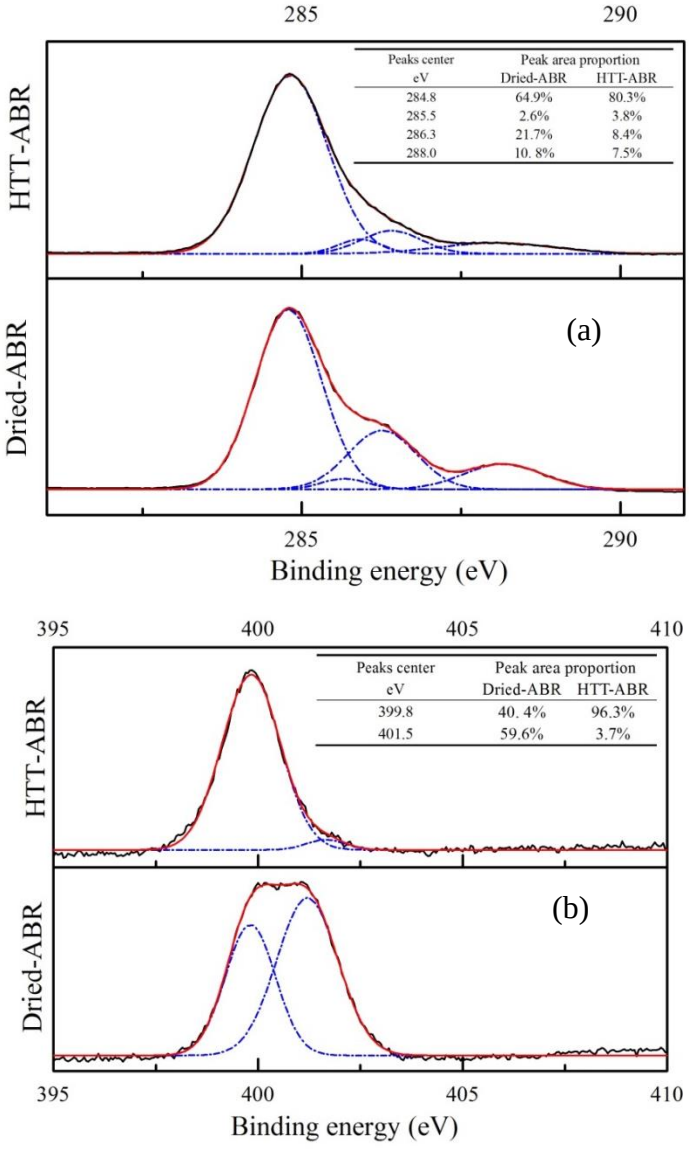

Figure 2.14. Spectra of XPS analysis for (a) C 1s and (b) N 1s of solid biofuels from HTT at 200 ℃ for 30min and directly drying raw antibiotic bacterial residue.

When the nitrogen functional groups are taken into account in the N 1s spectra of

Figure 2.14 (b), two fitting peaks at BEs of 399.8 eV and 401.5 eV can be observed. They might represent amide or amine (399.8 eV) and ammonia or protonated amine (401.5 eV), respectively [20, 21]. Theoretically, hydrolysis reactions occurring in HTT would degrade protein and amino acid into solvable smaller chain molecules. Some kinds of these molecules could even easily protonated in the presence of hydronium and hydroxide ions. All of these matters are likely to enter the aqueous phase, as was observed in the previous study[11, 15]. In Figure 2.14 (b), the area percentage of the deconvoluted peak at BE of 401.5 eV decreased from 59.6% for raw ABR to 3.7% for the HTT produced solid biofuel, indicating actually the dissolution of amine protonation and ammonia. This correspondingly increased the relative ratio of amide or amine in the solid biofuels from 40.4% in the raw ABR to 96.3% in the 200 ℃ HTT-ABR. The result agrees well with the reports of Liao [21] and Zhao [20] obtained in characterizing the sewage sludge after HTT, and also verifies the N content variation shown in Table 2.2 for different solid biofuels.

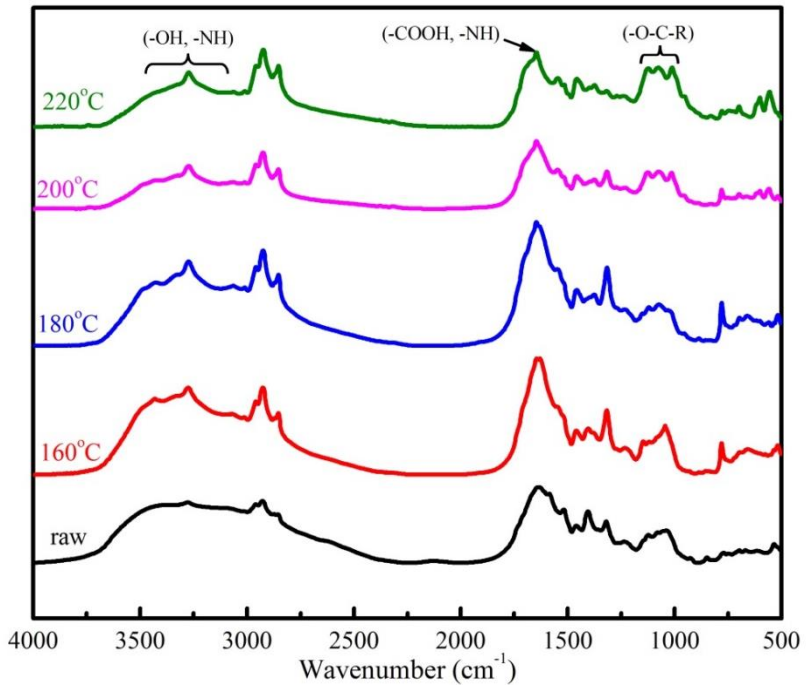

Figure 2.15. FTIR spectra of the dry antibiotic bacterial residue and its hydrothermally treated residue

Figure 2.15 presents the FTIR spectra of dried raw ABR and HTT-ABRs at

different HTT temperatures. There are many irregular and complex absorption peaks, indicating the complicated composition of ABR. Performing HTT incurred some changes in the FTIR adsorption peaks, although the changes were not tremendous. The shoulder around 3200 cm^{-1} to 3700 cm^{-1}, which is supposed to be the overlapping peaks of hydroxyl and amino groups, was overall weakened after HTT especially at 200 ℃ and 220 ℃, indicating the decrease of hydroxyl groups in the solid biofuels due to the dehydration[11]. The peak intensity at about 1650 cm^{-1} tended to be weaker with raising the HTT temperature from 180 ℃ to higher values, revealing the removal of carboxyl groups through the hydrolysis. The IR adsorption spectra in 1270-980 cm^{-1} typify the C-O-R groups to indicate especially the presence of pectin consisting of monosaccharides, polysaccharides or celluloses in raw ABR [22]. HTT tended to simplify the FTIR spectra in this region, showing the removal of carbohydrate components through dehydration and hydrolysis reactions.

2.3.4. Mass and energy recovery in the solid fuels

Figure 2.16 gives the solid recovery from ABR in the different HTT conditions. The case of dried basis raw ABR amount was considered as 100%. Then the absolute mass of the dried basis HTT ABRs dividing the dried raw ABR will be the solid recovery. It can be seen the highest recovery appeared at HTT at 160 ℃ for 30 minutes, as high as 49%. As the HTT temperature or holding time increased, the solid recovery decreased eventually. Thus the lowest recovery is for HTT at 240 ℃ for 30 minutes as 35.4%. It corresponded well with the COD concentration results which can be explained that HTT dissolve some fraction of the solid substance in ABR and the higher temperature and longer holding time will boost this process by enhancing the hydrolysis, dehydration reaction of the protein, sugars, etc[15]. This observation implies that the HTT temperature and holding time should not be too high or long for keeping a certain high recovery.

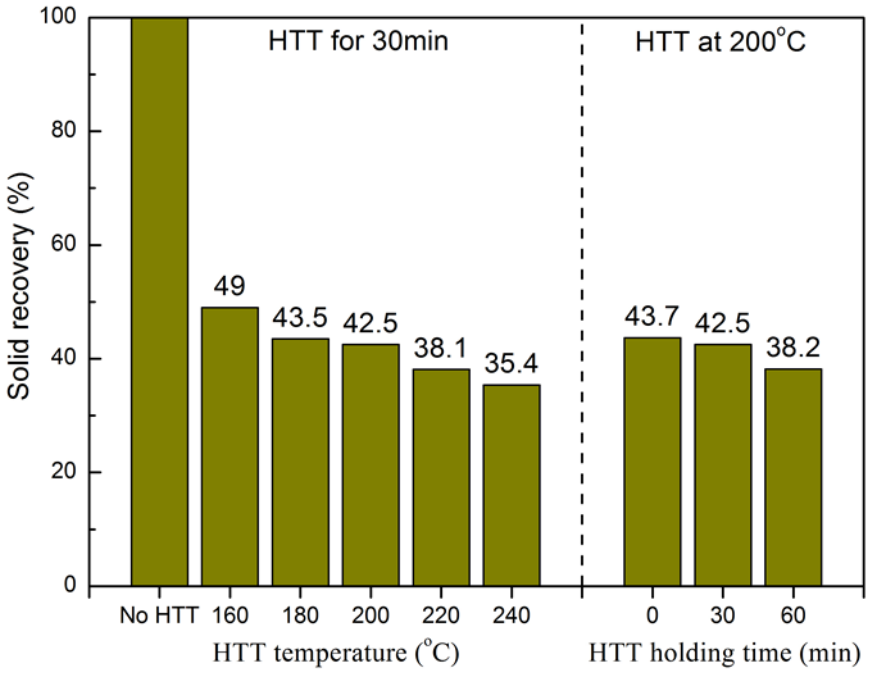

Figure 2.16 Mass balance of solid ABR and liquid

Figure 2.17 shows the energy recovery ratio in the HTT produced solid biofuel under different temperatures. The recovery ratio was assigned to be 100% for the case of raw antibiotic mycelial dreg, and the recovered energy for each HTT temperature was obtained multiplying the mass and LHV of the HTT produced solid biofuels. The figure shows that via HTT, above 55% of the energy antibiotic mycelial dreg can be recovered in the solid biofuels. Increasing the HTT temperature from 160 ℃ to 200 ℃ did not much vary the energy recovery ratio. With hydrolysis during HTT, a small part of organic matters are converted into gases (mainly CO_2 and vapor), while some others are dissolved into the liquid phase[15]. Although the increasing of HTT temperature did not much change the energy recovery ratio as shown in Figure 2.17, it considerably elevated HHVs of the resulting solid biofuels, as shown in Table 2.2. This means that raising the HTT temperature decreased the recovered amount of solid biofuels but increased HHV at the same time. Thus, at the optimal HTT temperature about 200 ℃, the relatively high HHV of the HTT produced solid biofuel can be ensured.

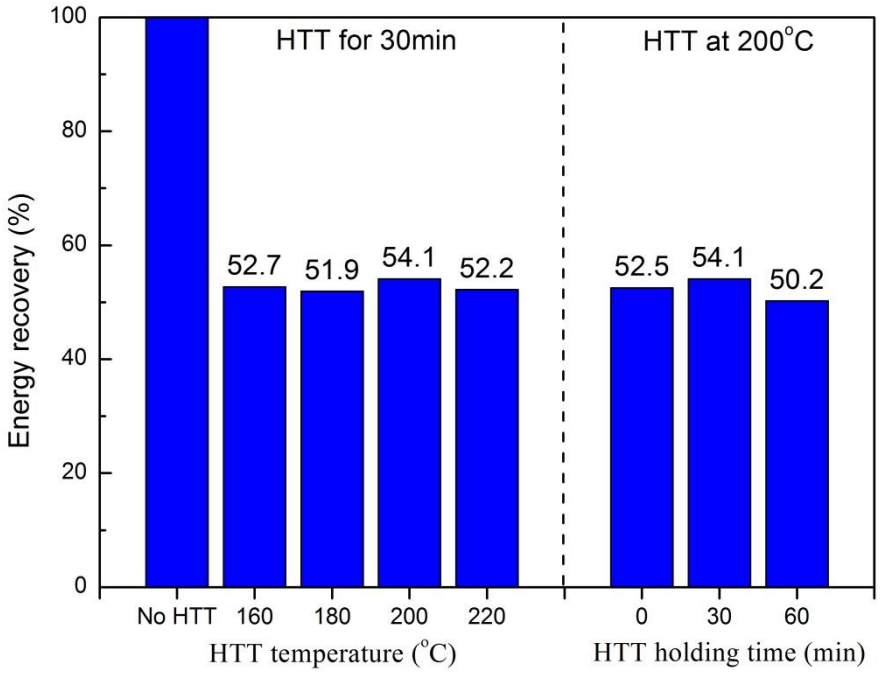

Figure 2.17. Energy recovery by HTT in the solid fuels

2.4. Conclusions

In this chapter, the antibiotic bacterial residue (ABR) was subjected into an autoclave reactor to primarily investigate the feasibility of solid fuel production from it by HTT. The effect of HTT on the properties of the solid fuel products and aqueous products was revealed and discussed. The fundamental understanding of HTT of ABR was discussed based on the characterization of the solid and liquid products. Finally, the solid recovery and energy recovery from ABR by HTT were determined. The findings are concluded as follows.

1) The dewaterability of ABR was significantly improved by HTT in term of the sedimentation performance, the dehydration and the drying. The improvement depends not much on the HTT operation temperature or holding time. The higher temperature or longer residence time will boost better dewaterability. After HTT temperature up to 220 ℃, the drying performance of the residue will be weakened. Therefore, the best condition for ABR dewatering should be around 200 ℃. HTT

can also restrict water adsorption of solid matters in ABR. The reason should be due to HTT enhances the hydrolysis of the pectin substance, which is high in oxygen and has strong hydrophilism in ABR.

2) HTT of ABR is accompanied with some loss in volatile matters and certain increase in ash content, HHV of the resulting solid biofuel was increased by 37% (19.3 kJ/g to 26.5 kJ/g) and LHV was elevated by 46% (16.7 kJ/g to 24.4 kJ/g) through HTT at 220 ℃ in comparison with the directly dried raw ABR. Both XPS and FTIR analyses of the HTT produced solid biofuels revealed that the increase in the heating value was mainly due to the HTT-accompanied reactions including dehydration, dehydroxylation, decarbonylation and decarboxylation occurring to the organic matters which lowered the oxygen content of the solid biofuel. In the view point of the heating value upgrading, the HTT temperature should be higher than 180 ℃. Nitrogen content in the solid matters of ABR was found to be reduced by 27 % (7.7 wt% to 5.6 wt.%) through HTT at 200 ℃, as a result of hydrolyzing protein or amino acid. Corresponding to this, more than half of the N in the dried raw ABR (solid-N) was transferred into the HTT centrifugate to become Kjeldahl nitrogen (K-N).

3) The COD of the centrifugate was quite high as over 200g/L which due to the strong dissolution of the solid matter into the aqueous phase. Due to the decomposition of effect of HTT on the antibiotic substance shown by the model solution, it can be expected that HTT is really suitable to confirm the safe disposal of the hazardous ABR. In the viewpoint of high COD and low antimicrobial effect by antibiotics, the liquid product is anticipated to be suitable for the biogas production by anaerobic digestion.

4) Solid fuels produced from ABR by HTT can give a mass recovery to 35% to almost 50%. The higher HTT temperature showed lower recovery due to the stronger dissolution effect of HTT on ABR. However, as the higher HTT temperature will increase the heating value of the produced solid fuels, the

interesting finding is that all the energy recovery from ABR to in solid fuels by HTT showed higher than 50%. And the best HTT condition in the view point of energy recovery is 200 ℃, 30 minutes. It was same as the best condition for the improvement of the dewaterability.

5) The most proper HTT temperature for solid fuel production from ABR would be 180 ℃ to 200 ℃ based on the consideration of improvement in dewaterability and heating values of the solid fuels.

References

[1] Zhao P, Shen Y, Ge S, Chen Z, Yoshikawa K. Clean solid biofuel production from high moisture content waste biomass employing hydrothermal treatment. Applied Energy. 2014;131:345-67.
[2] Prawisudha P, Namioka T, Yoshikawa K. Coal alternative fuel production from municipal solid wastes employing hydrothermal treatment. Applied Energy. 2012;90:298-304.
[3] Lu L, Namioka T, Yoshikawa K. Effects of hydrothermal treatment on characteristics and combustion behaviors of municipal solid wastes. Applied Energy. 2011;88:3659-64.
[4] He C, Giannis A, Wang J-Y. Conversion of sewage sludge to clean solid fuel using hydrothermal carbonization: Hydrochar fuel characteristics and combustion behavior. Applied Energy. 2013;111:257-66.
[5] Zhao P, Ge S, Ma D, Areeprasert C, Yoshikawa K. Effect of hydrothermal pretreatment on convective drying characteristics of paper sludge. ACS Sustainable Chemistry & Engineering. 2014;2:665-71.
[6] Zhao P, Shen Y, Ge S, Yoshikawa K. Energy recycling from sewage sludge by producing solid biofuel with hydrothermal carbonization. Energy Conversion and Management. 2014;78:815-21.
[7] Namioka T, MOROHASHI Y, YAMANE R, YOSHIKAWA K. Hydrothermal treatment of dewatered sewage sludge cake for solid fuel production. Journal of Environment and Engineering. 2009;4:68-77.
[8] Meng D, Jiang Z, Kunio Y, Mu H. The effect of operation parameters on the hydrothermal drying treatment. Renewable Energy. 2012;42:90-4.
[9] Liang L, Sun R, Fei J, Wu S, Liu X, Dai K, et al. Experimental study on effects of moisture content on combustion characteristics of simulated municipal solid wastes in a fixed bed. Bioresource technology. 2008;99:7238-46.
[10] Jiang Z, Meng D, Mu H, Yoshikawa K. Study on the hydrothermal drying technology of sewage sludge. Science in China Series E: Technological Sciences. 2010;53:160-3.
[11] Funke A, Ziegler F. Hydrothermal carbonization of biomass: a summary and discussion of chemical mechanisms for process engineering. Biofuels, Bioproducts and Biorefining. 2010;4:160-77.
[12] Committee JIS. Coal and coke. Determination of gross calorific value by the bomb calorimetric method, and calculation of net calorific value. Tokyo: Japanese Standards Association. 2003.
[13] Neyens E, Baeyens J, Creemers C. Alkaline thermal sludge hydrolysis. Journal of Hazardous Materials. 2003;97:295-314.
[14] Fan J, De Bruyn M, Budarin VL, Gronnow MJ, Shuttleworth PS, Breeden S, et al. Direct microwave-assisted hydrothermal depolymerization of cellulose. Journal of the American Chemical Society. 2013;135:11728-31.
[15] Peterson AA, Vogel F, Lachance RP, Fröling M, Antal Jr MJ, Tester JW. Thermochemical biofuel production in hydrothermal media: a review of sub-and supercritical water technologies. Energy & Environmental Science. 2008;1:32-65.

[16] Hernando MD, Mezcua M, Fernández-Alba A, Barceló D. Environmental risk assessment of pharmaceutical residues in wastewater effluents, surface waters and sediments. Talanta. 2006;69:334-42.
[17] Dewdney J, Maes L, Raynaud J, Blanc F, Scheid J, Jackson T, et al. Risk assessment of antibiotic residues of β-lactams and macrolides in food products with regard to their immuno-allergic potential. Food and Chemical Toxicology. 1991;29:477-83.
[18] Ibarra J, Munoz E, Moliner R. FTIR study of the evolution of coal structure during the coalification process. Organic Geochemistry. 1996;24:725-35.
[19] Muthuraman M, Namioka T, Yoshikawa K. A comparison of co-combustion characteristics of coal with wood and hydrothermally treated municipal solid waste. Bioresource technology. 2010;101:2477-82.
[20] Zhao P, Chen H, Ge S, Yoshikawa K. Effect of the hydrothermal pretreatment for the reduction of NO emission from sewage sludge combustion. Applied Energy. 2013;111:199-205.
[21] Liao B, Lin H, Langevin S, Gao W, Leppard G. Effects of temperature and dissolved oxygen on sludge properties and their role in bioflocculation and settling. water research. 2011;45:509-20.
[22] 贡丽鹏, 郭斌, 任爱玲, 刘仁平, 宋汉宁. 抗生素菌渣理化特性. 河北科技大学学报. 2012:190-6.

Chapter 3 Pilot Scale Hydrothermal Treatment of Antibiotic Bacterial Residue

3.1. Introduction

In Chapter 2, the technical feasibility of solid biofuel production from antibiotic bacterial residue (ABR) by hydrothermal treatment (HTT) has been investigated in a lab scale experimental research. The mechanism of HTT on ABR was also studied. However, for the practical application of HTT for safe treatment or recycling of ABR, further studies should be done. This chapter is devoted to scaling up of HTT for ABR treatment so as to confirm the feasibility of our proposal in the pilot plant. Also, in order to reduce the energy utilization of HTT, the modification of HTT process was conducted in the pilot plant. The study boundary for this chapter is in the dotted line circle as shown in Figure 3.1. Compared to Chapter 2, steam heat supplying will be additionally included in this chapter.

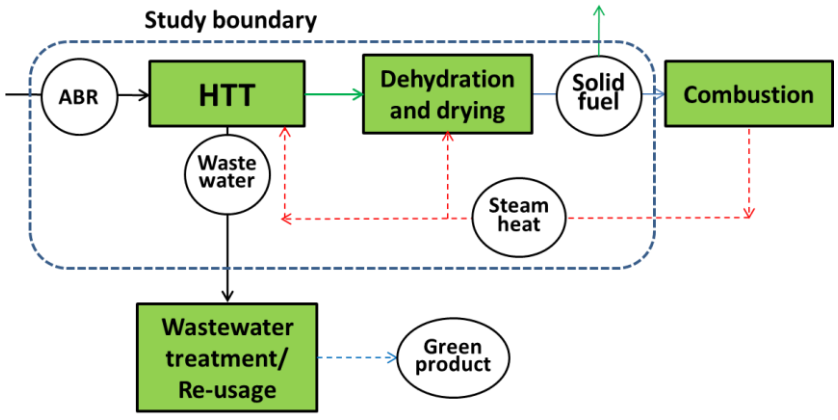

Figure 3.1. Study boundary of Chapter 3.

A set of pilot scale equipment was built up and ABR was hydrothermally treated in the pilot plant. The product properties were then analyzed and compared with the

result from the lab scale experiment. Besides, the mass balance and the energy balance for the pilot scale HTT were revealed. In order to improve the energy efficiency of HTT, material preheating process was induced. The effect of the preheating on the process was discussed in terms of the operation time, the mass balance and the energy recovery.

3.2. Apparatus and experimental methodologies

3.2.1. Pilot scale hydrothermal treatment plant and the experimental procedures

The antibiotic bacterial residue (ABR) is hydrothermally treated in a set of pilot scale apparatuses. The experimental and analysis procedure is shown in Figure 3.2 as flow chart form. Firstly, the raw ABR was treated in a hydrothermal treatment (HTT) reactor. After finishing the treatment process, the pressure in the HTT reactor was released by discharging the steam to become condensed liquid. The HTT-residue in the reactor was then mechanically dehydrated to get dehydrated liquid and dehydrated residue. After that, the dehydrated residue was dried to get the solid fuels (HTT-ABR). For comparison, the raw ABR without HTT was directly dried to obtain Dried-ABR. As products, the dehydrated liquid and ABR-based fuels were measured by a series of analytical methods.

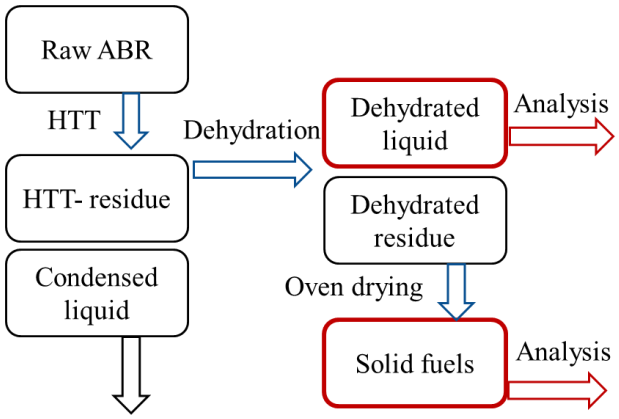

Figure 3.2. Flow chart of the pilot scale experiments

As shown in the upper part of Figure 3.3., the pilot plant for HTT mainly consists of 4 units. The main reaction in the process occurs in the HTT reactor which has a motor rotator for enhancing the mass and heat transfer. A steam boiler is used for providing the heat for the HTT reaction by supplying saturated or even over heated steam into the reactor. The material storage tank is installed for ABR that is ready for the treatment. Pressing filter is installed for separating the liquid fraction from the HTT-residue, so as to get the solid products and liquid products. The HTT reactor type used in this study was vertical, which is different from many previous studies [1-4]. In this type of reactor, the liquid will probably not immerse the axis of rotation. However, in the horizontal reactor, the axis of rotation will be at the middle of the reactor, which is obviously easy to immerse in liquid so that it leads to leakage under the high pressure and high temperature condition. Therefore, in the present study, even though the horizontal type is better for mixing the material than the vertical rotation, the vertical axis rotation was chosen, which is shown in the middle of the lower part in Figure 3.3. The steam feeding will be inserted deep into the bottom of the HTT reactor. The steam boiler and the pressing filter are shown next to the HTT reactor respectively. The specifications of the main apparatuses abovementioned are listed in table 3.1.

Table 3.1. Apparatus specification.

Main units	Boiler	HTT reactor	Pressing filter
Capacity	1ton/h	2000L	2.5m^2
Electricity using parts	Control unit, Burner, Water purifier, Pump, Draft.	Motor, Speed transformer.	Pump, Compressor, Air pump.
Electricity	2kw	13kw	5.5kw

The boiler was firstly started up to prepare steam. At the same time, a 1000w pump was used to feed the raw ABR from the storage tank into the reactor up to

around 1ton. When the steam in the boiler was over heated to reach 240℃ at the pressure of 2.4MPa, the steam valves between boiler and the HTT reactor will be opened to inject the steam into the reactor. The steam pressure, temperature and flow rate near the steam inlet of the reactor was measured and recorded continuously. The motor rotator was also started up to enhance the mixing of material and steam in the reactor. When the temperature in the reactor reached the targeted value, the steam supplying would be controlled to maintain the temperature for 15 minutes to 30 minutes. After all the reaction finished, the steam supplying and rotation were stopped. The steam in the reactor was released until the pressure in the reactor became the same as the atmospheric pressure, while the temperature was lowered down to 100℃. The HTT-residue in the HTT reactor was then discharged from the bottom by a high pressure pump to compress the residue and separate the liquid out in the compressing filter. The separated liquid was sampled for the downstream analysis. The solid part from the pressing filter was also collected and dried for the downstream analysis. The operation conditions for the pilot test are shown in Table 3.2. The test 1 and 2 were for the comparison of the different HTT temperatures. The test 3 was conducted by a modified HTT process and with shorter holding time at 15 minutes. The motor rotating speed for material mixing in the HTT reactor was kept at 100 r/min for all the experiments.

Table 3.2. Summary of experimental conditions

Test	Temperature (℃)	Holding time (min)	Sample amount (kg)	Motor speed (r/min)
1	120	30	680	100
2	180	30	1190	100
3	180	15	1187	100

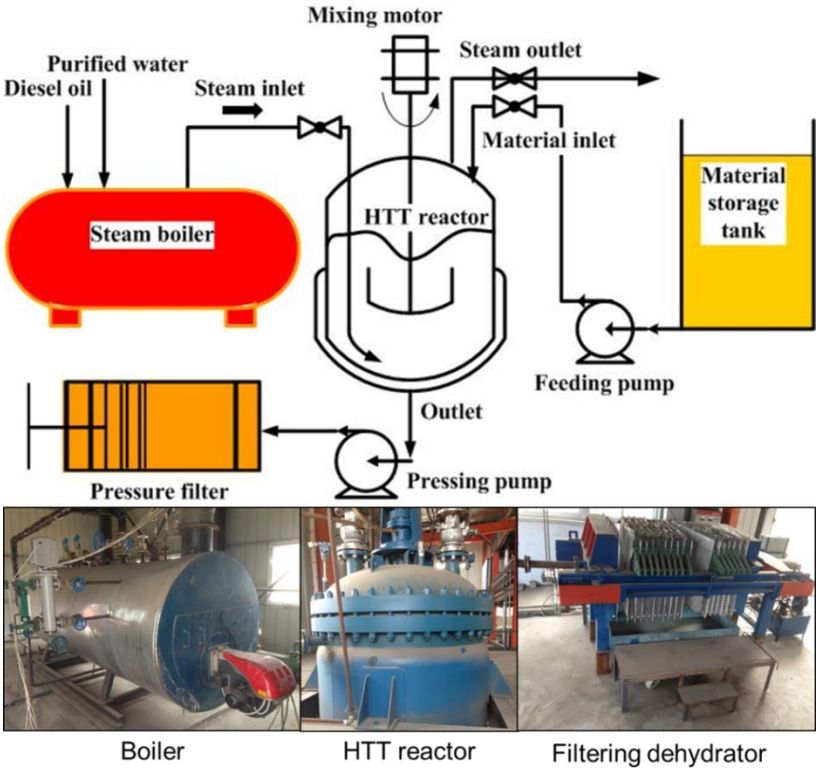

Figure 3.3. Sketch diagram and pictures of the hydrothermal treatment apparatus.

Figure 3.4 shows the key parameters for the test 1(Figure 3.4(a)) and test 2 (Figure 3.4(b)). The temperature in the HTT reactor increased as the steam supplying increased. When the temperature in the reactor reached the targeted temperature, it can be seen that the steam supplying changed so little which means the energy for maintaining the HTT reactor at a certain temperature just needs small amount of energy. Or it can be concluded that the reaction of ABR in the HTT reactor almost did not consume or release energy. Therefore, in this study, we assumed that there is no energy release or usage for the reactions occurred during HTT. After finishing the holding time at the targeted temperature, the steam in the reactor was released, which lead to the reduction of temperature and pressure in the reactor.

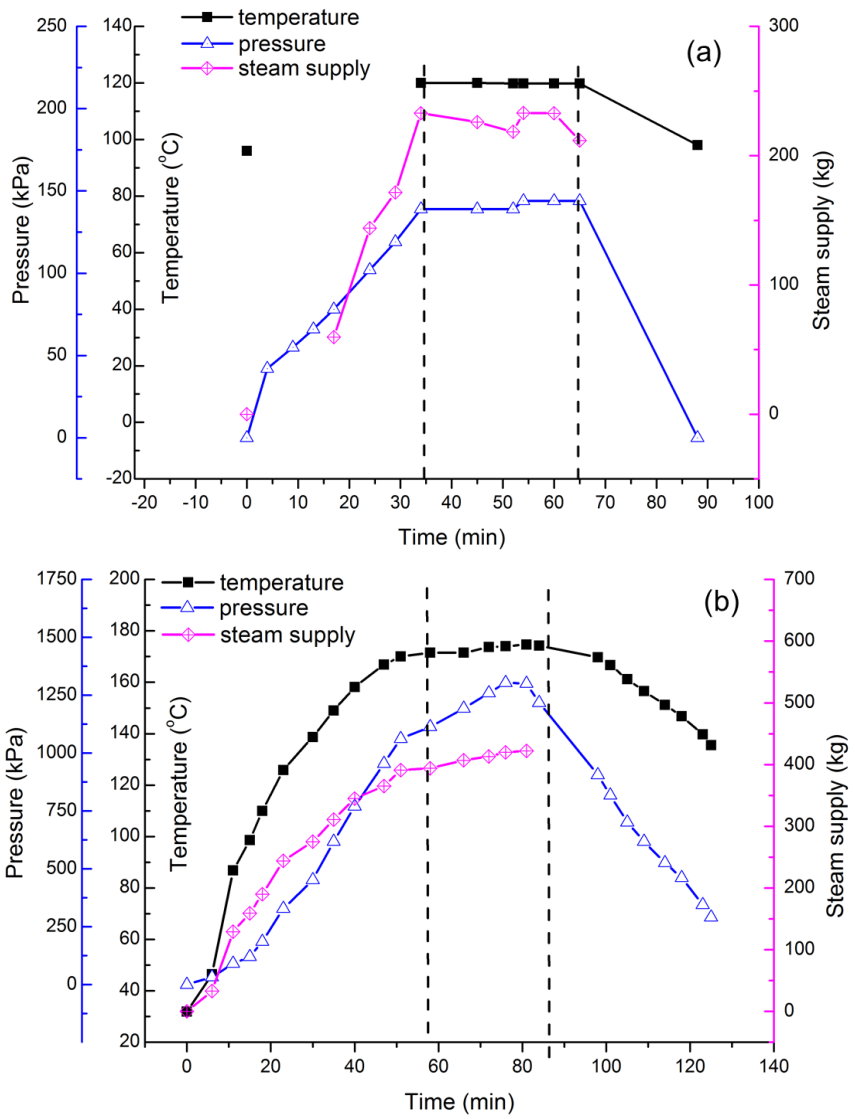

Figure 3.4. Key parameters in the hydrothermal treatment reactor for test 1(a) and test 2(b).

3.2.2. Analytical methods

The dried solid biofuels dropped from the oven drying were milled to powder by a roller crusher. In order to confirm the uniformity of the solid biofuels for the downstream analysis, the powder like samples then were sieved through a 200 m filter. The basic analysis for solid fuel such as the proximate and ultimate analyses for fuel properties (including element composition) and the oxygen bomb calorimeter (SCLR-5000) for the higher heating value (HHV) were conducted for the produced fuels.

The dehydrated liquids from the compressing filter were measured by several types of analysis. Firstly, the Chinese standard methods (GB/T 5009-2003, China) were used to measure the soluble chemical oxygen demand (SCOD) of the centrifugate. The pH value of the liquids was directly measured by a pH meter (Mettler Toledo FE20). For the nitrogen behavior in the centrifugate, the liquid was diluted proper times to conduct ammonium ion (NH_4^+) determination by the spectrophotometer directly to get NH_4^+.

The boundary for mass balance and energy balance analysis was shown in Figure 3.5, including the feeding unit, the hydrothermal treatment (HTT) unit and the dehydration and drying unit. All the energy in the form of heat thermal energy, chemical energy (fuel heating value) and electricity will be taken into account as energy. The baseline of the thermal energy calculation is chosen as the enthalpy of water at 25 ℃. At the boundary circle, it can be seen that the input mass in this system is water, diesel oil and raw ABR. The output are exhaust steam, dehydrated liquid and vapor, and solid fuel. The energy input is diesel oil in the boiler, raw ABR at feeding and the relatively small amount of electricity each unit consumes. The energy output mainly occurs at the exhaust steam and energy loss in the boiler, the heat loss from the HTT reactor and the hot liquid and solid fuel from the dehydration and drying.

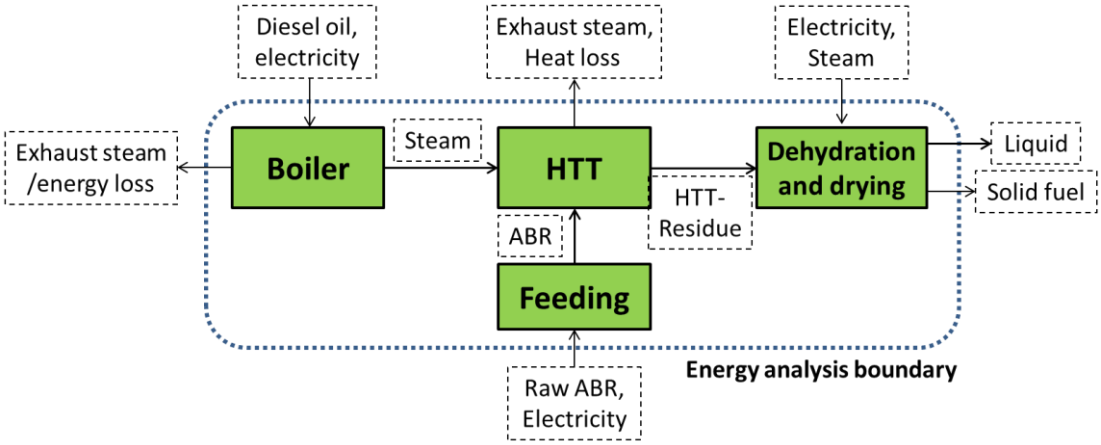

Figure3.5. Boundary of mass balance and energy balance

The energy balance analysis will be firstly focused on the HTT unit calculated by the equation from (1) to (8) including input and output terms as follow:

Input:

$$\text{Steam heat} = \sum_0^n(\text{Enthalpy (p, t)} - \text{Enthalpy(25℃)}) \times \text{Steam mass} \quad (1)$$

where the summary ranges in the steam supplying period from 0 to n; Enthalpy of steam or water can be checked from a EasyQuery enthalpy and entropy V2.6 program, p means pressure of the steam at the inlet; t means the temperature of steam at the inlet. Steam mass was measured by the steam flowmeter.

$$\text{Energy in ABR} = \text{LHV} \times \text{ABR-mass} \times (1\text{-Moisture content}) + (\text{Enthalpy (t)-Enthalpy(25 ℃)}) \times \text{ABR-mass} \times \text{Moisture content} \quad (2)$$

where LHV was lower heating value of Dried-ABR obtained from the calorific oxygen bomb; t represents the temperature of ABR.

$$\text{Electricity} = \text{power capacity} \times \text{operation time} \quad (3)$$

Output:

$$\text{Exhaust steam heat} = \sum_0^n(\text{Enthalpy (p, t)} - \text{Enthalpy(25℃)}) \times \text{Steam mass} \quad (4)$$

$$\text{Hot liquid heat} = (\text{Enthalpy (100 ℃)} - \text{Enthalpy (25 ℃)}) \times \text{liquid mass} \quad (5)$$

$$\text{Solid fuel energy} = \text{LHV} \times \text{solid fuel mass} \quad (6)$$

$$\text{Energy converted into liquid} = \text{Energy in ABR} - \text{Solid fuel energy} \quad (7)$$

$$\text{Energy loss} = \text{Steam heat} + \text{Electricity} - \text{Exhaust steam heat} - \text{Hot liquid heat} \quad (8)$$

Based on the energy balance on HTT, the systemic energy balance would be analyzed. All the electricity input was calculated by equation (3). The boiler thermal efficiency was assumed to be 80% [5]. The diesel input from the boiler can be

estimated by steam heat / 0.8. Hence, the exhaust steam heat and energy loss in the boiler will be diesel oil energy + electricity– steam heat. For the feeding, the energy input includes the energy in ABR and electricity. For the dehydration and drying unit, the energy input will be electricity and the drying thermal heat. The energy consumption for drying in the commercial plants was about 1.2 kg (steam)/kg (water) according to previous results [6]. At a lab scale (capacity, 100 kg/h), it was around 70~75% for gas-agitated double screw type dryer [7]. The thermal drying was assumed to be 83.3% in the thermal efficiency by steam drying in this study.

3.3. Results and discussions

3.3.1. Properties of the products from hydrothermal treatment of antibiotic bacterial residue

Figure 3.6 shows the appearance of ABR, the dehydrated HTT-ABR and the liquid products. Apparently, the raw ABR sample is a kind of yellow and slurry residue, which can be fed by a liquid pump. By mechanically dehydrated, ABR will become a kind of sticky sludge. By HTT under 120 ℃ for 30 minutes, the dehydrated ABR would be pieces but not like sludge, indicating the lower moisture content in the dehydrated ABR. And the color of the sample was deep brown. As the HTT temperature increased to 180 ℃, the dehydrated ABR apparently became drier sample. The color turned out to be darker than ABR and HTT dehydrated ABR with a lower HTT temperature, implying slight carbonization should have occurred which was proven by other researchers [8, 9]. The dehydrated liquid produced from HTT both showed deep brown color, indicating the organic solid substance dissolved into the liquid phase, correlating well with the result from the lab scale experiment. And the higher HTT temperature led to the deeper color of the liquids, verifying again that the higher HTT temperature will result in more organic solid substance dissolving into the liquid or lead to the carbonization of the organic component in the liquid.

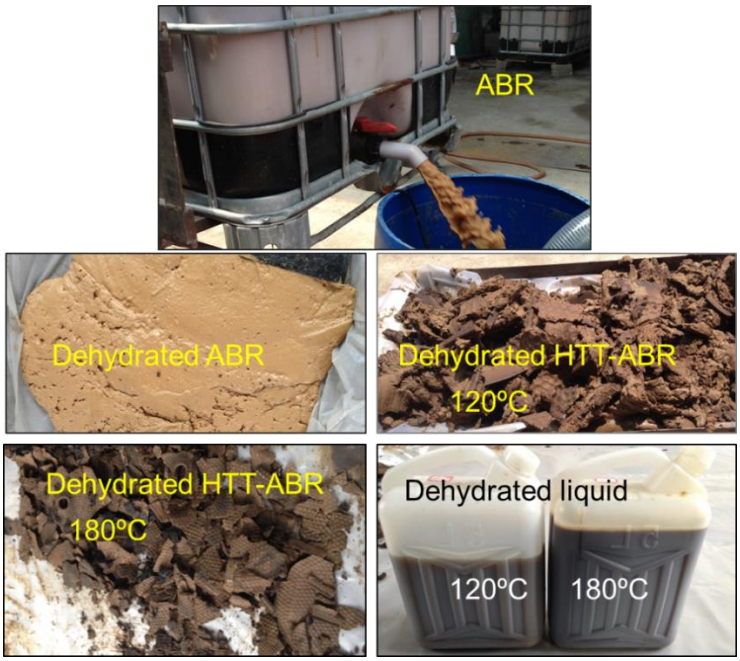

Figure 3.6. Picture of solid products

Table 3.3 shows the fuel analysis of ABR before and after HTT, reflecting the effects of different HTT conditions on the physical and chemical properties of ABR. After HTT, the produced residues were subjected to compressing filter for mechanically dewatering. The moisture content of the dehydrated samples was shown in the table to interpret the dewaterability of ABR drove from HTT under various conditions. From the results, an obvious trend of decreasing in moisture content in centrifuged samples can be observed after HTT and as the HTT temperature increased where it dropped from 75 wt.% for raw ABR to 38 to 40 wt.% for 180 ℃ treated samples, indicating that the dewaterability of ABR was improved by HTT. This phenomenon agrees well with the lab scale experiment and could be observed for other kinds of biomass material as well [1, 10, 11], which can be explained by the fact that the cell of the biomass was crashed through the hydrolysis and the low temperature pyrolysis processes then the bound water was liberated. For the proximate analysis, ABR was full of volatile matter (VM) and ash content, showing no detectable fixed carbon (FC) content. During HTT, degradation reactions occurred through the hydrolysis[9]. Simultaneously, the smaller molecules polymerized to form

big molecules then aggregated to solid fragment. In this period, the degradation is much faster than aggregation. Therefore, a de-volatilization was shown reducing the VM content in certain amount after HTT. With a higher temperature, the lower volatile mater content was shown. Correspondingly, the ash content was increased as a function of the temperature. Surprisingly, the ash contents were also significantly higher than those from the lab scale HTT experiment. This was presumed to result from the heating and mixing ways by steam supply for the pilot test, which probably led to stronger dissolution of organic ingredients in ABR than jacket heating and mechanical agitation employed in the lab scale experiments. In addition, smaller amounts of hydrogen and oxygen appeared in the solid biofuel from the pilot tests compared to those from the lab experiments, suggesting dehydration of organic matters in ABR took place to bigger extents. Deeper dehydration also resulted in the equivalent HHV of the HTT-ABRs (17.9 ~ 24.2 MJ/kg) to that of the raw ABR (25.1MJ/kg), despite that the former has a higher ash content than the latter.

When it comes to ultimate analysis, only the raw ABR and HTT-ABR at 180℃ for 30 minutes was shown in the table. It is apparent that all the samples are abundant in oxygen content and nitrogen content. Owing to the decarboxylation and dehydration of the biomass[8, 9], after HHT, the oxygen contents of ABR significantly decreased from 22.2wt.% to 12.1wt.%, and the concentration of hydrogen also became much lower. Besides, the high nitrogen content is intrinsic characteristic of ABR related to the medicine processing [12]. Since the nitrogen is the source of the fuel NOx emission, the feature of high nitrogen content is an apparently drawback of this material as bio-fuel. It is interesting that the nitrogen concentration was also dramatically reduced from 7.2 wt.% for raw material to 1.9 wt.% for HTT-ABR, indicating again that HTT has de-nitrification effect on ABR. The decreasing level in nitrogen in the pilot experiment was much higher than the lab scale experiment, which should be attributed to the difference in the heating and

mixing method in the pilot test as mentioned earlier. It could be expected that the NOx emission of the HTT-ABR based solid fuel combustion will be decreased in comparison with the raw ABR. One more difference for the pilot with the lab scale experiment was the carbon concentration was lower after HTT while the lab scale showed C content increase, this can also be explained by the fact that the increase of the ash content in the pilot test was more significant than the lab scale experiment, corresponding with the decreasing in HHV by HTT in the pilot test, thus, it implies that in the pilot scale reaction, proper mixing method and HTT temperature should be taken care of so as to reduce the dissolution of the solid.

Table 3.3. Properties of ABR-based solid fuels

HTT conditions		Raw ABR	120 ℃ 30min	180 ℃ 30min	180 ℃ 15min
Moisture in dehydrated ABR		75	52	38	40
Moisture in naturally dried ABR		-	37	21	30
Proximate analysis [a](%)	VM[a]	88.8	77.6	65.7	67.8
	Ash[a]	11.2	22.4	34.3	32.2
	FC	0	0	0	0
Heating value (MJ/kg)	HHV[a]	25.1	24.2	17.9	21.2
	LHV[b]	24.1	23.2	16.9	20.1
Ultimate analysis[a]	C	47.1		42.8	
	H	10.2		5.4	
	O[c]	22.2		12.1	
	N	7.2		1.9	
	S	2.1		3.5	

a. Dry basis, b. calculated by equation (9), c. calculated by difference.

The pH value of the dehydrated liquid from the pressing filter was slight decreased (see Table 3.4) to 5.07 from 5.50 for the raw ABR, corresponding to generation of a certain amount of organic acids. Meanwhile, the pH value in the lab scale experiment increased with HTT. It should be due to the steam releasing in the lab scale experiment started at lower temperature around 140 ℃ but it started immediately after the treatment finished. What is more, the stirring was stronger in the pilot test than in the lab scale experiment. All of these differences were helpful for

ammonia escape from the liquid to make the pH value decreased. The NH_4^+ concentration was remarkably improved from 1820 to 3190 mg/L, which was consistent with remarkably lower nitrogen content in the solid biofuel than that of the raw ABR. The soluble COD (SCOD) of the suspension was as high as 88,290 mg/L and was 18.3% higher than that of the raw ABR, indicating deep degradation and hydrolysis of the organic ingredients in ABR.

Table 3.4. Properties of the solid product from the hydrothermal treatment of ABR

	pH value	NH_4^+ concentration in the dehydrated liquid (mg/L)	Solvable COD in the dehydrated liquid (mg/L)
Raw ABR	5.50	1820	74670
120 ℃, 30min	5.39	2320	78030
180 ℃, 30min	5.07	3190	88290

3.3.2. Mass balance and energy balance in the hydrothermal treatment process

The mass balance in the HTT reactor for HTT of ABR at 180 ℃, 30 minutes is shown in Table 3.5. 1187kg was dropped into the reactor for reaction. In 1187kg of ABR, there was 142kg of Dried-ABR, the rest was 1045kg of liquid. The temperature of the fed ABR in this test was 31 ℃. For HTT of this amount of ABR, 422kg of steam at temperature in the range from 110 ℃ to 195 ℃ was needed. At the output term, the exhausted steam which was discharged to the atmosphere was 309kg. After finishing the pressure releasing, the amount of the HTT suspension stay in the reactor was as much as 1300kg, at the temperature of 100 ℃, in which the HTT-ABR solid matter was only 49kg while the liquid fraction was 1251kg. It means that the recovery ratio of the HTT-ABR solid fuel from ABR was only 34.5%. This amount was lower than the lab scale HTT, which was earlier mentioned as 35% to 49%. Again, this should be due to the fact that the dissolution of the solid matter was much higher in the pilot scale HTT than the lab scale HTT. Lower temperature or shorter holding time might be better in the commercial HTT process in the view point of energy recovery in solid

fuel.

Table 3.5. Mass balance of the hydrothermal treatment of ABR at 180 ℃

	Input	
	Weight(kg)	Temperature (℃)
Steam	422	110~195
Dried-ABR	142	31
Moisture in ABR	1045	31
Sum	1609	
	Output	
	Weight(kg)	Temperature (℃)
Exhausted steam	309	100~170
Liquid	1251	100
HTT-ABR	49	100
Sum	1609	

Table3.6. Energy balance of the hydrothermal treatment of ABR at 180 ℃ for 30 minutes

Input			Output		
Terms	(MJ/batch)	(%)	Terms	(MJ/batch)	(%)
Electricity	62	2	Solid fuel energy	980	29
Energy in Dried-ABR	3408	100	Energy converted in liquid	2428	71
Thermal energy in moisture	27	1	Thermal energy in liquid	392.8	12
Steam heat	1095 (1045*)	32 (30*)	Exhaust steam heat	528	15
			Energy lost	263.2	8
Total	4592		Total	4592	

*steam supplying for HTT reactor to reach 180 ℃.

Based on the mass balance shown in Table 3.5, the energy balance in the HTT reactor was calculated and listed in Table 3.6. The energy in each term was displayed both in absolute value and in percentage value. The energy content in the dried-ABR fed into the reactor is consider as 100%. We can see that the energy input into the HTT reactor mainly came from the hot steam in the form of the thermal energy, which was about 1095MJ/batch, occupying 32% of the solid matter energy. This number was similar as the previous studies [1, 4], indicating that the vertical HTT reactor type should have not affected on the heat transfer so much in this pilot scale HTT

experiment. Notably, to reach the target temperature, the supplying steam was about 1045MJ/batch and 30% lower than the total steam heat (1095MJ/batch, 32%). This confirms again that once the temperature in the reactor reached the target, the extra energy to maintain the HTT reaction is very little. This low energy consumption to maintain the reaction probably was benefited from an external thermal insulator which will reduce the heat loss from its surface. Also, the reaction during HTT of ABR should not consume or release energy. The electricity and the thermal heat in the raw ABR gave 62 and 27MJ/batch respectively, which was only 3% in total.

For the energy output from the HTT reactor, the energy received in the HTT-ABR solid fuel (980MJ/kg, 29%) was much lower than the solid matter as Dried-ABR (3408MJ/kg, 100%) in the input, which due to the solid matter significantly dissolved into liquid phase as mentioned earlier. It can be said that the energy recovery by HTT in the pilot scale was 29%, much less than the lab scale study of ~50% due to the enhancement in the dissolution of solid matter in the pilot test. Compared to the studies on HTT of municipal solid waste, sewage sludge or paper sludge for solid fuel production [4, 10, 13], the energy recovery for HTT of ABR was much lower probably due to the natural differences of feedstock. The energy reduction in the solid fuel was considered to be converted into liquid, as much as 2428MJ/kg, where the COD in the dehydrated liquid evidenced the high organic matters inside, which has a potential to produce methane biogas by anaerobic digestion[14]. Before the HTT-ABR suspension was discharged, the high pressure was reduced to atmospheric pressure by discharging the exhaust steam. The hot exhaust steam contained about 528MJ/kg and 15% of energy, which is almost half of the steam injected. After the exhaust steam was discharged, the temperature of the suspension was around 100℃ to show a thermal energy in it, as high as 392.8MJ/kg, 12%. The rest of the energy would be energy loss about 263.2MJ/kg, 8%, which is unavoidable.

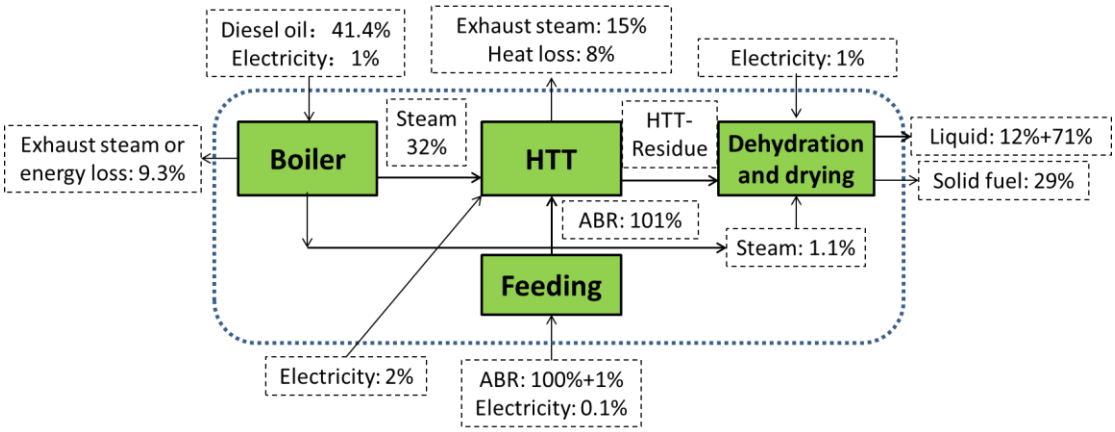

Figure3.7. Energy balance of the pilot scale HTT for solid fuel production

The energy balance for the total process is displayed in Figure 3.7. The energy input and output through the boundary were listed in the black dotted block. According to the previous study, the drying of the dehydrated HTT ABR will consume about 1.2 times of the water in form of hot steam [6]. Thus, as the natural drying will produce 20wt.% moisture content HTT-ABR solid fuel, the drying process to produce 49kg of dry basis HTT-ABR would consume around 14.7kg steam. Considering the steam from the boiler was at the condition of 240℃, 2.4MPa, the energy will be 39.6MJ/batch, 1.1%. For the whole process, it can be seen that the main energy input is from the steam boiler, as assuming 80% of the thermal efficiency for the boiler, the diesel needed should be 41.4 % of the total energy for treating 100% energy of ABR. Apart from the diesel energy, other energy consumption was mainly in the form of electricity, which was 4.1% in total. If we assume 40% of the thermal efficiency to convert the thermal energy into electricity[6, 15], the term should be around 10.3%. In the output, 29% would be in the solid matter. It should be noted that 15% of the energy was in exhaust steam, which can be considered as high quality energy for its high pressure and temperature. It means that there should be big potential to use this part of the thermal energy to preheat or as steam input for the next batch of HTT. Further concern will be focused on this case. Besides, the energy recovered in the solid matter was as low as 29%. If consider to combust the solid fuel to produce steam, this amount is not enough for one batch HTT treatment, therefore,

further study should be conducted to improve the energy recovery ratio.

3.3.3. Modification study on hydrothermal treatment process

As the exhaust steam after the reaction was shown as high as 15%, in this study, a modified HTT process was proposed to reuse the exhaust steam for the next batch to preheat the raw ABR. The modified process is shown in Figure 3.8. The exhaust steam will go through a heat exchanger which stores raw ABR for next batch HTT reaction, so that the high temperature steam will be able to transfer the heat to the raw ABR. Thus, when the preheated feedstock is fed into the HTT reactor, certain amount of the thermal energy will be brought back to the reactor. The hot steam consumption will probably be reduced in the next reaction to reduce the energy consumption.

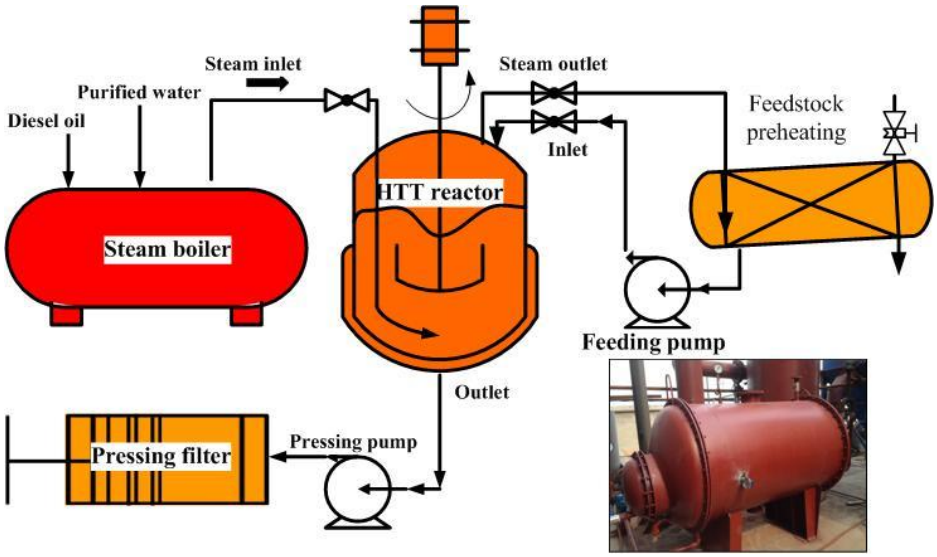

Figure 3.8. Sketch diagram of modified hydrothermal treatment process and picture of the material preheating apparatus.

In addition to the exhaust steam recycling, the holding time of the HTT process was also reduced from 30 minutes to 15 minutes to see how the holding time affect the mass balance and the energy recovery.

The key parameters in the HTT reactor for modified process are displayed in Figure 3.9. The raw ABR will be heated to the temperature in the HTT reactor from

the temperature of 75 ℃. It is worthy to mention that, in the preheating by the exhaust steam from previous batch, the raw ABR could be preheated to over 100 ℃ while the temperature in the HTT reactor were still as high as 130 ℃. This obviously indicates that the exhaust steam from the HTT reactor is able to preheat the next batch material to the boiling point. However, due to the time consuming of the material discharging for the previous batch, when this batch of HTT started, the temperature of the material was reduced to 75 ℃. Therefore, further attention should be paid on the optimization of the commercial HTT process so as to improve the exhaust steam recycling. From Figure 3.9, we can also see that the steam consumption was dramatically reduced due to the shorter HTT holding time and a lower energy consumption.

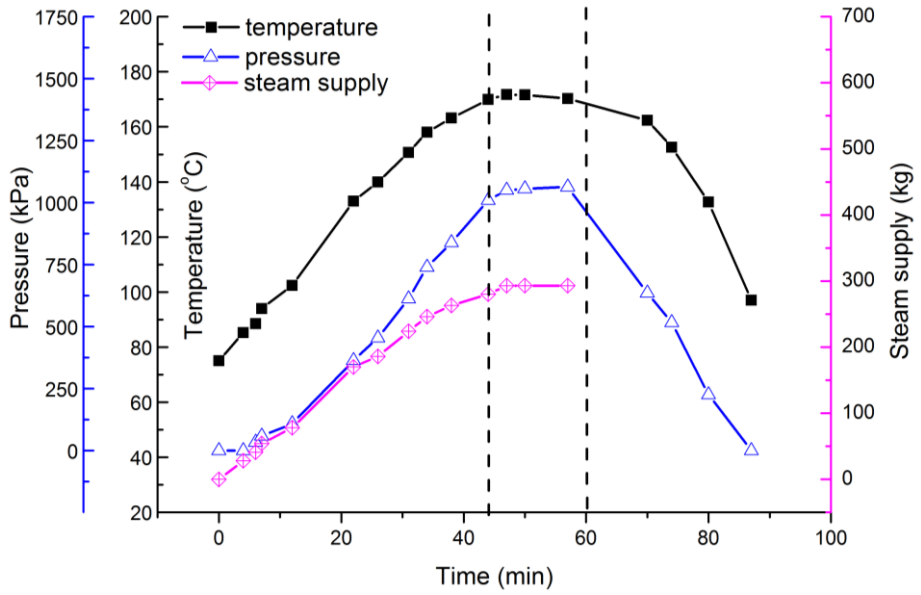

Figure 3.9. Key parameters in the hydrothermal treatment reactor for modified process

The mass balance in the HTT reactor for HTT of ABR at 180 ℃ with 15 minutes is shown in Table 3.7. ABR feeding was 1176kg, then dried-ABR will be 141kg, the rest was 1035kg of liquid. The temperature of the fed ABR in this test was 75 ℃, which contained a certain amount of thermal energy. Thus, for HTT of this amount of ABR, only 293kg of hot steam at the temperature in the range from 110 ℃ to 195 ℃ was needed. At the output term, compared to the previous batch, the amount of

exhausted steam was reduced to 248kg, this might be caused from the less steam injected into the HTT reactor. After finishing the pressure releasing, the rest liquid was 1221kg at the temperature of 100 ℃, in which the HTT-ABR solid matter was only 59kg and the liquid was 1162kg. The HTT-ABR solid fuel recovered from ABR shows 41.8%, which was much higher than the previous batch and comparable to the lab scale HTT, which was earlier mentioned as 35% to 49%. The shorter holding time could reduce the dissolution of the solid matter into the liquid, resulted in the higher solid fuel recovery, which agreed well with the proximate analysis shown in Table 3.3.

Table 3.7. Mass balance for the modified hydrothermal treatment of ABR at 180 ℃

Input		
	Weight(kg)	Temperature (℃)
Steam	293	120~199
ABR	141	75
Moisture in ABR	1035	75
Sum	1469	
Output		
	Weight(kg)	Temperature (℃)
Exhausted steam	248	100~170
Liquid	1162	100
Solid matter	59	100
Sum	1469	

Table3.8. Energy balance in the hydrothermal treatment reactor of ABR at 180 ℃

Input			Output		
Terms	(MJ/batch)	(%)	Terms	(MJ/batch)	(%)
Electricity	62	2	Solid fuel energy	1188	35
Energy in Dried-ABR	3384	100	Energy converted in liquid	2196	65
Thermal energy in moisture	216	6	Thermal energy in liquid	365	11
Steam heat	758	22	Exhaust steam heat	424	13
			Energy lost	247	7
Total	4420		Total	4420	

Based on the mass balance shown in Table 3.7, the energy balance in the HTT

reactor was calculated and listed in Table 3.8. We can see that the hot steam supplied was 758MJ/batch, occupying only 22% of the solid matter energy, which was sharply decreased compared to the previous batch without exhaust steam recycling. This could owe to the hot ABR brought 6% of the thermal energy into the reactor as these two terms were 29%, which was almost the same as the supplying steam (30%) for heating up to the target temperature. Besides, the electricity gave 62 MJ/batch, which was only 2% in total. For the energy output from the HTT reactor, the energy received in the solid matter as HTT-ABR (1188MJ/kg, 35%) was much higher than the previous batch, which is due to the less solid matter dissolution in shorter HTT holding time as mentioned earlier. It can be said that the energy recovery by HTT in the pilot scale was 35%. This number was still much less than the lab scale study of ~50% due to the enhancement in the dissolution of solid matter in the pilot test by different mixing and steam feeding. The energy in Dried-ABR was converted into liquid as much as 2196MJ/kg, 65% that is still very high. Therefore, the energy production from the dehydrated liquid would be a considerable idea to improve the system. The hot exhaust steam contained about 424MJ/kg and 13%, which slightly smaller than the previous batch. The temperature of the suspension was around 100 ℃ after exhaust steam discharging, to show the thermal energy of 365MJ/kg, 11%. The rest of the energy would be energy loss about 247MJ/kg, 7% which is less than the previous batch. It can be explained by the shorter heat up and holding time resulting in the lower heat loss from the HTT reactor.

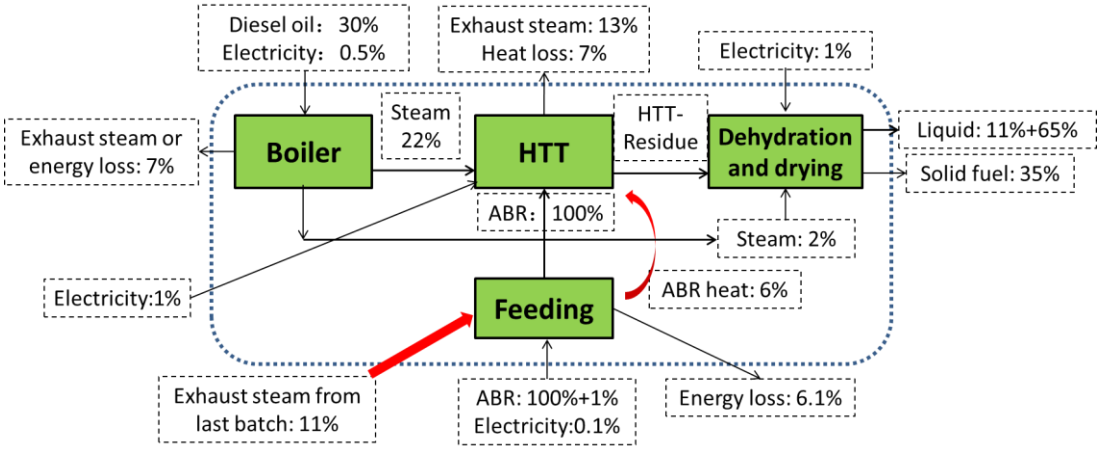

Figure 3.10. Energy balance of the modified pilot scale HTT for solid fuel production

The energy balance for the modified HTT process is displayed in Figure 3.10. The energy input and output through the boundary were listed in the black dotted block. Due to the shorter holding time, the hydrolysis of ABR by HTT would be weaker, as a result, the natural drying of HTT-ABR at 180 ℃ for 30 minutes could reduce the moisture in dehydrated residue to 30wt.%. Thus, the drying process to produce 59kg of dry base ABR will proximately consumes 25kg steam. Then, the energy consumption will be 67.4MJ/batch, 2%, indicating that the shorter holding time will not bring too much difference in the dehydration process, which is similar as the lab scale study. The main input is coming from the steam boiler with the thermal efficiency of 80%, where the diesel fuel required should be 30 % of the total energy for treating 100% energy of ABR. The electricity was considered to reduce to 2.6% due to the shorter holding time. If the thermal efficiency of converting thermal energy into electricity is 40% [15], the term should be around 6.5%. Therefore, the total energy consumption for HTT of ABR in the thermal heat should be 36.5%. In the output, 35% would be in the solid fuel, which means the modified process still showed obstacle to produce enough energy in the solid fuel to maintain the process itself, which was quite different from the previous studies that there is a net surplus energy in the form of solid fuel by HTT of biomass wastes[1, 4, 13]. In a word, by exhaust steam recycling, the thermal energy needed for treating 100% energy of ABR

was significantly reduced by almost 30% from 51.7% to 36.5%.

It should be mentioned that the exhaust steam recycling process in this study still have a potential to improve the efficiency. As shown in Figure 3.7 in the feeding unit, there was still around 5% of the thermal heat with higher quality can be recycled to the next HTT batch. In the real commercial process, it can be achieved by employing more than one HTT reactor to receive the exhaust steam and heat up the reactor directly to reduce the thermal energy loss. Besides, the dehydrated liquid from HTT process has very high COD value, which can be used to produce methane biogas by anaerobic digestion. This can be considered as another way to improve the energy recovery ratio.

3.3.4. The modified hydrothermal treatment performance in full scale plant

It has been proved by the experiment shown in section 3.3.3 that recovering the exhaust steam by the heat exchanger to preheat ABR can reduce the energy consumption. In the experiment, it was found that ABR in the storage tank can be preheated by exhaust steam up to 100 ℃ while the temperature in the HTT reactor was still as high as 120 ℃. However, before the preheated ABR was fed into the HTT reactor for the next batch, discharge of steam and material of the present batch was firstly conducted. During this period, the preheated ABR was cooled down from 100 ℃ to 75 ℃, resulting in 6% heat loss in the heat exchanger as shown in Figure 3.10.

In the practical HTT process, more than one HTT reactor should be applied. Therefore, we propose a HTT process, as shown in Figure 3.11, that the exhaust steam will be recycled to the next HTT reactor fed with wet ABR. Thus, ABR can be continuously heated by fresh steam right after the preheating finished. One the other hand, due to the bigger size of HTT reactor ($10m^3$) in a commercial plant, the mass and heat transfer will be more difficult. For better estimation of the performance of

the steam recycling, it is assumed that ABR for the next batch can be heated up from ambient temperature to just 100 ℃.

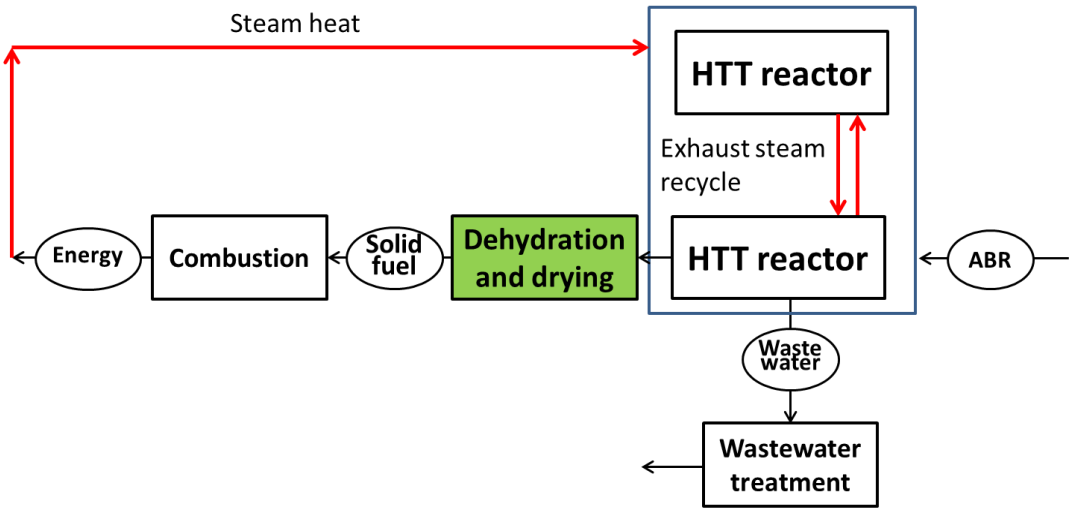

Figure 3.11. Full scale of HTT process to improve the exhaust steam recycling

As a consequence, 6% heat loss in the heat exchanger can be avoided and most of the exhaust steam heat (11% in total) will go to the next HTT batch. The energy balance of the commercial plant is shown in Figure 3.12 where the energy input terms shown in red circle will be reduced. The steam heat consumption for HTT will be dramatically reduced from 22% to 16% and the diesel oil consumption will be reduced to 22.5%. As same as in section 3.3.3, the electricity used in one batch will consume 6.5% of the energy from fuel. Therefore, the total energy needed from fuel would be 29% which is much less than the solid fuel production (35%). Compared to the no steam recycling process, the energy consumption can be dramatically reduced by 44% from 51.7% to 29%. Additionally, because the steam needed for heating ABR from 75 ℃ to 100 ℃ was 80kg, the water consumption will be reduced from 293kg to 213 kg for treating approximately one ton of ABR. Compared to the steam needed in the conventional HTT process, it can be significantly reduced by 49.5%. HTT operating time will also be reduced.

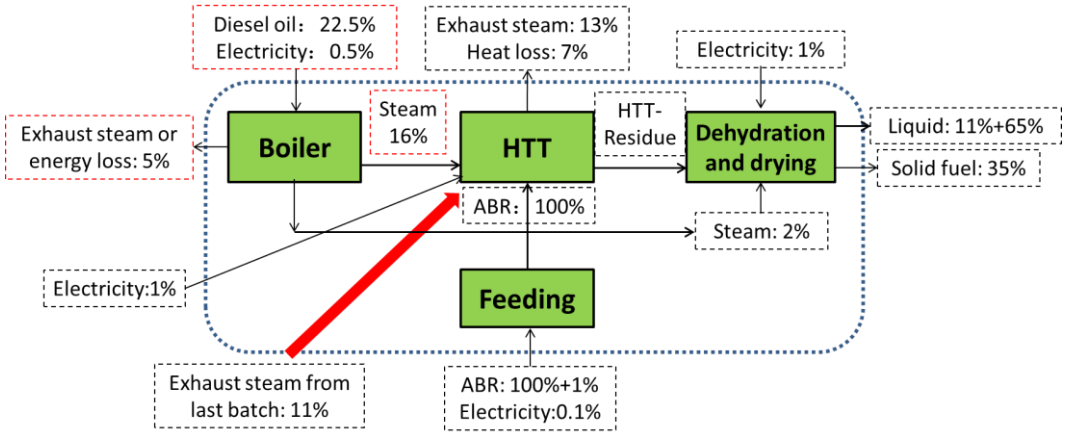

Figure 3.12 Energy balance of the modified commercial HTT for solid fuel production

3.4. Conclusions

A set of pilot scale equipment has been built up and ABR was hydrothermally treated in the pilot plant. The product properties were then analyzed and compared with the result from lab scale experiment. Besides, the mass balance and the energy balance for the pilot scale HTT were investigated. In order to improve the energy efficiency of HTT, material preheating process was induced. The results were concluded as follows.

1). The pilot scale HTT of ABR showed similar improvement in dewaterability of ABR. By HTT, ABR could be mechanically dehydrated to 38~52wt.% moisture content material, while the raw ABR could only reach 75wt.%. As the HTT temperature increased, the dewaterability was increased from 52wt.% at 120 ℃, 30 minutes to 38wt.% at 180 ℃, 30 minutes. The natural drying performance was also improved with increasing the HTT temperature or holding time.

2). The mass recovery and energy recovery in the ABR-based solid fuels was reduced in comparison with the lab scale experiment. In the 180 ℃, 30 minutes HTT, the mass recovery was 34.5% and the energy recovery was 29%. Due to the rotation mixing in the pilot scale reactor was enhanced and the steam feeding further boost the mass transfer in the reactor, the dissolution of the solid matter in ABR would be

increased. This led to the lower mass recovery than the lab scale experiment. Also, the heating value of the ABR-based solid fuels will be decreased by increasing the HTT temperature or holding time. Similar with the lab scale experiment, the dehydrated liquid from HTT process has a high COD value, which means that the methane production from the liquid need to be considered.

3). By recycling the exhaust steam from the previous batch, the energy consumption for the same amount of ABR can be significantly reduced by almost 30%. Further improvement of the exhaust steam recycling was estimated to show a great potential on energy and water saving by 44% and 49.5%, respectively. It can be apparently expected that production of solid fuel from ABR by HTT will be feasible.

References

[1] Prawisudha P, Namioka T, Yoshikawa K. Coal alternative fuel production from municipal solid wastes employing hydrothermal treatment. Applied Energy. 2012;90:298-304.
[2] Lu L, Namioka T, Yoshikawa K. Effects of hydrothermal treatment on characteristics and combustion behaviors of municipal solid wastes. Applied Energy. 2011;88:3659-64.
[3] Namioka T, Morohashi Y, Yoshikawa K. Mechanisms of malodor reduction in dewatered sewage sludge by means of the hydrothermal torrefaction. Journal of Environment and Engineering. 2011;6:119-30.
[4] Areeprasert C, Zhao P, Ma D, Shen Y, Yoshikawa K. Alternative solid fuel production from paper sludge employing hydrothermal treatment. Energy & Fuels. 2014;28:1198-206.
[5] De Mello F. Boiler models for system dynamic performance studies. Power Systems, IEEE Transactions on. 1991;6:66-74.
[6] Werther J. Potentials of biomass co-combustion in coal-fired boilers. Proceedings of the 20th International Conference on Fluidized Bed Combustion: Springer; 2010. p. 27-42.
[7] Kim H-S, Shin M-S, Jang D-S, Na E-S. A study for the thermal treatment of dehydrated sewage sludge with gas-agitated double screw type dryer. Journal of Environmental Science and Health. 2005;40:203-13.
[8] Hu B, Wang K, Wu L, Yu SH, Antonietti M, Titirici MM. Engineering carbon materials from the hydrothermal carbonization process of biomass. Advanced Materials. 2010;22:813-28.
[9] Peterson AA, Vogel F, Lachance RP, Fröling M, Antal Jr MJ, Tester JW. Thermochemical biofuel production in hydrothermal media: a review of sub-and supercritical water technologies. Energy & Environmental Science. 2008;1:32-65.
[10] Namioka T, MOROHASHI Y, YAMANE R, YOSHIKAWA K. Hydrothermal treatment of dewatered sewage sludge cake for solid fuel production. Journal of Environment and Engineering. 2009;4:68-77.
[11] Zhao P, Ge S, Ma D, Areeprasert C, Yoshikawa K. Effect of hydrothermal pretreatment on convective drying characteristics of paper sludge. ACS Sustainable Chemistry & Engineering. 2014;2:665-71.
[12] Ferenczy L, Mai A, Ott I, Ambrus G, Lang T. Process for the improvement of antibiotic production by in vivo genetic recombination. Google Patents; 1988.
[13] Zhao P, Shen Y, Ge S, Yoshikawa K. Energy recycling from sewage sludge by producing solid biofuel with hydrothermal carbonization. Energy Conversion and Management. 2014;78:815-21.
[14] Zhong W, Li Z, Yang J, Liu C, Tian B, Wang Y, et al. Effect of thermal–alkaline pretreatment on the anaerobic digestion of streptomycin bacterial residues for

methane production. Bioresource technology. 2014;151:436-40.
[15] Bhat I, Prakash R. LCA of renewable energy for electricity generation systems—A review. Renewable and Sustainable Energy Reviews. 2009;13:1067-73.

Chapter 4 Combustion Behaviors of Hydrothermally Treated Antibiotic Bacterial Residue

4.1. Introduction

In Chapters 2 and 3, it has been verified that the hydrothermal treatment (HTT) can degrade the residual antibiotics in antibiotic bacterial residue (ABR) and improve the dewaterability of ABR to allow its safe disposal and high-efficiency production of solid biofuel. Although HTT can partially remove nitrogen present in ABR, there is yet little understanding about the nitrogen monoxide (NO) emission characteristics from burning ABR-based solid fuels obtained by HTT. The nitrogen content in the hydrothermally prepared solid biofuel of ABR is still high as 5.8 wt.%, and it would be highly necessary to control the NO emission from its combustion [1-3]. Besides, as the ash from biomass usually content certain amount of harmful alkali metals that would probably cause slagging and fouling problems for the boilers which has attracted significant attentions [4-6]. Considering the high N and typical ash composition in the ABR-based fuels, the purpose of this chapter is to investigate the ABR-based fuels combustion characteristics which consist of the NO emission characteristic before and after HTT and the effect of HTT on slagging and fouling tendency of the ash of ABR-based fuel.

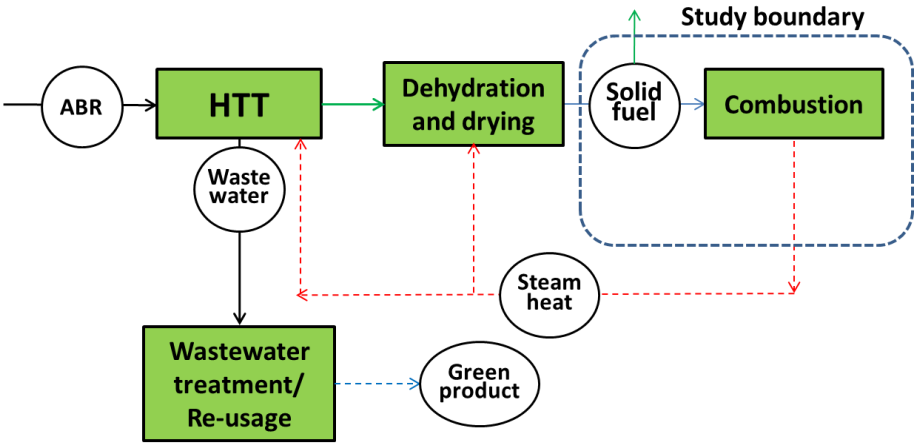

Figure 4.1. The study boundary of Chapter 4.

ABR before and after HTT are combusted via both conventional and air-staged modes to investigate the corresponding NO emission characteristics, whereby clarifying the effect of HTT on NO emission and the mechanism about the NO emission reduction due to HTT. For these research objectives, in this study, ABR with and without HTT was pyrolyized at 1273 K. The X-ray Photoelectron Spectroscopy (XPS) and Thermo Gravimetric (TG) analyses of both the dried raw ABR (Dried-ABR) and HTT-ABR are conducted to understand the transfer of nitrogenous components in their pyrolysis and combustion. Slagging and fouling index of ABR ash were calculated to investigate the slagging and fouling tendency of the ash. The mechanism about how HTT affect on the ash behavior will be clarified based on the ash behavior in the fuel preparation which will be discussed in detail.

4.2. Material and Methodology

4.2.1. Fuel characterization

The raw antibiotic bacterial residue (ABR) tested in this study was produced from the fermentation process producing cephalosporin C, and the HTT-ABR used for combustion tests was made via the condition-optimized HTT at 200 ℃ for 30 minutes

[7]. A brown coal was also tested for comparison. Table 4.1 shows the properties of all the tested fuels. Before combustion, the fuels were all dried at 102 ℃ for 24 h in an atmospheric air oven, then milled and sieved to 0.3~0.4 mm to minimize the particle size influence. Comparing to coal, the biofuels from ABR have no fixed carbon, and their combustible matters are volatile only. For both HTT-ABR and coal, they have the similar ash contents of about 15 wt.% (dry basis). The ABR-based biofuels have obviously high nitrogen contents, reaching 7.7 wt.% and 5.8 wt.% (daf basis) for Dried-ABR and HTT-ABR, respectively. During HTT, hydrolysis of nitrogenous substances like protein, amino acid and other in ABR can reduce the nitrogen content in its produced solid matters [8]. The coal sample has a lower oxygen content than the ABR fuels do. All the tested fuels have the similar sulfur content and relatively high higher heating value (HHV) of about 20 MJ/kg.

Table 4.1. Properties from proximate and ultimate analyses of tested fuels.

Fuel sample	Proximate analysis (wt.%, dry)				HHV (MJ/kg)	Ultimate analysis (wt.%, daf)				
	M	Ash	VM	FC		C	H	S	N	O
Dried-ABR	5.8	8.4	91.6	0	19.3	43.5	6.7	0.76	7.7	41.9
HTT-ABR	2.4	14.8	85.2	0	24.6	53.3	6.6	0.9	5.8	33.6
Coal	1.9	15.1	37.3	47.6	22.7	75.3	4.22	0.72	1.1	18.7

Figures 4.1 and 4.2 show the results from pyrolyzing and combusting of the three fuels in TGA (SHIMADZU D50). The pyrolysis was conducted in Ar atmosphere and the combustion was conducted in Ar + 21 vol.% O_2 to avoid thermal NO formation. The temperature program was from room temperature to about 1173K at 50 K/min. Figure 4.1 verifies further that both Dried-ABR and HTT-ABR have no fixed carbon. The weight loss curves for them, however, showed still two distinctive stages of devolatilization (see dotted vertical lines). For the tested coal, its pyrolysis curve can be also divided into two stages, with the first stage for release of volatile and the second stage representing carbonization to form char. Because there is no formation of char, we distinguish the two devolatilization stages of ABR-based fuels as the

releases for light and heavy volatiles, respectively. Then, from Fig. 4.1 we can see that the demarcation of the two stages occurred roughly at the similar time of 500 s or temperature of 800K. While the light volatile released quickly, the release of heavy volatile was very slow to show that it is possibly through a kind of cracking reactions strongly depending on the temperature. Figure 4.1 further confirms that Dried-ABR has the lower ash content and higher light-volatile content than HTT-ABR does. Carefully examining the TGA curves for both the ABR fuels, we can figure out that the heavy volatile takes about 15 wt.% and 20 wt.% for Dried-ABR and HTT-ABR, respectively.

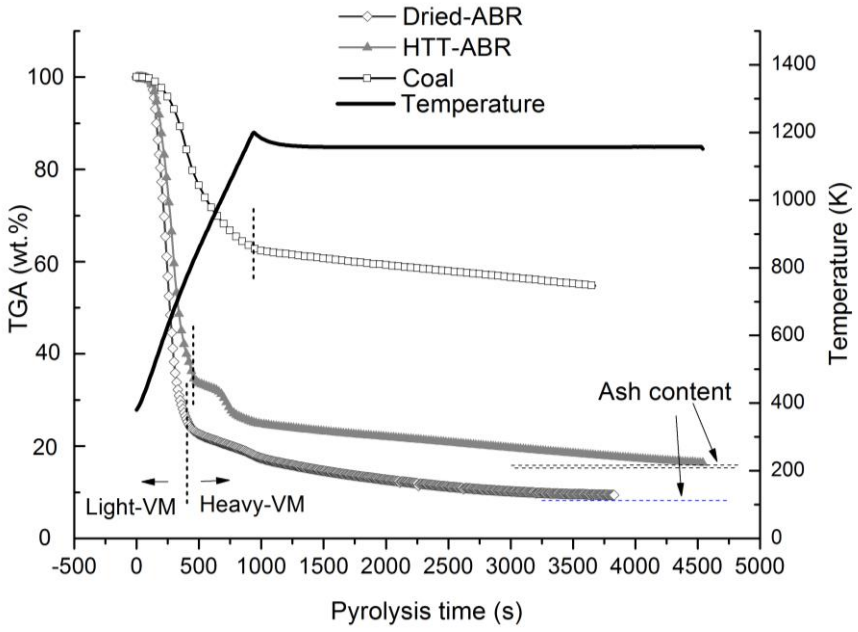

Figure 4.1. Pyrolysis tests in TGA with Ar atmosphere of all solid fuels.

The TGA and DTG curves shown in Fig. 4.2 for the combustion of the ABR-based fuels further verified the preceding analysis about two types of volatiles. In Fig. 4.2, the ABR fuel samples have two distinctive DTG peaks, while also an inflection point shown on their TGA curves. For each fuel, its inflection area just corresponds to the transition period in its DTG curve between two big DTG peaks. The second DTG peak starts at about 370 s and 430 s for Dried-ABR and HTT-ABR, respectively. It is obvious in Fig. 4.2 that HTT lowered the combustion rate so that the

HTT-ABR fuel shifted its two DTG peaks to the right-hand side to make the first peak to have lower intensity and wider time span. The obviously delayed second DTG peak for HTT-ABR clarifies that it has reduced the activity for combustion. Furthermore, the first big peak for both Dried-ABR and HTT-ABR consists of two fractional peaks, indicating that, in their light volatiles, there would be rather two slightly different types of volatiles (further studies are needed for understanding the difference between them). By matching with the pyrolysis data shown in Fig. 4.1, we can reasonably suppose that the combustion corresponding to the second DTG peak for Dried-ABR and HTT-ABR is mainly for their heavy volatiles. For the tested coal there was only one big DTG peaking area and it is peaked at the left corner of the area to indicate the combustion of the coal volatile. Then, its flatten DTG peak area, till the peak end, of the coal DTG curve should correspond to the char combustion.

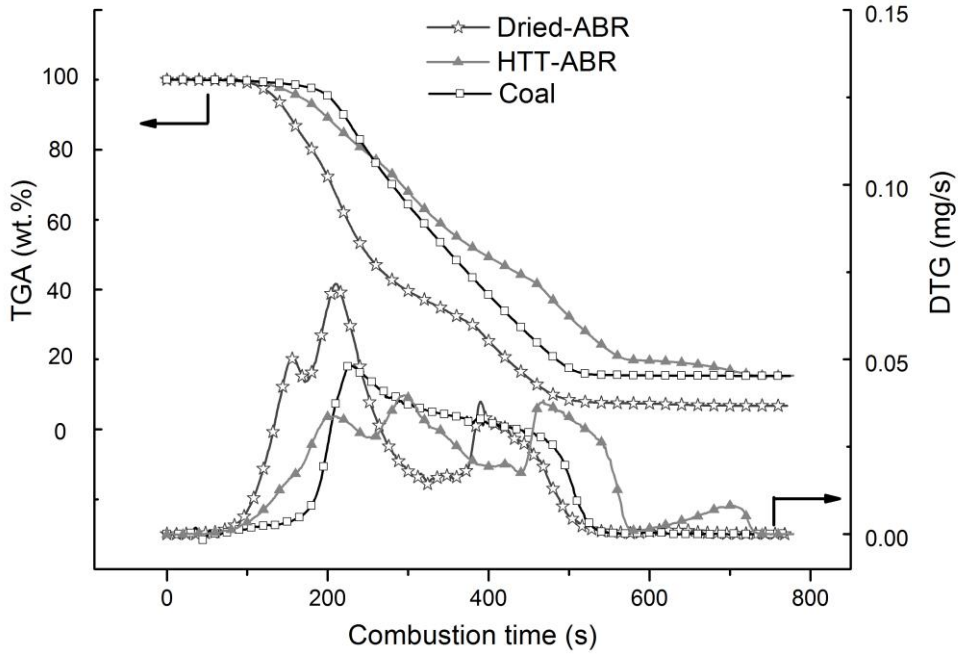

Figure 4.2. Combustion tests in TGA and $Ar+O_2$ atmosphere of all solid fuels.

The study also characterized the tested fuels using X-ray Photoelectron Spectroscopy (XPS, ESCALAB250Xi). For the analysis, a sample was, in succession, dried in a vacuum dryer, degased at 10^{-7} Pa for 3 h and neutralized by Ar-ion

sputtering. Monochromatic Al K Alpha (350W, hv =1486.8eV) X-ray was used to excite the fuel sample. All spectra were obtained at 20 eV of pass energy in the fixed transmission mode. The resolution and analysis area were 0.05 eV and 0.8 mm^{-2}, respectively. The analysis was automatically performed at 3 ~ 5 different positions on the surface to obtain the high-quality N 1s spectra.

4.2.2. Combustion and pyrolysis tests

All combustion and pyrolysis experiments were conducted in an electrically heated fixed bed reactor schematically shown in Fig. 4.3. It mainly consists of a gas supply section, an online flue gas cleaning and analysis section and the fixed bed reactor. The reactor is made of quartz glass and divided into three parts, an outer tube, an inner tube and a top cover having a secondary gas inlet. The outer tube has a flue gas outlet on its top and a primary gas inlet at its bottom. The two gas inlets enable the reactor to simulate various combustion modes (will be shown later). A sintered quartz porous plate at the middle height of the inner tube supported the tested fuel sample. A gas mixture of argon (99.99%) and O_2 at a volumetric ratio (Ar/O_2) of 79:21 was adopted as the oxidant to avoid any thermal NO emission. An online flue gas analyzer (Testo 350XL, Japan) monitored the composition of the flue gas from the reactor. The measured NO_2 was constantly below 8 ppm in all experiments, thus only NO was considered in this study when analyzing the NOx emission .

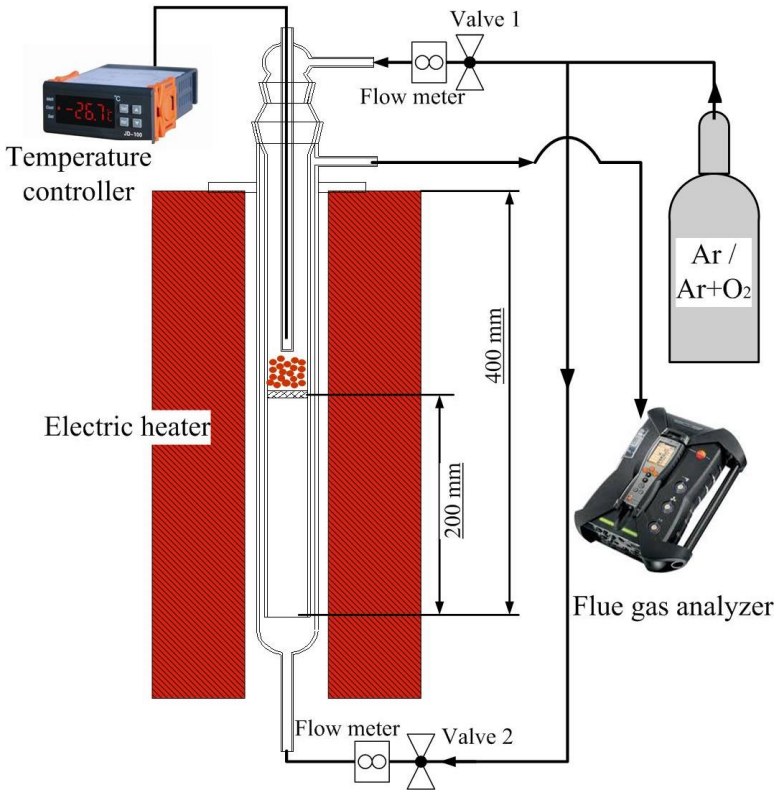

Figure 4.3. A schematic diagram of the adopted experimental fixed bed combustor.

For all combustion tests, 0.25 g fuel sample was mixed with 5 g silica sand to maintain a certain bed height for enhancing the gas-solid interaction and also preventing the possible ash agglomeration during combustion. The modes of conventional combustion (CC) and air-staged combustion (ASC) were performed by considering that the latter is one well-known technology for lowering NO emission. When conducting CC, the fuel sample was placed in the inner tube and the oxidant gas was injected from the primary gas inlet at the top cover (through valve 1) at the flow rate of 2 L/min. For ASC, the oxidant gas was injected through the primary and secondary gas inlets with the flow rates of 1.5 L/min and 0.5 L/min, respectively. We then can assume that all the combustions in this study are conducted under the same fuel to air ratio, while 25% of the total oxygen was sent as the secondary oxygen in ASC. Inside the inner tube, the sample was pyrolyzed and preliminarily burned in O_2-deficient condition. The pyrolysis gas flowed down and was fully burned out through interacting with the sufficient O_2 supply from the secondary gas inlet in the

interstice between the inner and outer tubes. For all tests, the flue gas was monitored online in a Testo flue gas analyzer to get the instantaneous NO concentration (in ppm). The combustion temperature was varied in 1073~1273 K where the furnace was heated up to the setting temperature firstly and then tube fed with sample would be put into the furnace to be rapidly heated up for combustion test. In this work, all combustion tests were conducted for the same amount of fuel in the same flow rate of oxidant (O_2+Ar) to compare the specific NO emission in milligram NO per gram fuel and also the fuel-N conversion calculated from the emission.

For understanding the mechanism of NO emission reduction in fuel combustions, all solid fuels were pyrolyzed in the same reactor at 1273 K to measure the released NH_3, one of the main NO precursors. The NH_3 yield from pyrolysis was determined with the standard method of JIS K0099-2004. Firstly, NH_3 in the pyrolyzing gas was fully absorbed using 200 mL 0.1N sulfate acid. The resulting solution was in turn measured with a Thermos 9512 ammonia analyzer to obtain the NH_4^+ concentration. Finally, the total released NH_3 was calculated from multiplying the concentration and the volume of the absorption solution.

With the instantaneous NO concentration (ppm) given by the Testo gas analyzer, the total amount of NO emitted (mg/g) in a testing period was calculated by

$$\text{NO emission} = \frac{40}{22.4 * \text{Mass of fuel}} * \sum_{0}^{n} \left(\frac{\text{Gas flow rate}}{60} * \frac{\text{NO concentration}}{10^4} * \Delta t\right), \quad (1)$$

where, the mass of fuel is 0.25 g, $\sum$ indicates the calculation period of fuel combustion, gas (flue gas) flow rate is 2 L/min, Δt means the time period between two adjacent data points which is 1 s in this study. The fuel-N conversion to NO was defined as the percent of nitrogen converted into NO from fuel-N:

$$\text{Fuel} - \text{N conversion to NO} = \frac{14 * \text{NO emission}}{30 * \text{Fuel} - \text{N}} * 100\%, \quad (2)$$

where 14/30 represents the molar weight ratio of N in NO, NO emission is determined by Eq. (1), and fuel-N is the nitrogen mass per gram of fuel (mg/g) from Table 4.1.

4.2.3. Slagging and fouling tendency calculation

The solid fuel properties and the corresponded ash composition of the ABR-based fuels from different HTT conditions has been respectively presented in Tables 2.2 and 2.3 of Chapter 2. It will be used for further study on the fuel ash behavior and deposition tendencies during the combustion process. For the prediction of coal ash slagging and fouling tendency, the empirical indices [4, 6, 9-11]，despite their shortage due to the complex conditions in combustion process, are widely used and probably remain the most secure basis for decision making[4, 9].

For example, the modified base-to-acid ratio (A/B) with phosphorous pentoxide (A/B_{+P}) index from Pronobis et al. [6, 11]is used here,

$$A/B_{+P} = \frac{Fe_2O_3+CaO+MgO+K_2O+Na_2O+P_2O_5}{SiO_2+TiO_2+Al_2O_3} \quad (3)$$

where the chemical name of each oxide will refer their percentage. Besides, the B/A simplified form ($R_{(a/b)}$) was taken in the previous study[12].

$$R_{(a/b)} = \frac{Fe_2O_3+CaO+MgO}{SiO_2+Al_2O_3} \quad (4)$$

The minimum ash softening temperature occurs when R_b= 35–55% and with increasing the ratio K_{Al} = SiO_2/Al_2O_3, the softening temperature migrates to lower contents of alkali compounds. Researchers have previously presented the results of regression analysis of correlations between hemispherical temperature and fouling

temperature and $R_{(b/a)}$ and K_{Al} for more than 180 coals to obtain three areas: By R(b/a) < 0.75---the lower, the higher HT and FT are and in consequence the danger of slagging decrease too; by R(b/a) < 0.15 both temperatures exceed 1600 ℃; The lowest levels of HT and FT as well as the strongest hazard occur by R(b/a)≅0.75; By R(b/a) =0.75~2.0 HT and FT grow with increasing values of R(b/a); By R(b/a)> 2.0 the dependence is not noticeable.

Fouling index (F_u) is given as

$$F_u=(B/A)*(K_2O+Na_2O) \quad (5)$$

if F_u <0.6, low fouling inclination; 0.6< F_u <40, high inclination; F_u >40, extremely high for fouling and tendency of sintering of deposits.

Slag viscosity index

$$S_R=\frac{SiO_2}{SiO_2+Fe_2O_3+CaO+MgO}*100 \quad (6)$$

corresponds to high viscosity and therefore to low slagging inclination. If the S_R >72, low slagging inclination; 65< S_R < 72, medium inclination; S_R< 65, high.

For the Fe_2O_3/CaO ratio, the value in the range of 0.3~3.0 will increase the slag formation.

Apart from these, recently, the alkali index has become popular as a threshold indicator for fouling and slagging [13, 14]. It expresses the quantity of alkali oxides in the fuel per unit of fuel energy, as shown below:

$$AI=\frac{kg(Na_2O+K_2O)}{GJ} \quad (7)$$

where AI means alkali index, Na_2O and K_2O respectively represents the weight of

these alkali oxides (kg) in per kilogram of fuels. GJ means the energy density in per kilogram of fuels. When the AI values are in the range of 0.17-0.34 kg/GJ, the fouling is probable. The fouling will be certain to occur if the value is higher than 0.34 [10, 14].

Additionally, a bed agglomeration index has been developed for the fluidized bed reactors

$$BAI=\frac{Fe_2O_3}{Na_2O+K_2O} \quad (8)$$

bed agglomeration will occur when BAI is lower than 0.15.

The abovementioned indexes were mainly used for coal fuel or biomass mixed with coal. However, they were also used by several studies for pure biomass ash [13, 15]. Additionally, considering that the metal species of the studied biofuels is similar with coal, the indices for coal should be applicable characterization of the ash from AMR-based fuel.

4.3. Results and discussions

4.3.1. NO emission characteristics of burning ABR-based biofuels

NO emission and fuel-N conversion behaviors

Figure 4.4 shows the specific NO emission calculated by Eq (1) and its corresponding Fuel-N conversion into NO obtained from Eq. (2) for all the tested fuels in the CC mode at different combustion temperatures. Similar to many other studies [2, 3, 16], the NO emission and its corresponding fuel-N conversion into NO increased with increasing the temperature from 1073 to 1273 K. Except for the effect of enhanced reaction kinetics between N species and O_2, for the biomass fuels like

Dried-ABR and HTT-ABR with low, even without fixed carbon, the quicker release of volatile N at raised temperatures from fuels should be also a reason for increasing their NO formations and fuel-N conversions at higher temperatures. In this case (fuel without fixed C), the volatile N is the only precursor of NO formation [17, 18].

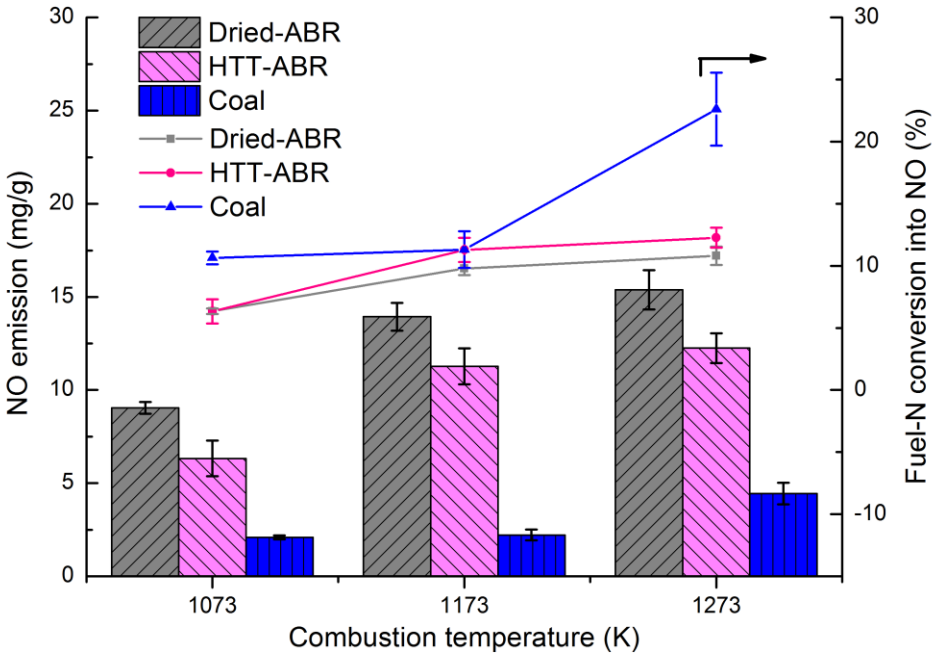

Figure 4.4. NO emission and fuel-N conversion in burning fuels via CC mode.

The absolute NO emission for Dried-ABR, HTT-ABR and coal followed the same order as that of their N contents clarified in Table 4.1. Nonetheless, the Fuel-N conversion into NO is generally highest for coal and lowest for Dried-ABR. Between Dried-ABR and HTT-ABR, the difference in the fuel-N conversion into NO is little (about 2 percent) and tends to slightly increase with raising the temperature. At 1073 K there was actually no difference in the fuel-N conversion into NO for Dried-ABR and HTT-ABR. Figure 4.1 has shown that the devolatilization rate is essentially the same for the two ABR-based fuels. On the other hand, the tests were all for the same amounts of fuel and O_2. Considering the higher ash content of HTT-ABR than Dried-ABR (Table 4.1), the actual excessive oxygen ratio should be slightly higher for

HTT-ABR, which would be the major reason for the slightly higher fuel-N conversion of HTT-ABR. For Dried-ABR, it must release more instantaneous volatile into the combustion atmosphere to give the higher reduction capability to NO and in turn its slightly lower fuel-N conversion [1]. The highest fuel-N conversion for coal, as shown in Fig. 4.4, would be due to its lower volatile content, leading to less volatile in its atmosphere to reduce the formed NO from char combustion [19].

The NO emission from burning HTT-ABR is lower than that from burning Dried-ABR, even though the burning of HTT-AMAR had a slightly higher excessive oxygen ratio as indicated above. This means that through HTT it obviously reduced the NO emission of ABR fuel combustion. As an example, we can see that the combustion at 1073 K had the NO emission of 6.5 mg/g for HTT-ABR but 9 mg/g for Dried-ABR. This effect of HTT on NO emission from burning its resulting fuel is similar to that observed in burning sewage sludge after HTT (Zhao. al. [20]) and can be attributed to the removal of some N species from the produced fuel, as shown in Table 4.1 by the lower N content for HTT-ABR.

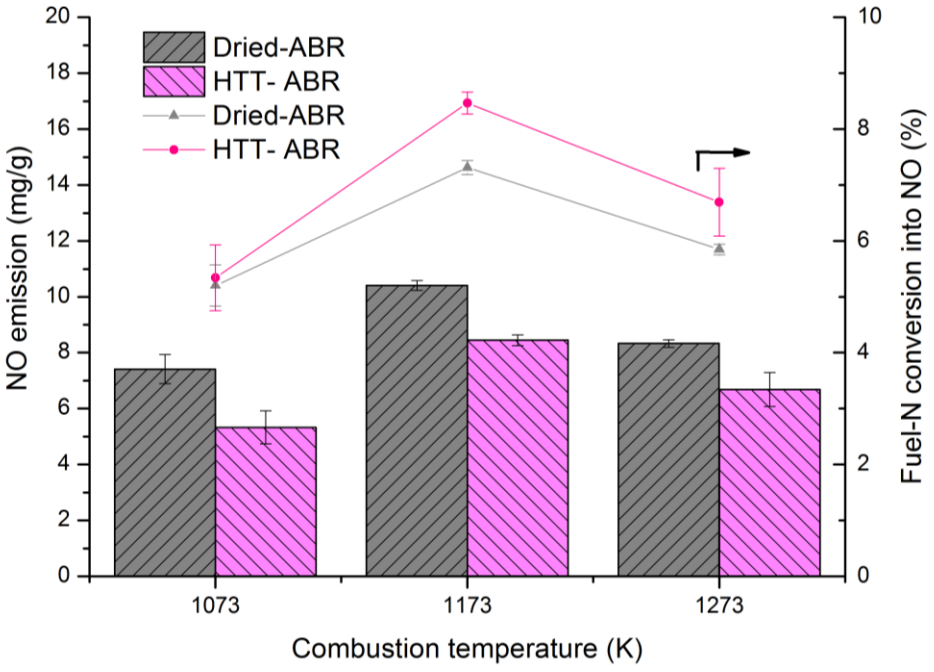

Figure 4.5. NO emission and fuel-N conversion in burning ABR fuels via ACS mode.

Figure 4.5 shows the NO emission and its corresponding fuel-N conversion into NO from burning Dried-ABR and HTT-ABR in the ASC mode. Different from the results for the CC mode shown in Fig. 4.4, here, the NO emission and the fuel-N conversion are peaked at 1173 K to have reversely the lower NO emission and fuel-N conversion at the tested highest temperature of 1273 K. The first increase in the NO emission and fuel-N conversion from 1073 K to 1173 K can be similarly understood as for the data in Fig. 4.4 in terms of the increased NO-formation kinetics and quicker release of volatile nitrogen precursors at the higher temperature.

Compared to CC, the ASC reduces NO remission because of its suppressed NO formation in the primary combustion zone under oxygen-lean, even oxygen-deficient conditions [19, 21]. In our tests, the O_2 amounts fed into the primary and secondary combustion zones are fixed. At very high temperature, such as 1273 K, the high-speed volatile release from ABR fuels, in which there was actually no fixed carbon, would make the combustion in the primary zone O_2-deffient to form very less NO, or even to leave many reducing volatiles in the primary exhaust gas. In the secondary combustion zone, where another 25% of the total oxygen is supplied, all fuel volatiles are fully combusted but the NO formation is much reduced due to the less O_2 amount. Overall, there have thus the conversely lower NO emission and fuel-N conversion into NO at the higher temperature, as shown in Fig. 4.5. The result clarifies that when with 25% as the secondary O_2 supply (75% as the primary), for Dried-ABR and HTT-ABR, their primary combustion may be under oxygen-lean conditions at temperatures below 1173 K but oxygen-deficient conditions at above 1273 K.

As shown in Fig. 4.5, the NO emission from burning HTT-ABR was also obviously lower (by 1.5 - 2 mg/g) than that from Dried-ABR at all the tested temperatures, which should be mainly due to the lower N content of HTT-ABR comparing to that of dried raw ABR. Nonetheless, the fuel-N conversion into NO kept higher for HTT-ABR than for Dried-ABR. As analyzed above, it should be mainly

due to the actually slightly higher excess oxygen ratio for burning HTT-ABR. Obviously, all these results comply well with those obtained for CC from Fig. 4.4.

Reduction in NO emission by HTT and ASC

Both Dried-ABR and HTT-ABR fuels are further combusted with different modes to clarify the potential of reducing the NO emission via HTT, ASC and their combination. The benchmarked tests below, in terms of percentage of reduction in the NO emission, include Dried-ABR in CC versus HTT-ABR in CC, HTT-ABR in CC versus HTT-ABR in ASC, and Dried-ABR in CC versus HTT-ABR in ASC. The last comparison hopes to clarify the reduction potential for NO emission via combining HTT and ASC. Figure 4.6 shows the result, where the percentage is all against the higher NO emission of each pair of compared tests under the same combustion conditions.

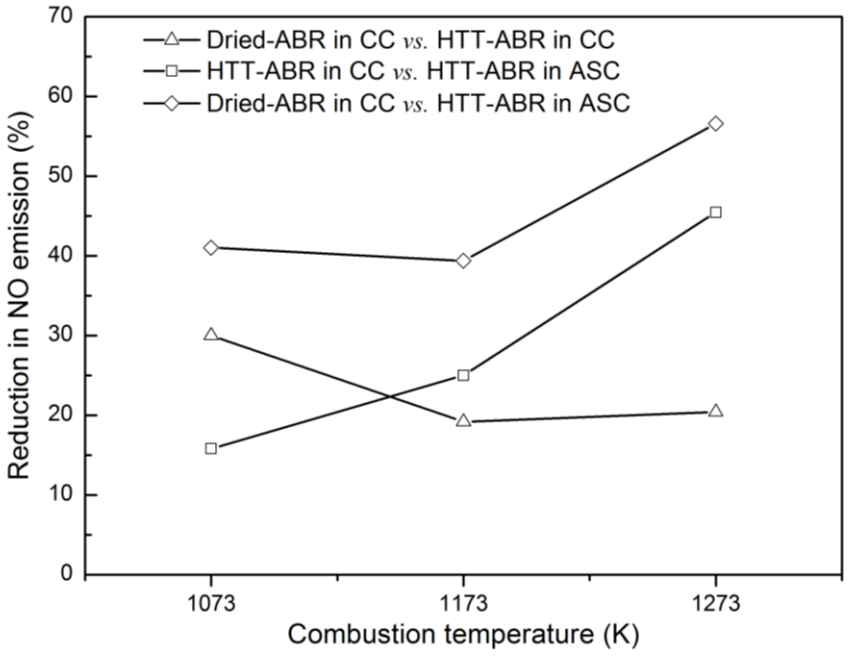

Figure 4.6. Percentage of NO reduction by HTT and ASC for different combustion modes.

In the CC mode, the reduction in the NO emission for HTT-ABR, against that for

Dried-ABR, is only due to HTT, which reached 30% at 1073K and decreased to about 20% at 1173 K and 1273 K. The lower N content in HTT-ABR would be the major reason for this lowered NO emission. Figures 4.3 and 4.4 show that the conversion of fuel-N into NO is similar at 1073 K but higher at the higher temperatures. Thus, the reduction percentage in the NO emission between the two fuels should be mainly subject to the difference in N contents between Dried-ABR (7.7 wt.%) and HTT-ABR (5.8 wt.%, 25% lower) at 1073 K. This percentage then decreased for 1173 K and 1273 K due to the higher fuel-N conversion into NO of HTT-ABR at these temperatures. As a result of the similar difference in fuel-N conversion for such two temperatures, the NO reduction percentage is about 20% at both 1173 K and 1273 K. The result indicates that, for the combustion of ABR-based fuel, the lower nitrogen in the solid fuels, the lower NO emission will be. As shown in Table 2.2, the nitrogen in ABR can be removed by HTT and a higher HTT temperature helps to reduce more nitrogen in the fuel. However, the nitrogen reduction trend slowed down when the temperature was high than 200 ℃ where nitrogen was reduced only from 5.8% (200 ℃) to 5.6% (220 ℃). This small difference probably can be neglected for the NO emission. From this aspect, the HTT temperature should not be higher than 200 ℃.

For the case of ASC, the reduction in the NO emission due to ASC (HTT-ABR in CC vs. HTT-ABR in ASC) increased with raising the temperature, from about 16% at 1073K to about 45% at 1273K. As analyzed for Fig. 4.5, in the case of ASC, the quickly released volatiles including nitrogenous species in ABR fuels at high temperatures lowered the NO emission. This is because at high temperatures the rapidly generated reducing volatiles in the primary combustion zone decreased its excessive oxygen ratio, even forming O_2-decifienct conditions, to considerably reduce the NO formation [21]. The volatiles including nitrogenous species (NH_3, HCN, etc.) can also further reduce NO when they flow into the secondary combustion zone for their burnout by reacting with the secondary oxygen. Therefore, the higher the

combustion temperature, the larger the NO reduction due to adopting ASC, as is shown in Fig.4.6 by combusting the same HTT-ABR via CC and ASC modes.

Finally, Fig. 4.6 compares the cases for CC of Dried-ABR and ASC of HTT-ABR. The plot was based on actually measured combustion results of such two cases, and the comparison was made for the specific NO emission per gram of fuel. At 1073 and 1173 K, the NO emission from ASC of HTT-ABR was about 40% lower than that from CC of Dried-ABR. This reduction percentage further increased to 57% at 1273 K. Further noting that the fuel amount of HTT-ABR should be lower than that of Dried-ABR from drying the high-water antibiotic residue directly (the former being 50-70% of the latter), one can induce that via HTT and further ASC of the HTT-produced solid fuel, it can indeed greatly reduce the absolute NO emission by, for example, over 50% in comparison with the case of "drying + CC". This is a result similar to the report made for combining HTT of sewage sludge and then combustion of its produced solid fuel [20].

Time-series variation in NO concentration

The variation of the flue gas NO concentration with burning time was investigated to understand more about the effect of HTT and combustion mode on the NO emission, as was previously done in testing the decoupling combustion [3, 22, 23]. Figure 4.7 shows the instantaneous NO concentration (ppm) in CC of coal and Dried-ABR at 1273 K. The curves with experimental data represent the actual measurement, while the fractional curves shown with dashed lines refer to the deconvolution fitting according to the Guass curve fitting function. The two deconvoluted fractional curves can be suggested to represent two types of different NO sources. For coal (top plot), they are considered to be from volatile-N (left) and char-N (right) [18, 24], respectively. Corresponding to the two types of volatiles for ABR-based fuels (Figs. 4.1 and 4.2), the two deconvoluted curves for Dried-ABR in

the lower-side plot of Fig. 4.7 should be due to the nitrogen released respectively with the light and heavy volatiles, which are denoted herein as LV-N (left) and HV-N (right).

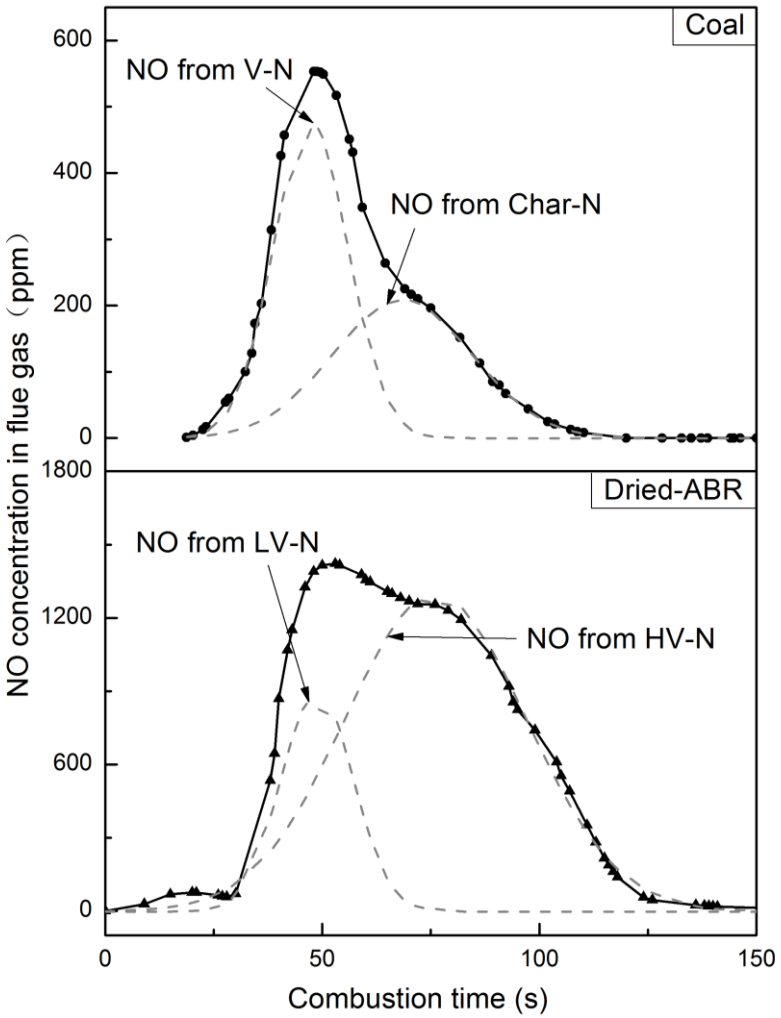

Figure 4.7. Time-series of the NO concentration and its curve deconvolution for burning coal and Dried-ABR at 1273 K.

Based on the deconvolution approach, comparing the different cases varying with the fuel and combustion mode allows then the identification of what type of nitrogen is dominant in forming NO when burning a fuel or in realizing the NO reduction shown in Fig. 4.6 due to HTT and ASC. From the plots for coal in Fig. 4.7 (upper-side) we can see that the integrated areas of the left and right deconvolution curves are equivalent, indicating that both volatile-N and char-N are important to the

NO emission of coal combustion, as was verified by many literature studies [17, 18]. Considering the lower-side plots for Dried-ABR, we can see that the area of left curve is much smaller than that of the right curve, indicating that the overall NO emission should be from the HV-N particularly. Or, this means that the converted HV-N is much more than the converted LV-N, although needing a further justification.

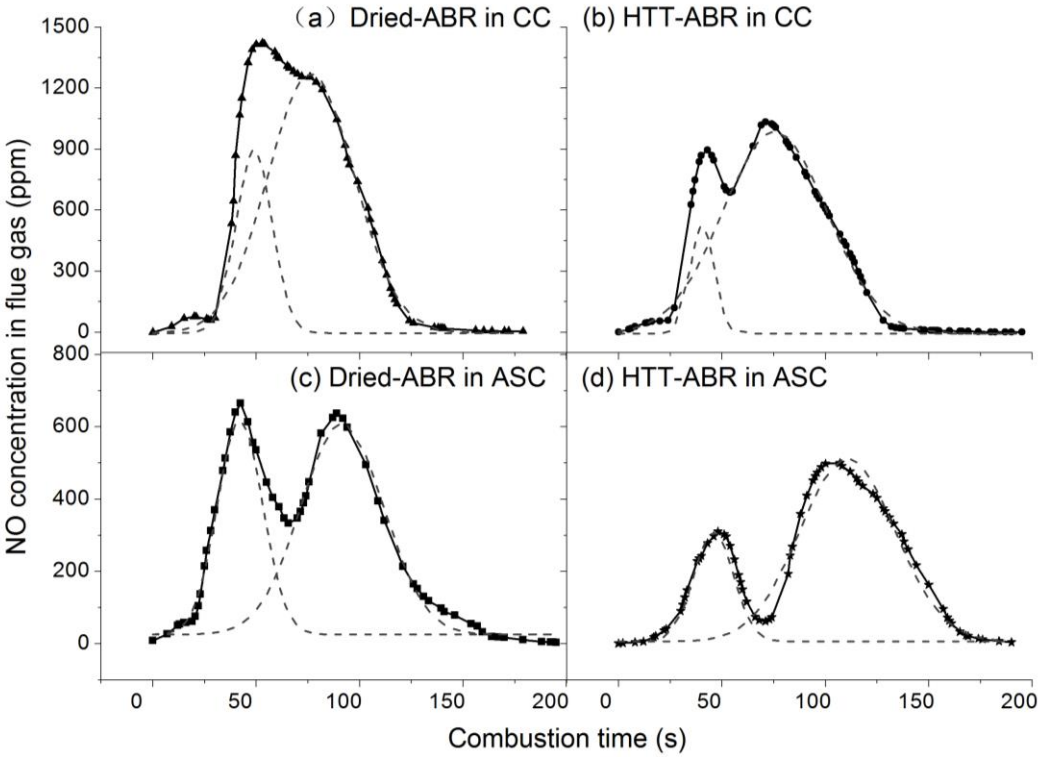

Figure 4.8. Time-series of the NO concentration and its curve deconvolution for burning Dried-ABR and HTT-ABR via both CC and ASC modes at 1273 K.

Figure 4.8 compares the time-series of the NO concentration and its deconvolution fitting for combusting both Dried-ABR and HTT-ABR via CC and ASC modes at 1273 K. The left inset is for Dried-ABR, while the first and send rows are for CC and ASC modes, respectively. Table 4.2 summarizes the integrated areas of all deconvoluted curves in Fig. 4.8 and the estimated variation ratio in the curve area to analyze the relative NO reduction caused by adopting either HTT or ASC. Here, the integrated curve area is actually equivalent to the NO emission. It is interesting to find that the experimental time-series of the NO concentration curve exhibited two

obvious peaks, especially for the fuel HTT-ABR (Fig. 4.8(b)) and the ASC mode (Fig. 4.8(c), 4.8(d)). This actually further verified that there should be two types of volatile nitrogen for the ABR-based fuels, which are denoted as LV-N and HV-N corresponding to the left and right peaks. The curve deconvolution then provides a general approach or technique to quantify the respective contributions of such two types of nitrogen to the overall NO emission (concentration) curve for each case.

Table 4.2 Deconvoluted information for NO emission curves of Fig.4.8.

Fuel and combustion mode	Emission or curve area		HV-N to LV-N	Reduction by HTT (%) [a]		Reduction by ASC (%) [b]	
	LV-N	HV-N		LV-N	HV-N	LV-N	HV-N
Dried-ABR by CC	18748	68191	3.64				
HTT-ABR by CC	7532	63137	8.38	59.8	7.4		
Dried-ABR by ASC	16569	30014	1.81			11.6	56.0
HTT-ABR by ASC	7270	29174	4.01	56.1	2.8	3.5	53.8

a: Against the case of Dried-ABR for the same combustion mode.
b: Against the case of CC mode for the same fuel.

Figure 4.8 shows that for all the cases the right deconvolution curve has a much bigger area than the first deconvolution curve, verifying that for ABR fuels, its NO formation should be mainly due to the conversion of the defined HV-N. Based on the curve heights and also widths in Fig. 4.8, we can obviously see that the curves in the second row indicate the lower NO emission than the first row (because the flue gas flow rates were very similar), whilst Fig. 4.8 (b) implies also the lower NO emission than Fig. 4.8 (a) shows. These indications just comply with the results clarified from Figs. 4.4 to 4.6 based on the actually measured NO emission and fuel-N conversion. Consequently, it is quite reasonable to use the areas of deconvoluted curves to analyze the relative contribution of each kind of nitrogen.

First, via the ratio of HV-N to LV-N, Table 4.2 shows that the contribution from HV-N is 1.8 to 8.4 times of that from LV-N, that is 8.4 for CC of HTT-ABR and 1.8 for ASC of Dried-ABR. For the same combustion mode, HTT-ABR has the higher

ratio of HV-N to LV-N (than Dried-ABR), and for the same fuel, the ASC mode has the lower ratio (than CC). Second, comparing Dried-ABR and HTT-ABR for both CC and ASC modes, Table 4.2 shows that the relative decrease in the NO emission (also the area in Fig. 4.8) is much higher for LV-N (55-60%) than for HV-N (3-7%). The absolute decrease in the area is also higher for LV-N (more than 10000 for LV-N against 1000-5000 for HV-N). Consequently, the dominant reason for HTT to reduce NO emission is due to its decreased NO formation from LV-N. This shows plausibly that HTT removed mainly LV-N which may be easier to be removed than HV-N. Similarly, comparing the CC and ASC modes for a given fuel in Table 4.2, it is clarified that HV-N dominates the decrease in the curve area both relatively and absolutely. Its relative area decrease reaches 54-57% and absolute area decrease is more than 30000. Thus, the reduction in the NO emission due to adopting ASC is dominantly due to the reduced conversion of HV-N, which takes above 90% of its total reduction. The result sounds reasonable by considering that the easy-release LV-N should be converted into NO mainly in the primary combustion zone under a high atmospheric O_2 concentration, where the conversion of the slow-release HV-N into NO should occur in the secondary zone under a reduced O_2 concentration. This implies that for the controlling of NO emission in the combustion of ABR, air-staged combustion would be a sufficient method. In the real fluidized bed combustion, the bed temperature and primary air flow rate condition should be controlled to make sure the secondary devolatilization occur in the bed zone where the oxygen is locally deficient.

More about effects of HTT on NO emission

The preceding results clarify that HTT removes certain nitrogenous components from ABR via hydrolysis (see Table 4.2), and this in turn reduces the NO emission of ABR combustion (Figs. 4.4 to 4.6). The analysis above shows also that there are two types of volatile nitrogen in ABR, light volatile N (LV-N) and heavy volatile N

(HV-N). The removed nitrogen via HTT should be mainly LV-N (Table 4.2). Herein, all fuels are tested with XPS to identify the nitrogen species existing in the fuels, and further the NH_3 amount released in fuel pyrolysis is measured to verify what kind of nitrogen would be removed through HTT.

Figure 4.9 shows the XPS spectra of all tested fuels, and its dash-line plots are the deconvoluted curves representing different types of nitrogen species. Literature studies have reported that, in coal, some specific heteroaromatic rings are the main nitrogen functionalities, and the representative ones are the N-containing pyridine, pyrrole and quaternary [25, 26]. In Fig. 4.9, the three deconvoluted curves are just at the binding energies (BEs) of 398.7 eV for pyridine, 400.1 eV for pyrrole and 401.1 eV for quaternary. This, on the one hand ratifies the approach, and on the other hand, provides a comparison with the deconvolution for the tested biomass fuels. For the latter, two fitting curves are obtained at BEs of 399.8 eV and 401.5 eV to represent the N-C bonds in amide or amine and N-H bonds in ammonia or protonated amine [20, 27]), respectively. A slight difference in BEs for such two curves from those reported in the previous study [24] could be attributed to the different natures of fuels from ABR and sewage sludge.

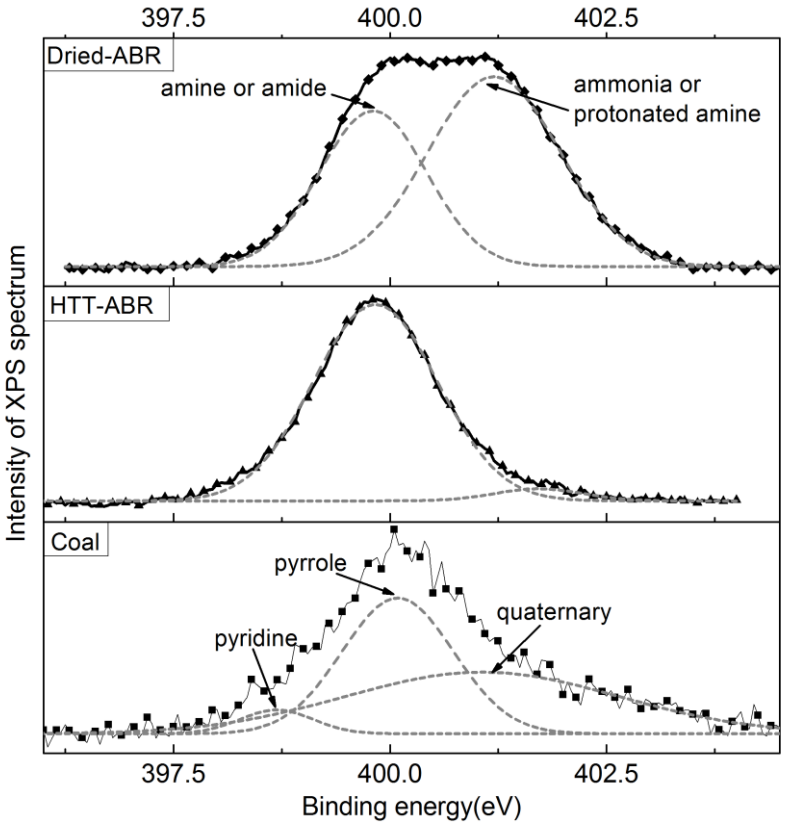

Figure 4.9. Spectra of XPS for N 1s of all tested fuels

Comparing the XPS spectra of Dried-ABR and HTT-ABR shown in Fig. 4.9, we can see that the hydrolysis reactions occurring with HTT of ABR dramatically weakened the deconvoluted curve at BE of 401.5 eV that represents amino acid or ammonia, while it correspondingly increased the intensity of amide or amine. This decrease in amino acid or ammonia is presumed to occur with the removal of some related volatile matters, thus justifying that the NO reduction by HTT comes mainly from the lowered LV-N content of HTT-ABR. Figure 4.10 further shows the amount of released NH_3 (mg/g) and its corresponding conversion against the total fuel nitrogen measured in pyrolysis of the tested fuels at 1273 K.

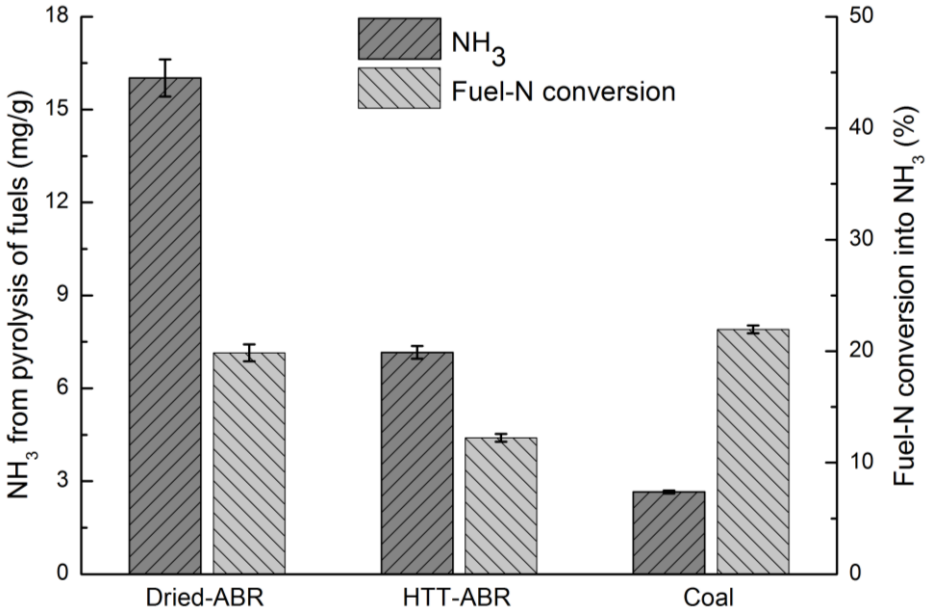

Figure 4.10. Ammonia released in pyrolysis of the tested fuels and its corresponding conversion against total fuel-N.

As shown in Fig. 4.10, the released NH_3 amount is distinctly different by following order of Dried-ABR >> HTT-ABR >> coal. The conversion relative to fuel-N into NH_3 does not have so large difference, but it is obvious that HTT-ABR is only 13%, which is lower than about 20% for Dried-ABR and coal. Combining the preceding XPS spectra, we can reasonably induce that the more released NH_3 in pyrolyzing Dried-ABR should come from its higher content of amino acid and/or ammonia. Because of the removal of these nitrogenous species via HTT, the HTT-ABR has thus the lower NH_3 release as well as its lower conversion of fuel-N into NH_3. This lower NH_3 release may also cause the volatile product from HTT-ABR to have possibly lower reduction capability toward NO. It thus more or less contributes to the higher fuel-N conversion into NO clarified in Figs. 4.3 and 4.4 when comparing with the burning of Dried-ABR.

4.3.2. Ash behavior and slagging/fouling tendency

Ash behavior in fuel preparation process

Ash in ABR would partially dissolve into water in HTT and be leached out in centrifugation. The mass of ash remaining in the HTT produced solid biofuels was calculated as the ash content of the fuels in Table 2.2 and the total mass of the biofuels. Its mass in 200 g raw ABR without centrifugation was used to determine the original ash content in ABR. Fig. 4.11 shows the percents of ash in the HTT produced solid biofuels from different temperatures, where the pink bar indicates the ash lost during the fuel preparation process, which includes dissolution in HTT and leaching via centrifugation. About 17% ash in ABR was lost via leaching in centrifugation (denoted as "No HTT" in Fig. 4.11). Comparing to ABR (100% ash), the ash loss for the 160 ℃ HTT-ABR was the highest which reached 55%. Increasing the HTT temperature decreased the ash loss. For example, ash decreased to 40% for the HTT at 220 ℃. The results mean that at higher HTT temperatures, more ash components tended to precipitate and retain in the solid biofuels, whereas at lower HTT temperatures, there were more ash species dissolving into the liquid phase and in turn leached out by centrifugation after HTT.

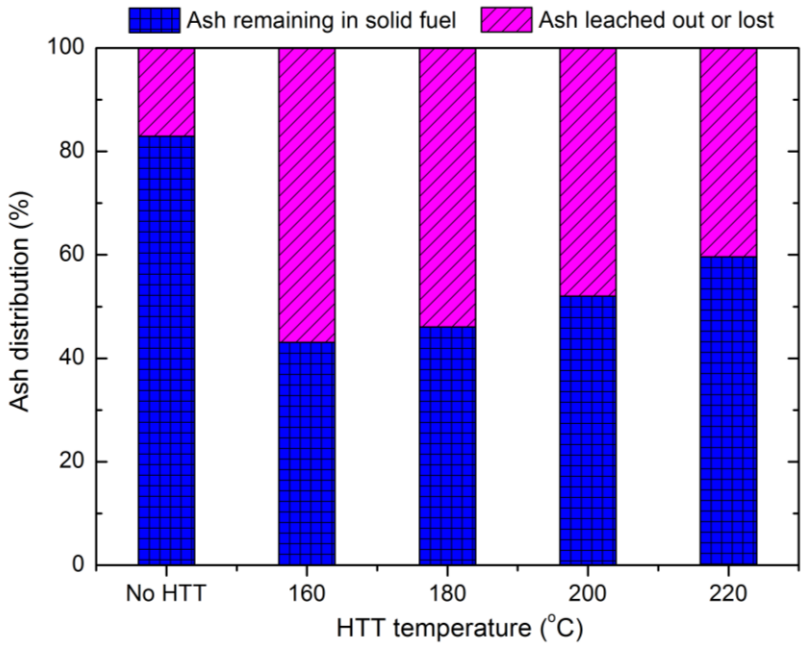

Figure 4.11. Percentage of ash remaining in HTT produced solid biofuels excluding the leached ash during fuel preparation.

Figure 4.12 shows further the absolute masses of major ash components remaining in HTT-ABR produced from 200 g of ABR under different treating temperatures. The mass of each kind of ash component or species was calculated with the total ash amount (Table 2.2 and Fig. 4.11) and the XRF-measured content (Table 2.3). The basis for this comparison was the absolute ash mass in the dried ABR, which was about 3300 mg and denoted as "No HTT" in Fig. 4.12. Then this total mass of ash was decreased to 1700 mg through HTT at 160 ℃ and its consequent centrifugation, and all the plotted ash species contributed an obvious decrease. For example, the oxides of alkali earth metals (CaO and MgO in violet bar) and phosphorus pentoxide (red bar) decreased from about 2800 mg in "No HTT" case to 1500 mg for HTT at 160 ℃. The amounts of sulfate and alkali metal oxides in the fuel ash correspondingly decreased from about 600 mg and 210 mg to about 150 mg and 40 mg, respectively. With increasing the temperature of HTT from 160 ℃ to 220 ℃, all the ash components except for alkali metal oxides (pink bar) showed slight increase in their absolute amounts. The most obvious increase was shown for the phosphate (from 110 mg to 540 mg corresponding to the HTT temperature rise from 160 ℃ to

220 ℃). The mass increase for alkali earth metal oxides (violet bar) was from about 1420 mg to about 1640 mg, while that for sulfate (blue bar) was very slight because its amount was only about 150 mg. The absolute amount of alkali metal oxides decreased with increasing the HTT temperature, and it was about 40 mg and 20 mg for the cases of HTT at 160 ℃ and 220 ℃, respectively.

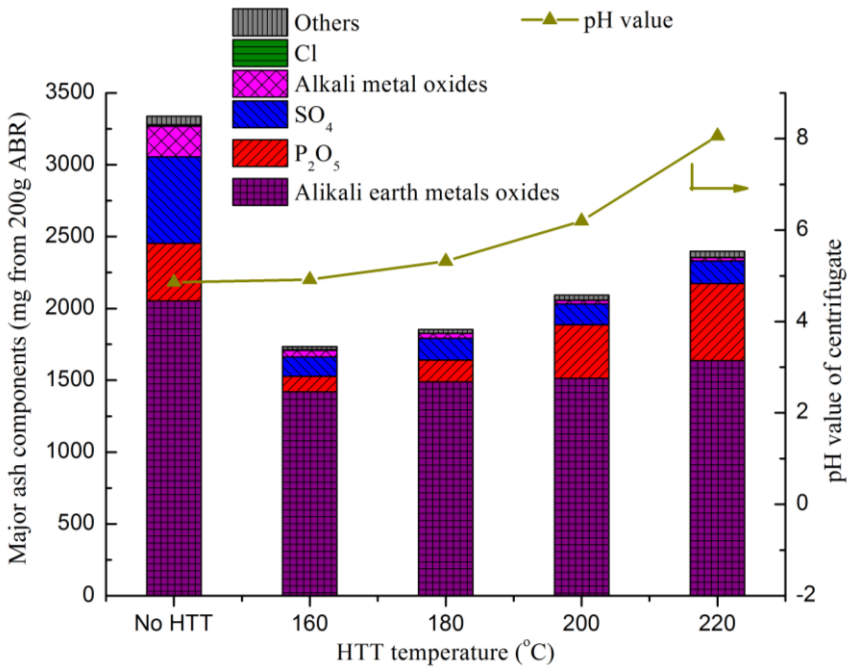

Figure 4.12. Absolute masses of major ash components remaining in solid biofuels from HTT of 200 g antibiotic mycelial dreg at different temperatures and the corresponding pH values of HTT liquid

As a summary, Figure 4.12 shows that increasing the HTT temperature promoted the precipitation of all ash components or species except for alkali metal oxides, and this made the ash amount in the HTT-ABR become more at higher temperature. The major reason is that HTT operation would increase the pH value of its liquid phase, thus lowering the solvability of metal oxides to retain more salts or oxide as fuel ash and to cause the gradually increased ash amount with the higher HTT temperature. The phosphorus pentoxide (phosphate possibly) in the biofuel from HTT at 220 ℃ was even higher than that in Dried-ABR (with centrifugation only). It means that some of phosphate originally transferred to the liquid phase in centrifugation (No

HTT) tended to precipitate at high-temperature HTT as ash in the HTT produced solid biofuels.

Noetheless, in comparison with Dried-ABR ("No HTT" in Figs. 4.11 and 4.12), HTT-ABR at all the tested temperatures had lower absolute ash amount. Especially, HTT lowered the absolute amounts of sulfur, chlorine, alkaline metals and also CaO, showing again the upgrading effect of HTT on the solid biofuel from ABR. The ash properties correlation with the combustion behaviors will be discussed later.

Slagging and fouling tendency

The chemical composition of ash of ABR-based fuels from different HTT conditions which has been shown in chapter 2 was converted into all oxide species and displayed in Table 4.3. Slagging and fouling indices calculation results are also listed in the lower part of Table 4.3.

Table 4.3 The major ash composition of antibiotic bacterial residue based fuels and the slagging and fouling indexs of the ash

Ash composition	No HTT	160 ℃	180 ℃	200 ℃	220 ℃
CaO	45.96	70.48	68.21	57.23	52.09
MgO	1.63	1.24	1.54	2.61	3.10
P_2O_5	16.33	9.79	12.59	25.95	31.57
SiO_2	1.089	0.62	0.46	0.29	0.28
K_2O	6.53	2.80	1.84	1.16	0.85
Na_2O	2.18	1.24	0.92	0.58	0.42
Fe_2O_3	0.82	1.09	1.08	1.45	1.69
Al_2O_3	0.41	0.16	0.15	0.14	0.14
Indices values					
$B/A_{(+P)}$	49.06	111.52	140.27	204.6	212.2
$R_{(b/a)}$	32.33	93.72	115.27	140.93	134.53
F_u	332.36	399.61	331.12	252.13	174.44
S_R	2.20	0.85	0.65	0.47	0.49
K_{Al}	2.67	4	3	2	2
Fe_2O_3/CaO	0.018	0.015	0.0156	0.025	0.032
AI	0.33	0.21	0.16	0.11	0.10
BAI	0.094	0.27	0.39	0.83	1.33

The $B/A_{(+P)}$ value of the ABR-based fuels are all very high exceeding 49 which are largely higher than the fuels studied by Pronobis et al. [6]. For the simplified basis to acid ratio $R_{(b/a)}$, it is obvious that the values for all the ABR-based fuels are much higher than 2, implying that the ash of ABR-based fuels all have very high slagging tendency. The higher HTT temperature increased the $R_{(b/a)}$. The reason of this should be due to the very high concentration of CaO contents in the ABR-based fuel which was considered as the base part in the index calculation. Afterward, at a higher HTT temperature, the pH value increased due to the production of ammonia, resulting in the further increasing of the CaO and P_2O_5 content in the fuels. It is also shown in Table 4.3 that the fusion index (F_u) has significantly high value far from the safe value of 40, which are ranging from 180 to 332. It means that the pure ABR-based fuels are probably to get fouling in the boiler. And as the HTT temperature increased, the F_u value eventually decreased, meaning that the ash was going closer to the safe level by HTT, attributed to the leaching effect on the alkali metal in HTT discussed earlier. S_R gives the viscosity index of the slag that is much lower than 65, indicating again the high slagging inclination of the ABR-based fuel. However, as the K_{Al} values of the tested fuels are all in the range of 1~4, the slag viscosity will probably be doubled according to the previous study [5], which means that the lower slagging tendency. All these observation indicates the very high possibility that ABR with or without HTT will lead to slagging or fouling problems when it is mono combusted in the real power plants. Further study should be focused on the co-combustion of ABR-based fuel with high melting ash coal or combustion blending with additives so as to avoid the ash caused problems [15, 28, 29].

In spite of the fouling and slagging tendency for all the ABR-based fuels, some other indexs showed positive effect of HTT on the ash properties. For instance, As for the iron calcium ratio n (Fe_2O_3/CaO), it seems to be safe for all the fuels in the range of 0.018~0.032 which is out of high deposition area of 0.3~3[6]. AI, as shown in the

talbe, was decreased dramaticaly after HTT and the reduction goes deeper with the increase in the HTT temperature. As a result, AI of ABR without HTT is 0.33 kg/GJ, which means the fouling and slagging is highly probable. Meanwhile, when the HTT temperature higher than 180 ℃, the vaule was reduced to lower than 0.16 [14], which is considered as a safe level. But the difference of AI in the solid fuel derived from 200 ℃ and 220 ℃ HTT was as small as 0.01. Therefore, it can be concluded that the better HTT temperature for the ash problem mitigation should be ranged from 180 to 200 ℃, which agrees well with the optimal temperature concluded in Chapter 2. Correspondingly, BAI keeps increasing from 0.094 to 1.33 with the increase of the HTT temperature, indicating that the HTT temperature higher than 160 ℃ will positively increase the value higher than 0.13 to keep ash in ABR from agglomeration in the fluidized-bed reactor according to the previous study [30]. The decrease in AI and increase in BAI for ABR-based fuel can be accounting for the leaching out of alkali metals in the HTT fuel preparation process.

As a summary, due to the low content of acid group and high content of basic group oxide, the slagging and fouling inclination of the ABR-based fuels are all very high. The releasing of the ammonia during HTT further boosts the dissolution of acid group while tend to keep basic group oxides, further increase the negtive effect. The cocombustion with coal or blending with additives should be considerred when combusting the ABR-based fuel in the boiler furnace. For the design of fluidized bed furnace, the bed temperature should be carefully controlled as low as possible to avoid the fouling or slagging problem for the combustion of ABR. On the other hand, as HTT has a leaching effect on the ash, the most critical alkali oxides can be leached out during HTT that leads to the relatively lower slagging and fouling tendencies for the ABR-based fuels after HTT.

4.4. Conclusions

This chapter investigated the combustion characteristics of the antibiotic bacterial residue (ABR) either by experiment and calculation. Firstly, the NO emission characteristics from combusting biofuels from ABR with/without hydrothermal treatment (HTT) in a batch-type fixed bed reactor according conventional combustion (CC) and air-staged combustion (ASC). Analysis of the fuel nitrogen functionalities and the deconvolution of the time-series of the flue gas NO concentration (or emission) clarified the mechanism about how the fuel pretreatment by HTT and the different combustion modes affect the NO emission. Secondly, the ash slagging and fouling tendency was studied by calculating and discussing several indexes of the ash, the mechanism of how HTT affect on the ash behavior was clarified based on the discussion of the ash behavior in the biofuel preparation.

1) Comparing the burning of directly dried ABR (Dried-ABR), the NO emission was 20~30% lower for the fuel after HTT (HTT-ABR). This HTT-induced reduction in the NO emission was found to be mainly due to the removal of certain N existing with the light volatile matters (LV-N) of ABR in the form of amino acid or/and ammonia. Through burning HTT-ABR via ASC, it was found that the reduction of the NO emission, in comparison with the CC of the same fuel, increased with raising the combustion temperature, and at 1273 K, it reached about 45%. Deconvoluting the time-series of the NO emission revealed that the reduced NO mission by ASC was mainly due to the suppressed NO formation from the nitrogen existing in the heavy volatile (HV-N) of ABR. In comparison with CC of the Dried-ABR fuel, it was found that via ASC of HTT-ABR, the reduced NO emission increased with raising the combustion temperature and can be 40-57% at 1073-1273 K to show the integrated effects of HTT and ASC on reducing NO emission of ABR combustion. Consequently, HTT of a fuel and further combusting the

HTT-produced fuel via air-staged mode would provide an effectively feasible way to reduce the NO emission in converting biomass fuels with high contents of moisture and nitrogen into energy via combustion.

2) Due to the low content of acid group and high content of basic group oxide, the slagging and fouling inclination of the ABR-based fuels are all very high. The releasing of the ammonia during HTT further boosts the dissolution of acid group while keeping basic group oxides, and further increases the negtive effect. The co-combustion with coal or blending with additives should be considered when combusting the ABR-based fuel in the boiler furnace. On the other hand, as HTT has a leaching effect on the ash, the most critical alkali oxides can be leached out during HTT that lead to the relatively lower slagging and fouling tendencies for the ABR-based fuels after HTT.

3) The optimum HTT temperature for solid fuel production from ABR in the viewpoint of NO emission reduction and the ash problem mitigation would be ranged from 180 to 200 ℃, which agrees well with the optimal temperature concluded in Chapter 2.

References

[1] Obernberger I, Brunner T, Barnthaler G. Chemical properties of solid biofuels—significance and impact. Biomass and Bioenergy. 2006;30:973-82.
[2] Qian FP, Chyang CS, Huang KS, Tso J. Combustion and NO emission of high nitrogen content biomass in a pilot-scale vortexing fluidized bed combustor. Bioresour Technol. 2011;102:1892-8.
[3] Chen H, Zhao P, Wang Y, Xu G, Yoshikawa K. NO Emission Control during the Decoupling Combustion of Industrial Biomass Wastes with a High Nitrogen Content. Energy & Fuels. 2013;27:3186-93.
[4] Jenkins B, Baxter L, Miles T. Combustion properties of biomass. Fuel processing technology. 1998;54:17-46.
[5] Bryers RW. Fireside slagging, fouling, and high-temperature corrosion of heat-transfer surface due to impurities in steam-raising fuels. Progress in energy and combustion science. 1996;22:29-120.
[6] Pronobis M. Evaluation of the influence of biomass co-combustion on boiler furnace slagging by means of fusibility correlations. Biomass and Bioenergy. 2005;28:375-83.
[7] Zhang G, Ma D, Peng C, Liu X, Xu G. Process characteristics of hydrothermal treatment of antibiotic residue for solid biofuel. Chemical Engineering Journal. 2014;252:230-8.
[8] Ma D, Zhang G, Zhao P, Areeprasert C, Shen Y, Yoshikawa K, et al. Hydrothermal Treatment of Antibiotic Mycelial Dreg: More Understanding from Fuel Characteristics Chemical Engineering Journal. 2015.
[9] Blomberg T. Which are the right test conditions for the simulation of high temperature alkali corrosion in biomass combustion? Materials and Corrosion. 2006;57:170-5.
[10] Miles TR, Baxter LL, Bryers RW, Jenkins BM, Oden LL. Boiler deposits from firing biomass fuels. Biomass and Bioenergy. 1996;10:125-38.
[11] Pronobis M. The influence of biomass co-combustion on boiler fouling and efficiency. Fuel. 2006;85:474-80.
[12] Ots A, Zelkowski J. Evaluation of coal tendency to slagging and fouling basing on coal data and laboratory investigation. XXXII Kraftwerkstechnisches Kolloquium, Dresden2000. p. 47-58.
[13] Masi á AT, Buhre B, Gupta R, Wall T. Characterising ash of biomass and waste. Fuel Processing Technology. 2007;88:1071-81.
[14] Vamvuka D, Zografos D. Predicting the behaviour of ash from agricultural wastes during combustion. Fuel. 2004;83:2051-7.
[15] Vamvuka D, Zografos D, Alevizos G. Control methods for mitigating biomass ash-related problems in fluidized beds. Bioresource Technology. 2008;99:3534-44.
[16] Zhu C, Liu S, Liu H, Yang J, Liu X, Xu G. NOx emission characteristics of fluidized bed combustion in atmospheres rich in oxygen and water vapor for high-nitrogen fuel. Fuel. 2015;139:346-55.

[17] Vermeulen I, Block C, Vandecasteele C. Estimation of fuel-nitrogen oxide emissions from the element composition of the solid or waste fuel. Fuel. 2012;94:75-80.
[18] Hernando MD, Mezcua M, Fernandez-Alba AR, Barcelo D. Environmental risk assessment of pharmaceutical residues in wastewater effluents, surface waters and sediments. Talanta. 2006;69:334-42.
[19] Tognotti L. Coal-Nitrogen Release and NOx Evolution in Air-Staged Combustion. Energy & Fuels. 1998;12:6.
[20] Zhao P, Chen H, Ge S, Yoshikawa K. Effect of the hydrothermal pretreatment for the reduction of NO emission from sewage sludge combustion. Applied Energy. 2013;111:199-205.
[21] COMMISSION TE. COMMISSION REGULATION (EU) No 37. Official Journal of the European Union. 2010.
[22] Cai L, Shang X, Gao S, Wang Y, Dong L, Xu G. Low-NOx coal combustion via combining decoupling combustion and gas reburning. Fuel. 2013;112:695-703.
[23] He J, Song W, Gao S, Dong L, Barz M, Li J, et al. Experimental study of the reduction mechanisms of NO emission in decoupling combustion of coal. Fuel Processing Technology. 2006;87:803-10.
[24] Chaiklangmuang S, Jones JM, Pourkashanian M, Williams A. Conversion of volatile-nitrogen and char-nitrogen to NO during combustion. Fuel. 2002;81:7.
[25] Martti JA, Jouni PH, Jouni LT. Importance of Solid Fuel Properties to Nitrogen. Combustion and Flame. 1993;95:22-30.
[26] Kambara S, Takarada T, Toyoshima M, Kate K. Relation between functional forms of coal nitrogen and NOx emissions from pulverized coal combustion. Fuel. 1995;74:7.
[27] Pietrzak R. XPS study and physico-chemical properties of nitrogen-enriched microporous activated carbon from high volatile bituminous coal. Fuel. 2009;88:1871-7.
[28] Mahoney DF, Kober AE, Risbud SH. Method of reducing high temperature slagging in furnaces. Google Patents; 1983.
[29] Wang L, Hustad JE, Skreiberg Ø, Skjevrak G, Grønli M. A critical review on additives to reduce ash related operation problems in biomass combustion applications. Energy Procedia. 2012;20:20-9.
[30] Bapat D, Kulkarni S, Bhandarkar V. Design and operating experience on fluidized bed boiler burning biomass fuels with high alkali ash. American Society of Mechanical Engineers, New York, NY (United States); 1997.

Chapter 5 Conclusions and future works

5.1 Conclusions

This work has proposed to deal with the antibiotic bacterial residue (ABR) by hydrothermal treatment (HTT) and combustion. According to that, the task of this study was to investigate the feasibility of solid fuel production from ABR; to optimize and scale up the HTT conditions of ABR for the further application of this process; to discuss the effect of HTT on the combustion characteristic of ABR; finally to discuss the feasibility of our proposal. The results of the whole study are summarized as follows:

1) The dewaterability of ABR was significantly improved by HTT in term of the sedimentation performance, the dehydration and the drying. The improvement depends not so much on the HTT operation temperature or holding time. The higher temperature or longer residence time will boost better dewaterability. After HTT temperature up to 220 ℃, the drying performance of the residue will be weakened. Therefore, the best condition for ABR dewatering should be around 200 ℃. HTT can also restrict water adsorption of solid matters in ABR. The reason should be due to HTT enhances the hydrolysis of the pectin substance, which is high in oxygen and has strong hydrophilism in ABR.

2) HTT of ABR is accompanied with some loss in volatile matters and certain increase in the ash content, and HHV of the resulting solid biofuel was increased by 37% (19.3 kJ/g to 26.5 kJ/g) and LHV was elevated by 46% (16.7 kJ/g to 24.4 kJ/g) through HTT at 220 ℃ in comparison with the directly dried raw ABR. Both XPS and FTIR analyses of the HTT produced solid biofuels revealed that the increase in the heating value was mainly due to the HTT-accompanied reactions including dehydration, dehydroxylation, decarbonylation and decarboxylation

occurring to the organic matters which lowered the oxygen content of the solid biofuel. Nitrogen content in the solid matters of ABR was found to be reduced by 27 % (7.7 wt% to 5.6 wt.%) through HTT at 200 ℃, as a result of hydrolyzing protein or amino acid. Corresponding to this, more than half of the N in the dried raw ABR (solid-N) was transferred into the HTT centrifugate to become Kjeldahl nitrogen (K-N).

3) The COD of the centrifugate was quite high as over 200g/L which due to the strong dissolution of the solid matter into the aqueous phase. Due to the decomposition effect of HTT on the antibiotic substance shown by the model solution, it can be expected that HTT is really suitable to confirm the safe disposal of the hazardous ABR. In the viewpoint of high COD and low antimicrobial effect by antibiotics, the liquid product is anticipated to be suitable for the biogas production by anaerobic digestion.

4) Solid fuels produced from ABR by HTT can give a mass recovery to 35% to almost 50%. The higher HTT temperature showed lower recovery due to the stronger dissolution effect of HTT on ABR. However, as the higher HTT temperature will increase the heating value of the produced solid fuels, the interesting finding is that all the energy recovery from ABR into solid fuels by HTT showed higher than 50% value.

5) The pilot scale HTT of ABR showed similar improvement in dewaterability of ABR. By HTT, ABR could be mechanically dehydrated down to 38~52wt.% moisture content material, while the raw ABR could only reach 75wt.% moisture content. As the HTT temperature increased, the dewaterability was increased from 52wt.% for 120 ℃, 30 minutes to 38wt.% for 180 ℃, 30 minutes. The natural drying performance was also improved with increasing the HTT temperature or the holding time.

6) The mass recovery and energy recovery in the ABR-based solid fuels was reduced in the pilot plant experiment in comparison with the lab scale experiment. For the

180 ℃, 30 minutes, the mass recovery was 34.5% and the energy recovery was 29%. Due to the rotation mixing in the pilot scale reactor was enhanced and the steam feeding further boost the mass transfer in the reactor, the dissolution of the solid matter in ABR would be increased. This led to the lower mass recovery than the lab scale experiment. Also, the heating value of the ABR-based solid fuels will be decreased by increasing the HTT temperature or the holding time. Similar with the lab scale experiment, the dehydrated liquid from pilot scale HTT process has high COD value, which means that the methane production from the liquid should be considered.

7) By recycling the exhaust steam from the previous batch, the energy consumption for the same amount of ABR can be significantly reduced by almost 30%. Further improvement of the exhaust steam recycling was estimated to show a great potential on energy saving of 44% and water consumption saving of 49.5%. It can be apparently expected that production of solid fuel from ABR by HTT will be feasible in the technical aspect. Also, the combustion of the solid fuel should be further considered.

8) Comparing the burning of directly dried ABR (Dried-ABR), the NO emission was 20~30% lower for the fuel after HTT (HTT-ABR). This HTT-induced reduction in the NO emission was found to be mainly due to the removal of certain N existing with the light volatile matters (LV-N) of ABR in the form of amino acid and/or ammonia. Through burning HTT-ABR via air-staged combustion (ASC), it was found that the reduction of the NO emission, in comparison with the conventional combustion (CC) of the same fuel, increased with raising the combustion temperature, and at 1273 K it reached about 45%. Deconvoluting the time-series of the NO emission revealed that the reduced NO emission by ASC was mainly due to the suppressed NO formation from the nitrogen existing in the heavy volatile (HV-N) of ABR. In comparison with CC of the Dried-ABR fuel, it was

found that via ASC of HTT-ABR, the NO emission reduction ratio increased with raising the combustion temperature and can be 40-57% at 1073-1273 K to show the integrated effects of HTT and ASC on reducing the NO emission of ABR combustion. Consequently, HTT of a fuel and further combusting the HTT-produced fuel via air-staged mode would provide an effectively feasible way to reduce the NO emission in converting biomass fuels with high contents of moisture and nitrogen into energy via combustion.

9) Due to the low content of acid group and high content of basic group oxide, the slagging and fouling inclination of the ABR-based fuels are all very high. The releasing of the ammonia during HTT further boosts the dissolution of acid group while tend to keep basic group oxides. The co-combustion with coal or blending with additives should be considered when combusting the ABR-based fuel in the boiler furnace. On the other hand, as HTT has a leaching effect on the ash, the most critical alkali oxides can be leached out in HTT that leads to the relatively lower slagging and fouling tendencies for the ABR-based fuels after HTT.

10) Comprehensively considering the all the factors about the dewaterability, energy density, and combustion performance of solid fuel, and energy consumption of HTT, the optimal HTT temperature should be ranged from 180~200 ℃.

5.2 Recommendations for future work

In this study, the feasibility of HTT for solid fuel production from ABR has been investigated in lab scale and pilot scale tests. The effects of HTT on the combustion characteristics of the produced solid fuel have been clarified in a fixed bed type combustor. It is proved that the combination of HTT and combustion can efficiently treat ABR in the viewpoint of safe disposal of hazardous material. However, further works should be done in the future.

1) For the pilot scale, HTT showed different energy recovery ratio in comparison with the lab scale, which should be attributed to the enhancing dissolution of the solid organic substance by different heating method in the pilot test. The rotating speed of the motor stirrer, HTT condition should be further optimized in the pilot scale HTT.

2) Both the lab scale and pilot scale study showed that around 50% or more fraction of the solid matter was dissolved into liquid phase in HTT. As a result, the COD concentration in the liquid product from HTT was quite high which was considered a high potential to be used as raw material for anaerobic digestion to produce methane. It was reported by Meng et al that HTT dehydrated liquid could be used for methane production through anaerobic digestion[1]. Therefore, one orientation for the future work will be to investigate the biogas production from the hydrothermally treated ABR liquid by anaerobic digestion. Biogas production will probably improve the energy balance performance of the whole system.

3) The fouling and slagging tendency was shown to be very high even HTT gives a positive effect on it. Co-combustion of ABR-based fuel with low fouling and slagging tendency coal should be considered to solve this problem. Besides, the combustion of HTT produced solid derived from ABR should be further studied under the continuous type combustion.

Reference

[1] Meng D, Mu H, Yoshikawa K. Study on Biochemical Methane Potential and Engineering Application of Sludge Dehydrated Water through Hydrothermal Drying Treatment. International Journal of Energy Science. 2013.

Acknowledgement

I would like to express my gratitude to all those who helped me in this research and the writing of this thesis.

My deepest gratitude goes to Professor Yoshikawa, my supervisor, for his constant encouragement and guidance in my growth during these years. Thanks so much for giving me the chance to study in Tokyo Institute of Technology (TIT) four years ago and guiding me into the amazing field of waste to energy. He let me enjoy the research and the life in Japan. His guidance, support and encouragement during my studies at TIT are indeed a favor for me.

I would like to also express my gratitude and special thanks to Professor Takahashi, my supervisor, for his instructive advice on my thesis. I am deeply grateful of his help in the completion of this thesis.

Appreciation is also extended to Professor Guangwen Xu and Professor Guangyi Zhang in the Institute Process of Engineering; Chinese Academy of Sciences who gave me chance to conduct one major part of experiments in Institute Process of Engineering. Thanks so much for the fund supply of the Strategic China-Japan Cooperative Program on “Science and Technology (S&T) for Environmental Conservation and Construction of a Society with Less Environmental Burden” of the National Nature Science Foundation of China and Japan Science and Technology Agency (NO. 21161140329).

Besides, I would like to show deep appreciate to Dr. Peitao Zhao and Dr. Yafei Shen who get me guidance in HTT in chapter 2 and combustion in Chapter 4 as well as Hongfang Chen, Liang Lu, Hu Wu and Chinnathan Areeprasert. I am also deeply indebted to all the colleague and friends for their direct and indirect help to me.

Finally, I am always grateful to my family members who kept supporting me no matter where I am, whatever I am doing. Without their supporting, I will not exist here and have not gone so a long way. I am also sending my thanks to Yixin Nong, the best friend in my life, and her family who care me a lot no less than my parents and keep giving me power all the time. I will fully devoted myself into the pursuing my dream and do my best in the future.